Preparation of Clay-dye pigment and its dispersion in polymers

A thesis submitted in fulfilment of the requirements for the degree of Master of Engineering

Jamuna Sivathasan
B. Eng.

School of Civil, Environmental and Chemical Engineering

RMIT University

September 2007

Acknowledgements

I wish to thank Professor Satinath Bhattacharya, my research supervisor for his ingenuity, inspiration and invaluable guidance throughout the Research work.

And

Also I wish to thank Dr. Ivan Ivanov my second supervisor for the useful discussions & advice concerning the Research project.

With Gratitude to,

The Rheology and Material Processing Center, RMIT University for funding the research and providing partial Scholarship

School of Civil, Environmental and Chemical Engineering for providing financial aid towards my attendance at international conference (CHEMECA-2006) and for offering mindful supports.

Special Appreciation to,

Assoc. Professor Dougal McCulloch and Mr. Philip Francis for their skilful training in using and working with Transmission Electron Microscopy

Mr. Frank Antolasic for his assistance with using Small Angle X-ray Scattering instrument

Mr. Mike Allan, Mr. Andrew Chryss and Mr.Farhad Younos for providing the skills, useful discussions and support throughout the experimental work

Ms Vikki Dahl dedicated proof reader for correcting the Thesis

All the members of Rheology and Materials Processing Center (RMPC) and fellow Postgraduate students for kind support and encouragements

Finally, to all whom I have not mentioned, rest assured you're on my reserved list-

Thank you.

Preface

This Thesis has been written for the degree of Master of Engineering in compliance with the guidelines of the School of Civil, Environmental and Chemical Engineering, RMIT University, Melbourne- Australia. This dissertation is the original work carried out by the author between February 2005 and February 2007, unless otherwise stated. Some of this work was previously presented in CHEMECA 2006 International Conference and was published in the Proceedings of CHEMECA 2006.This thesis contains in total of 138 pages and 44 figures.

Declared

---------- 14 / 09 / 2007

Jamuna Sivathasan

Abstract

This thesis is concerned with an experimental study of clay intercalation by organic dye molecule which is crucial for the successful development of a stable clay-dye pigment with combined advantages of organic dye and inorganic clay.

In this work Clay-dye pigments were prepared by two different methods with the selection of a suitable intercalation medium. Two different organic dyes were used with unmodified clay and modified clay to study the intercalation. Characteristics of clay-dye pigment have been investigated using X-Ray Diffraction (WAXS & SAXS), Thermo-gravimetric Analysis (TGA) and Transmission Electron Microscopy (TEM). X-ray and TGA studies of clay-dye complex prepared with unmodified clay suggested that the absorption of the dye into the clay interlayer space showed larger spacing and increased thermal stability; where, as the adsorption of the dye molecule onto the external surfaces of the clay showed mere increase of d-spacing. Clay-dye complex prepared with organo-clay showed decrease of d-spacing from the actual organo-clay, which confirmed the removal of organic molecule from the clay layer and hence the possible partial replacement of dye molecule to the clay interlayer surface. TEM study also visually confirmed the change of clay layer d-spacing due to organic dye molecular intercalation.

Examination of incorporation of clay-dye pigment into the polymer showed significant improvement in thermal and ultra violet (UV) stability for dye molecule intercalated into the clay layer; where as dye molecule adsorbed on the outer surface of the clay did not show any significant improvement in the thermal and UV stability. In the case of

modified clay dye pigment it was observed poor UV stability against UV exposure, which revealed that desorption of long chain aliphatic quaternary ammonium cation from clay interlayer by organic dye molecule was incomplete, which leads to poor stability against high energy.

In this thesis it is shown that the absorption of cationic dye by unmodified clay in aqueous medium mainly takes place in the interlayer clay surface. More likely the dye molecules with aromatic quaternary ammonium cation intercalate the clay layer and strongly interacts with the clay interlayer oxygen plane, where solvent dye (which is hydrophobic in nature) adsorption by unmodified clay mainly takes place on outer surface of the clay. Dye molecules are weakly interacted with outer surface oxygen plane by hydrogen bonding or Vander Waals forces. Modified clay enabled the solvent dye to intercalate inside the clay interlayer surface with the suitable non-aqueous medium (because of its expanded structure). The modified clay suspension in the selected non-aqueous medium shows only partial desorption of alkyl ammonium molecule from the clay layer with the presence of both cationic dye and solvent dye. Therefore the penetrated dye molecules must have weakly interacted with the interlayer oxygen plane as well as the remaining alkyl ammonium molecule present inside the clay layer. It is believed that the thermal and UV stability of organic dye can only be facilitated by a specific interaction (π-interactions) between aromatic alkyl ammonium cation of organic dye molecule and the interlayer oxygen plane of clay minerals. This interaction possibly enables the high thermal energy or the energy of the UV radiation to transmit immediately into the clay layer. Therefore organic dye molecules are protected from high energy loading and hence thermal and UV stability are improved.

List of Abbreviations

MMT	Montmorillonite
NaMMT	Sodium Montmorillonite
C15A	Cloisite 15A
U Clay	Unmodified clay
TOT	Tetrahedral Octahedral Tetrahedral
HT	Hydrogenated Tallow
CEC	Cation exchange capacity
CPNC	Clay polymer nanocomposites
PS	Polystyrene
R6G	Rhodamine 6G
Rhod B	Rhodamine B
SD	Solvent dye
MB	Methylene blue
MG	Methylene green
CV	Crystal Violet
TFT	Thioflavine T
BR	Bioresmethrin
2M2ODA	Dimethyl dioctadecyl ammonium chloride
DCM	Dichloromethane
HCl	Hydrochloric acid
XRD	X-ray diffraction
WAXS	Wide angle X-ray scattering

SAXS	Small angle X-ray scattering
IR	Infra red
TEM	Transmission electron microscopy
EDS	Energy dispersive spectroscopy
CCD	Charge-coupled diode
FET	Field effect transistor
CMA	Multi channel analyzer
NMR	Nuclear magnetic resonance
ESR	electron spin resonance
TGA	Thermo-gravimetric analysis
DTA	Differential thermal analysis
DTG	Derivative thermogravimetry
UV	Ultra violet

Table of Contents

Table of Figures

CHAPTER 1: Introduction

In today's globally competitive market, product distinction is a key to success. Therefore, the ability to produce unique and appealing special effects becomes a powerful marketing tool for manufacturers of plastic products. High shelf-appeal not only positions a product to attract the consumer, but also gives the impression of higher quality product. Hence colour plays an important role in any plastics manufacturing industry and the choice of pigment affects the key parameters such as colour efficiency, thermal, UV and oxygen stability, migration stability, homogeneous dispersion, and ease of processability, cost and its environmental impacts.

1.1 Dye History

Ever since the beginning of humankind, people have been using colorants for painting and dyeing of their surroundings, their skins and their clothes. Until the middle of the 19th century, all colorants applied were from natural origin. They were mainly aromatic compounds, originated from plants (e.g. the red dye alizarin from madder and indigo), insects (e.g. the scarlet dye kermes from the shield-louse *Kermes vermilio*), fungi or lichens [1]. Synthetic dye manufacturing started in 1856, when the English chemist W.H. Perkin, in an attempt to synthesize quinine, obtained instead a bluish substance with excellent dyeing properties that later became known as aniline purple, Tyrian purple or mauveine. Perkin patented his invention and set up a production line. This concept of research and development was soon to be followed by others and new dyes began to

appear on the market, a process that was strongly stimulated by Kekule's discovery of the molecular structure of benzene in 1865. In the beginning of the 20th century, synthetic dyestuffs had almost completely supplanted natural dyes[2]

1.2 Clay Intercalation and Polymer Nanocomposites

Intercalation of organic compounds into inorganic layered silicates has attracted wide scientific and practical interest. By studying and adjusting the host, guest and intercalation reaction materials can be designed with unique structures, novel chemical and physical phenomena, and enhanced mechanical properties. This has been extensively studied in such fields as intercalation of cationic surfactants into clay minerals, preparation of polymer/clay nanocomposites, adsorption of poorly water soluble organic pollutants, and the control of photo physical and photochemical reactions in restricted geometry. Over the last decade, the utility of inorganic nanoparticles as additives for enhancing polymer performance has been established and has motivated increased research and development in polymer nanocomposites.[3, 4].

1.3 Background and Objectives of the Research Project

Colour has become increasingly important over the years as product appearance and appeal to consumers have become major elements in the packaging and marketing of wide ranges of goods, from cosmetics to cars. There have been developments across the colour spectrum and in the field of special effects. Special effect colorants are being used to generate effects such as fluorescence, phosphorescence, pearlescence and holographics.

There are two types of colorants in use: dyes and pigments. Pigments are insoluble and must be adequately dispersed in the plastic to achieve a uniform colour. This can be a problem in very thin mouldings where particle agglomerates are highly visible. Moreover it contains heavy metals which are harmful to the environmental and hence limits its applications. Dyes are soluble in plastics and give a more transparent finish but it has the tendency to leach out from plastics.

There are many functional considerations when selecting colorants. For example, many plastics are processed at very high temperatures and shear, and products are exposed to heat and light. The colorants must tolerate these conditions to function adequately. Health, safety and environmental issues have also brought changes in the market place as manufacturers strive to meet national and international regulations. Factors to consider in colorant selection include the presence of heavy metal compounds, migration of colorants into food or packaged goods (contamination issues), toxicity in

fire, etc. Hence manufacturers are looking at ways to eliminate cadmium and lead pigments and to improve existing products, for example by coating pigment particles to improve compatibility with plastics and aid dispersion. Therefore researches are experimenting with new chemicals as colorants and developing new methods to protect organic dyes from aggregation effects and photochemical degradation.

Clay minerals are well known for their ability to adsorb organic materials. When organic cationic dyes are adsorbed by the clay minerals it causes the mineral to be coloured. Developing a clay based dye pigment for polymers may play significant role in improving many desirable properties of polymers, including enhanced thermal properties, increased UV and migration stability, improved mechanical, barrier properties and flame-retardant properties. They can be readily dispersed in polymers and they retain complete transparency due to the clay primary particle size. Successful development of clay-dye pigment and its commercialization requires in-depth understanding of the complex mechanism of clay intercalation by organic dye molecules and its dispersion in polymers. The objectives of this research work are:

- Study the clay intercalation by organic dye and develop a process to produce nanoclay-dye pigment with better stability and good performance
- Conduct structural characterization to verify the level of intercalation and stability of clay-dye pigment by using X-Ray diffraction (XRD) and Transmission Electron Microscopy (TEM)

- Investigate the thermal stability of clay dye pigment using Thermo Gravimetric Analysis (TGA) to reveal the effect of dye intercalation into the clay on improving thermal stability of organic dye.
- Compound the clay- pigment with polymer and examine the effect of clay-dye pigment on the thermal and UV stability of pigmented polymer clay nanocomposites.

1.4 Structure of the Research Project

The structure of the research project is shown schematically in Figure 1-1. Two different types of organic dyes (Cationic dye, Solvent dye) and two different commercially available clays were used to study the clay intercalation. Clay dye pigment samples were prepared by using two different methods. The level of intercalation was characterized by using X-ray diffraction method (XRD) and Transmission electron microscope (TEM). The thermal stability of the clay dye pigment was studied using Thermo gravimetric analysis (TGA). Then the clay dye pigment was compounded with polymer and its thermal and UV stability improvement was characterized by using TGA and by UV exposure experiment.

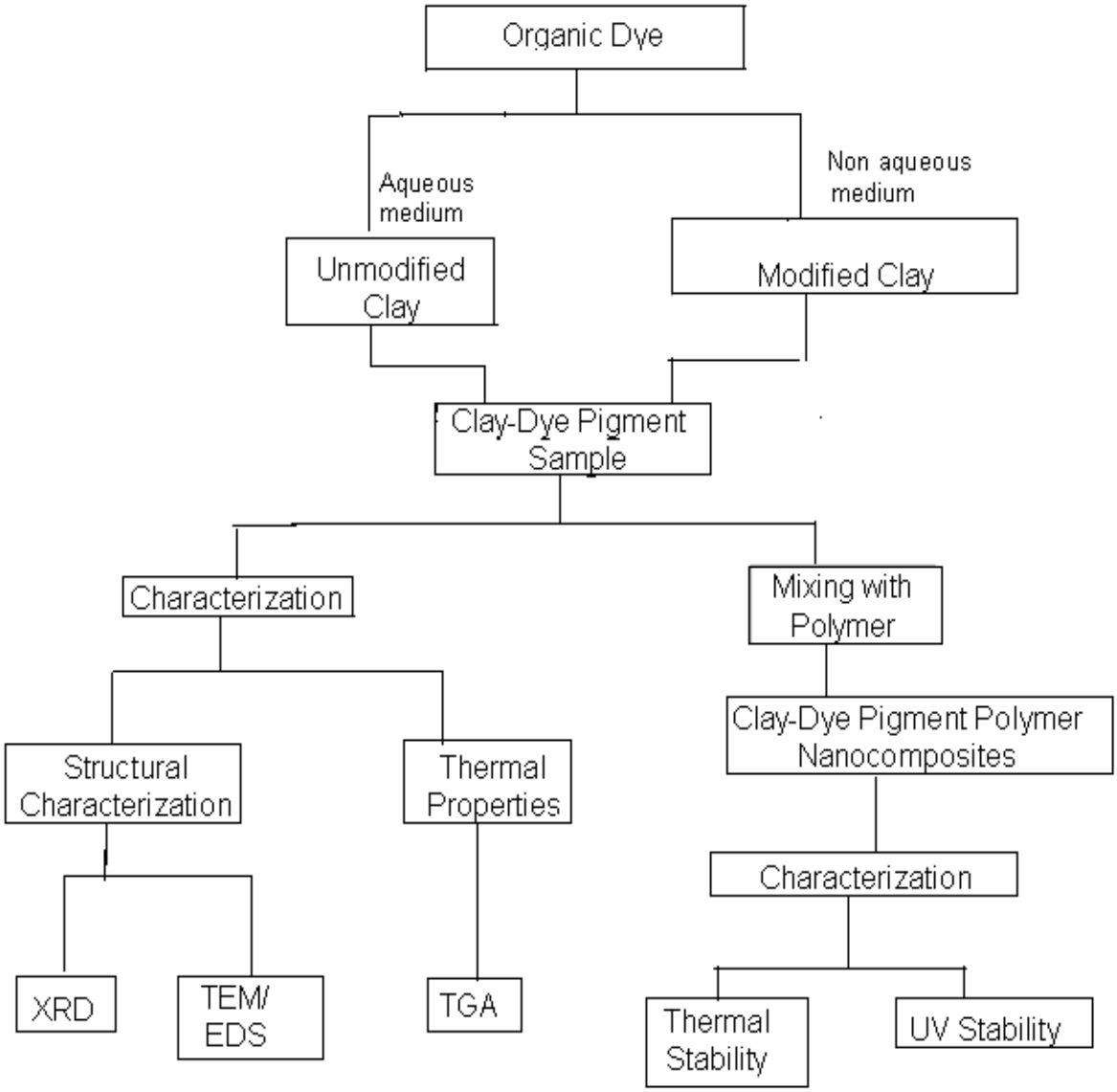

Figure 1-1: Schematic diagram of the research project structure.

CHAPTER 2: Theory and Literature Review

2.1 Introduction

Clays represent one of the traditional materials, whose applications have played an important role throughout human history. Recently, they have gained renewed interest from science and academia as well as industry for their unique and interesting properties, especially their capacity to adsorb not only inorganic but also organic materials, providing novel functional organic/ inorganic hybrid materials. Thus, investigations into their fundamental and molecular structure as well as their various characteristic properties can reveal their great potential in the development of new materials and systems composed of functionalized organic and inorganic compounds [5, 6]. Clay minerals are famous for their ability to adsorb organic compounds. Organic cationic dyes are adsorbed by the smectite minerals cause the mineral to be colored. The colored mineral may be used as a pigment for the color industry. Therefore understanding the mechanism of clay intercalation and dye molecular attachment onto the clay surface is crucial for the successful development of a stable clay-dye complex with combined advantages of organic dye and inorganic clay.

2.2 Dyes and Pigments

Colorants for plastics has great interest in areas such as packaging industry, automotive industry etc. Color increases the attraction of the product or even improves the durability of the product. Organic dyes, which dissolve and distribute on a molecular scale offer a wider range of color possibilities with higher intensities. But most of the common organic dyes have limited stability against UV, oxygen and temperature. Moreover they exhibit the tendency to leach out from polymer, so called bleeding of the dyes. Pigments on the other hand display better stability over organic pigments. They are mainly inorganic in nature with a particle size between 0.01 and 1μm[7]. However they have limited food packaging applications and are less desirable for environmental reasons, because of the presence of heavy metals which may contaminate the environment during recycling. They also show processing difficulties in dispersibility. Therefore, the development of a novel clay-dye pigment that is stable and non toxic would be advantageous for the plastics industry.

2.3 Dye Classification

All aromatic compounds absorb electromagnetic energy but only those that absorb light with wavelengths in the visible range (~350-700 nm) are colored [8]. Dyes contain *chromophores*, delocalized electron systems with conjugated double bonds, and *auxochromes*, electron-withdrawing or electron donating substituents that cause or

intensify the color of the chromophore by altering the overall energy of the electron system. Usual chromophores are -C=C-, -C=N-, -C=O, -N=N-, -NO2 and quinoid rings, usual auxochromes are -NH3, -COOH, -SO3H and -OH.

The vast array of commercial colorants is classified in terms of color, structure and application method in the Color Index (C.I.) which is edited since 1924 (and revised every three months) by the Society of Dyers and Colourists and the American Association of Textile Chemists and Colorists. The Color Index discerns 15 different application classes [8]; two among them are relevant to this research work (clay intercalation study), which are basic dyes and solvent dyes.

2.3.1 Basic Dyes:

Basic dyes are salts of the colored organic basis containing amino and imino groups and also combined with the colorless acid, such as hydrochloric or sulfuric. They are brilliant and most florescent among all synthetic dyes but have poor light and wash fastness. Basic dyes are cationic which has positive electrical charge and are used for anionic fabrics which are negative- charge-bearing, such as wool, silk, nylon, and acrylics where bright dying is the prime consideration. Basic dyes represent ~5% of all dyes listed in the Color Index.

2.3.2 Solvent Dyes:

Solvent dyes (lysochromes) are non-ionic dyes that are used for dyeing substrates in which they can dissolve, e.g. plastics, varnish, ink, waxes and fats. They are not often used for textile-processing but their use is increasing. Most solvent dyes are diazo compounds that underwent some molecular rearrangement. Also triarylmethane, anthraquinone and phthalocyanine solvent dyes are applied in textile and polymer processing industry.

Cationic dyes are well known for the study of clay intercalation (π- interactions between aromatic cations and clay minerals) for many decades. In this course of research attempt has been made to study the clay intercalation with solvent dye in comparison with cationic dye intercalation.

2.4 Structure and properties of Clay Minerals

The layered silicates commonly used in nanocomposites belong to the structural family known as the 2:1 phyllosilicates. Montmorillonite (MMT), hectorite and saponite are the most commonly used layered silicates. The layer structure of montmorillonite is presented in Figure 2-1.

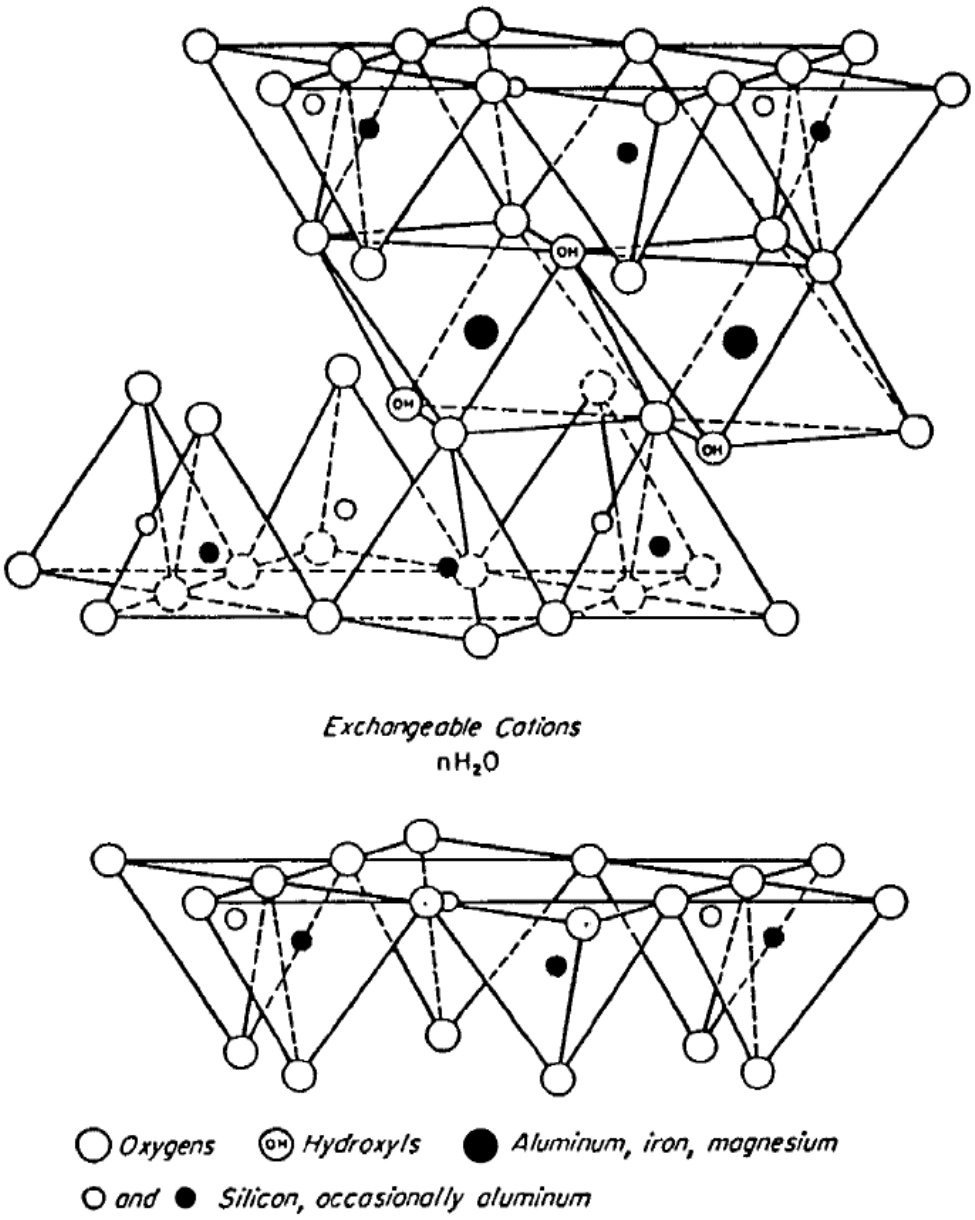

Figure 2-1: Diagramatic sketch of the structure of montmorillonite according to Hofman, Endell and Wilson, Marshall, and Hendricks. Adapted from L Margulies 1993.

In the layer structure, Si^{4+} and Al^{3+} ions occupy the central positions of tetrahedral and octahedral, respectively, arranged in layers in such a way that the Al octahedra form a layer between two layers of Si tetrahedra. Oxygen atoms and OH groups distributed at the corners of the tetrahedra and octahedra compensate for the positive charges maintaining electrical neutrality. Isomorphic substitution, i.e., replacement of Si or A1 by other ions with lower valency (for example, replacing Si^{4+} by Al^{3+} in the tetrahedra, or $Al^{3+}$by Fe^{2+} or Mg^{2+} in the octahedra), results in formation of net negative charges in the clay lattice. In naturally occurring clays these negative charges are neutralized by inorganic cations such as Na^{+}, Ca^{2+}, Mg^{2+}, etc. adsorbed on the surface. Water molecules are also present in the interlayer space. The adsorbed inorganic cations are exchangeable. Stacking of the layers leads to a regular van der Waals gap between the layers called the interlayer or gallery. The layer thickness is around 1 nm, and the lateral dimensions of these layers may vary from 30 nm to several microns or larger, depending on the particular layered silicate. This type of layered silicate is characterized by a moderate surface charge known as the cation exchange capacity (CEC), and generally expressed as meq/100 g. This charge is not locally constant, but varies from layer to layer, and must be considered as an average value over the whole crystal [9]. The large cation exchange capacity of certain clays (e.g., CEC of montmorillonite is about 0.915 meq/g clay) as well as their large specific surface area (e.g., 750 -800 m^2/g in montmorillonite) make them very efficient adsorbents for ionic or polar organic molecules [10].

2.4.1 Cationic Exchange Capacity (CEC) of the Montmorillonite Clay

Montmorillonite (MMT) is the most common phyllosilicates used for the production of Commercial clay polymer nanocomposites (CPNC). The typical chemical formulae of the MMT is given below,

$$[Al_{1.67}Mg_{0.33}(Na_{0.33})]Si_4O_{10}(OH)_2$$

Here $Na_{0.33}$ refers to the exchangeable cation in the interlamellar gallery, of which 0.33 equivalents is typical. Thus CEC of idealized MMT is 0.915 meq/ g clay (one ion per 1.36 nm^2), i.e. the anionic groups are spaced about 1.3 nm apart. The charge is located in the flat surface of the platelet. The specific surface area of MMT is 750-800 m^2/g (theoretical value is 834 m^2/g)[11]. However MMT composition varies across a relatively wide range not only with the geographic location but also with the deposit strata [12]. Thus the CEC ranges from 0.8- 1.2 meq/g.

2.4.2 Adsorption of organic Cation by clay

The nature of the interactions between the clay and the organic molecule is very diverse and ranges from strong columbic bonds (in the case of organic cations, which are adsorbed by cation exchange mechanisms) to much weaker hydrogen bonds or Van der Waals interactions. The adsorption of monovalent organic cations to MMT has been explained by considering two types of complexes: (i) a neutral complex between one monovalent organic cation and a negatively charged surface site, and (ii) a positively charged complex formed by non-coulombic interactions between an organic cation and the neutral complex. Thus organic cations can be adsorbed beyond the CEC of the clay and can cause charge reversal [13].

2.4.3 Primary and Secondary Adsorption of Organic Matter by Clay Minerals.

The sorptive properties of the smectite clays for organic molecules are greatly modified by replacing native exchangeable metallic cations with long chain or quaternary ammonium cations [14]. The replacement of the metallic cations initially present at the exchange site of the clay by organic ammonium cations converts the clay in to an organophilic substrate, which is capable of adsorbing polar and nonpolar molecules. These modified clays are commonly referred to as “organo-clays” and are two different types: those saturated with large quaternary ammonium cations with one or two long

alkyl chains (organophilic clays) and those saturated with small quaternary ammonium aliphatic and aromatic cations (adsorptive clays)[15]

The primary exchange of the metallic cation by the organic ammonium cation is usually carried out in aqueous systems. The driving force for this reaction is the tendency of the hydrophobic organic tails to be drawn away from the aqueous system and the tendency of the small inorganic cations to be fully hydrated in the aqueous system. The longer the aliphatic chains that constitute the cation, the stronger will be the tendency of the cation to be drawn away from the aqueous system. Inside the interlayer space the centers of the positive charges of the cations are located in the areas where maximum neutralization of the negative layer charges are obtained. Van der Waals forces occur between the oxygen planes and alkyl chains. If the ammonium cations are primary, secondary, or tertiary, with the ability of proton donation, the hydrophilic head of the cation is hydrated [15].

Interlayer spaces of unmodified smectites are hydrophilic in nature. Hydrophilicity originates from the electric charge of the layers and the presence of exchangeable cations in the interlayers. After primary adsorption of ammonium cations, there occur three phenomena in the interlayer space of smectite clays which are crucial for the secondary adsorption:

- Large organic cations break the structure of interlayer water and consequently the latter is easily replaced by organic molecules (hydrophobic adsorption)[16-18]

- Van der Waals or hydrophobic interactions may occur between the alkyl chains of the organic ammonium cations located inside the interlayer space and the adsorbed nonpolar molecules(organophilic adsorption) [19]

- The organic cations in the interlayers may serve as pillars, leading to a great space between the tetrahedral octahedral tetrahedral layers [20]

It is assumed that the secondary adsorption is accompanied by van der Waals interactions between the adsorbed organic molecules and the aliphatic chains of the exchangeable cation. Therefore the secondary adsorption of nonpolar molecules or of molecules of lower polarity by long chain ammonium montmorillonite complex increases with (i) increasing amount of primary adsorbed organic ions and (ii) increasing basal spacing.

Miscibility of interlamellar organic phase of the modified clay with the intercalation medium also influences the secondary adsorption. Jordan[21] studied Organophilicity of montmorillonite complexes with quaternary ammonium cations having two long aliphatic chains. These complexes readily swell in hydro carbon liquids

without the addition of any polar molecule. Dispersion in toluene takes place much more readily and completely with the quaternary double-chain ammonium complexes than with the primary single chain ammonium complexes. Jordan attributed the different behavior in the secondary adsorption to the complete coating of the former particles, which are more compatible with the hydrocarbons.

2.4.4 The effect of type of organic Cation in the Adsorption of Clay

The most common cation exchange method uses onium salt, quaternary ammonium being the most common. The reason for using the quaternary ammonium salts originates from consideration of the binding strength to MMT. The strength increases with the number of substituents in the ammonium cation [22].

$$NH_4^+ < RNH_3^+ < R_2NH_2^+ < R_3NH^+ < R_4N^+.$$

2.4.5 Clay Intercalation Study by Organic Cationic Dye

Attempts have been made to intercalate various dye molecules, in particular organic dyes inside layered inorganic lamella, especially anionic clays for various purposes and applications. Bergmann et al. [23] reported the first study on the metachromatic behavior of a cationic dye (methylene blue) on clay (Wyoming montmorillonite). Since then, interactions between organic molecules and clay particles in aqueous suspension have been extensively studied [24]

Sethuraman et al [25] carried out a comparative study on the kinetics of cation exchange reaction of Methylene blue (MB) with nonexpanding (kaolineite) and expanding clay (montmorillonite). They reported the total adsorption as small and the reaction rate high for nonexpanding clay because adsorption occurs only on surface; where as for expanding clay rapid adsorption takes place on the external surface at the beginning and it followed by a slow interlayer cation exchange. They concluded MB adsorption is irreversible until CEC is satisfied; adsorption can exceed the exchange capacity of the clay, but the amount excess in this level is readily desorbed.

Ghosal et al [26] showed that crystal violet can be adsorbed by montmorillonite in amounts greater than the exchange capacity. Rytwo et al[27] also showed that in addition to methylene blue (MB) and crystal violet (CV), thiflavin T (TFT) is also adsorbed in excess of the CEC on montmorillonite, with an exchange capacity of 80 mmol per 100 g

clay. In particular amounts of 140 and 160 mmol CV were adsorbed from solutions containing total amounts of 160 and 350 mmol CV per 100 g clay. Maximum adsorptions of TFT and MB were 140 and 120 mmol per 100 g clay, respectably.

The effect of ionic strength on the adsorptions of the monovalent dyes and divalent aromatic cations was investigated by Narine et al. [28]. They concluded that the dyes were irreversibly bound to the clay matrix and attributed metachromasy to the aggregation of the dyes on the clay surface and adsorption capacity increased with ionic strength of the solution.

Landau and coworkers [29] investigated the adsorption of cationic Rhodamine dye by Montmorillonite in solid state (mechanochemical) and aqueous suspension. Their investigation with XRD and DTA-TG studies suggested that the mechanochemical adsorption of organic cations take place on the external surface of the clay whereas in suspensions the adsorption takes place into the interlayer space.

2.4.6 The effect of loading of Cationic organic dye in Adsorption

Smectite clay minerals exhibit a high affinity for metachromic cationic dyes. The adsorption takes place largely by the mechanism of cation exchange; exchangeable metallic cations are released from the clay into the aqueous phase and organic cationic dye molecules are replaced. This cation exchange reaction is not reversible; exchangeable metallic cations do not replace the adsorbed dye. The adsorption cationic dye (Dye^{+}) by Na- montmorillonite (NaMMT) can be described by the following equation.

$$Dye^{+}_{(aq)} + NaMMT_{(s)} \qquad Na^{+}_{(aq)} + Dye\text{-}NaMMT_{(s)}$$

The type of different dye-clay associations were recently described by Yariv[15]. From spectroscopic investigation of adsorption of dyes by Laponite[30-32] it was proposed that three different types of clay-dye associations can take place. Direct π interactions between the O-plane of the clay and the aromatic rings of the dye, which may occur together with removal of water interlayer space. This type of association illustrated in Figure 2-2 as B1 & B2 type. At higher aggregation of the cationic dyes, clay flocculates and dye aggregation occurs in the interparticle space of the flocs (type C). The third type occurs due to higher dye aggregates on the external surface of peptized smectite layers or small tactoids (associations A1 & A2)

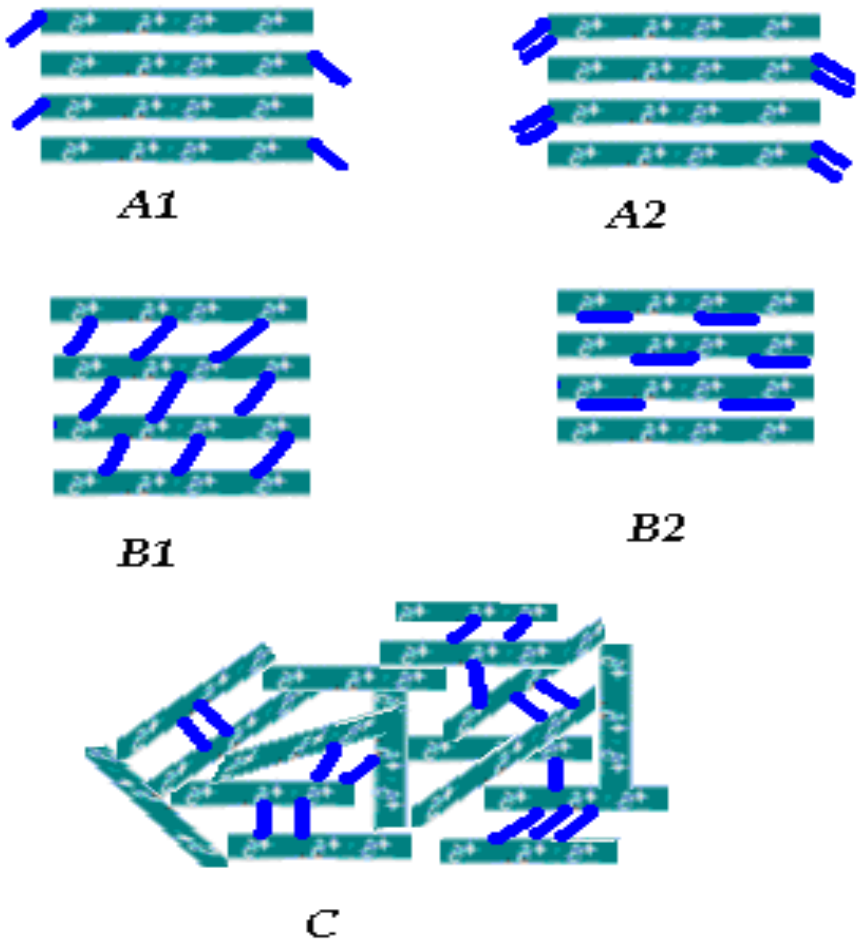

Figure 2-2 Schematic illustrations of different types of dye-clay associations: A1&A2- adsorbed dye cations located on the external surface. B1&B2- adsorbed dye cations located in the interlayer space. C- adsorbed dye cations located inside the interparticle space (reproduced from [15]).

Landau et al [29] reported on the effect of Rhodamine 6G (R6G) loading on adsorption by montmorillonite in aqueous suspension. From their thermal analysis they observed that the extent of interactions between the dye and the clay first increases with loading but decreases with excess dye. They reported when the amount of dye is below 35mmol R6G per 100 g clay the dye is located in the interlayer space and is able to form π bonds with the O-plane of the clay. With higher amount of dye the clay flocculates and the added dye locates in the interparticle space with no π interactions with O-plane as described by Yariv.

Pospisil et al [9] investigated the intercalation process and structure of montmorillonite intercalated with Rhodamine B cations using molecular modeling, X-ray powder diffraction and IR spectroscopy. From the X-ray diffraction and modeling they observed two structural phases for low dye concentration (phase 18 Å with bilayer arrangement of guests and phase 23 Å with the monolayer arrangement of guests). For high concentration (above 0.0037 mol/dm^{-3}) only one phase observed at ~ 18 Å. They reported it is possible for the coexistence of monomeric and dimeric arrangement for both phases. Furthermore they observed three types of dimmer in their molecular mechanics and dynamics simulations study: H-dimer (head-to-head, more stable), head- to-tail sandwich and head-to-tail J-dimer

2.4.7 Applications of Cationic Dye- Clay Interactions

In early work sorption of Methylene blue (MB) by clay minerals is used as a rapid method for determining cation exchange capacity, and clay content. Nevins et al. [33] compared CEC of different clay minerals obtained from MB titration with those obtained by ammonium acetate analysis and found close correlation between the two. Hills and Pettifer [34]studied the adsorption of MB in various rock types and showed a relationship between this adsorption and the smectite content.

R. Fahn et al [35] investigated the reactions of dye molecules with acid-activated montmorillonite to form light- resistant stable clay-dye complexes. They examined the amount of dye uptake as a function of time and the physical and chemical changes occurring in the acid activated montmorillonite as a result of dye adsorption. They observed good resistance to fading of montmorillonite dye complexes in light, which was a result of protected position of the dye molecule between the clay layers (due to intercalation process)

Margulies et al studied the photostabilization of pesticides by chromophores intercalated clays and discussed the mechanism by which photostabilization enhanced by chromophore modified clay. They describe the activity of the photolabile insecticide bioresmethrin (BR) coadsorbed onto MMT with a cationic dye methyl green (MG). In this case excited BR is the energy donor and MG is the acceptor. The energy transfer

process occurs when the distance between donor and acceptor is short and their orientation involves a specifically intimate alignment such that the dye can accept the radiation of the donor.

K. Ito et al., [36] studied Clay-fluoran dye intercalation to evaluate their performance as thermal recording media. They reported that clay previously incorporated with a bulky alkyl ammonium ion promoted the intercalation of the fluoran cationic dye and this intercalation procedure exhibited considerable resistance to color disappearance of the image by humidity in practical thermal printing method.

Batenburg et al. [7] studied the possibility of developing stable clay-dye complex by intercalating water soluble Methylene blue inside the montmorillonite clay for coating applications. They reported that the thermal stability of MB-clay complex increases of at least 100K from that of MB dye.

Fan Q. and coworkers[37] studied the feasibility of forming polypropylene (PP) material fibers infused with nano clay particles that creates dye sites to facilitate the dyeing of PP fibers. They reported that they have observed strong indication for dye sites formation in the PP matrix by infusion of the nanoclay and for better mechanical properties and manufacturing feasibility of PP nanocomposites they recommended that the level of clay addition to PP is about 2 % and dying it at 1 % of dye concentration

Dudkina et al [38] reported successful development of nanocomposites by intercalating nonlinear optical chromophores (with different chemical structure) into a host lattice of MMT and mixing it with maleic anhydride-grafted polypropylene. They concluded that intercalated dibenzilidene acetone type chromophores exist in the clay galleries in an aggregated form (probably as J-aggregates) and this feature strongly affects optical and nonlinear optical properties of nanocomposites. Further more they reported that the thermal stability of the chromophores significantly improved due to the intercalation into the MMT layer and improved color properties.

2.5 X-Ray diffraction characterization of Clay intercalation

The anisotropic nature of intercalated guests molecules has been observed since the beginning of clay chemistry. The adsorption property in clays permits the mutual interaction of the incorporated guests which form self-assembling molecular aggregates due to the two-dimensional layer surface, which is in contrast to silica colloidal surfaces [39]. The self-assembly interaction is variable depending on the structure of the clay minerals and guest organic compounds, the kind and amount of exchangeable metallic ions, and the amount of intercalated water in the interlayers. It is possible to obtain detailed information on the higher dimensional structure of the guest molecules by various spectroscopic analyses methods such as X-ray diffraction, neutron scattering or high resolution electron microscopy, nuclear magnetic resonance (NMR), electron spin resonance (ESR), as well as polarized spectroscopies which are able to clarify the orientations of the guests within the layers [40-44]. Among all of them X-ray diffraction method is most commonly used to study the extent of intercalation.

The instrument that measures X-ray scattering are divided into two types; more common wide-angle X-ray scattering (WAXS) and newer small angle X-ray scattering (SAXS) instruments. It is common to consider the scattering angle $2\theta = 2°$ as a boundary between these two; however there are newer WAXS instruments available to provide reliable scattering profile down to $2\theta = 1°$. WAXS offers a convenient method to determine the interlayer spacing of the silicate layers in the original layered silicates and

in the intercalated organ-clay complex (within 1-4 nm). The interlayer spacing, (d_{00}) is commonly determined from the XRD spectrum as arbitrary intensity versus 2θ. The spacing is then calculated from Braggs Law;

$$n\lambda = 2d \sin\theta \qquad (2.1)$$

Where, n is the order of diffraction, λ is the wave length, θ is the angle of diffraction and d- inter planar distance

Bragg's Law is derived by considering that the following two geometrical factors are satisfied [45];

- The incident beam is normal to the reflecting plane, and the diffracted beam is always coplanar
- The angle between the diffracted beam and the transmitted beam is always 2θ

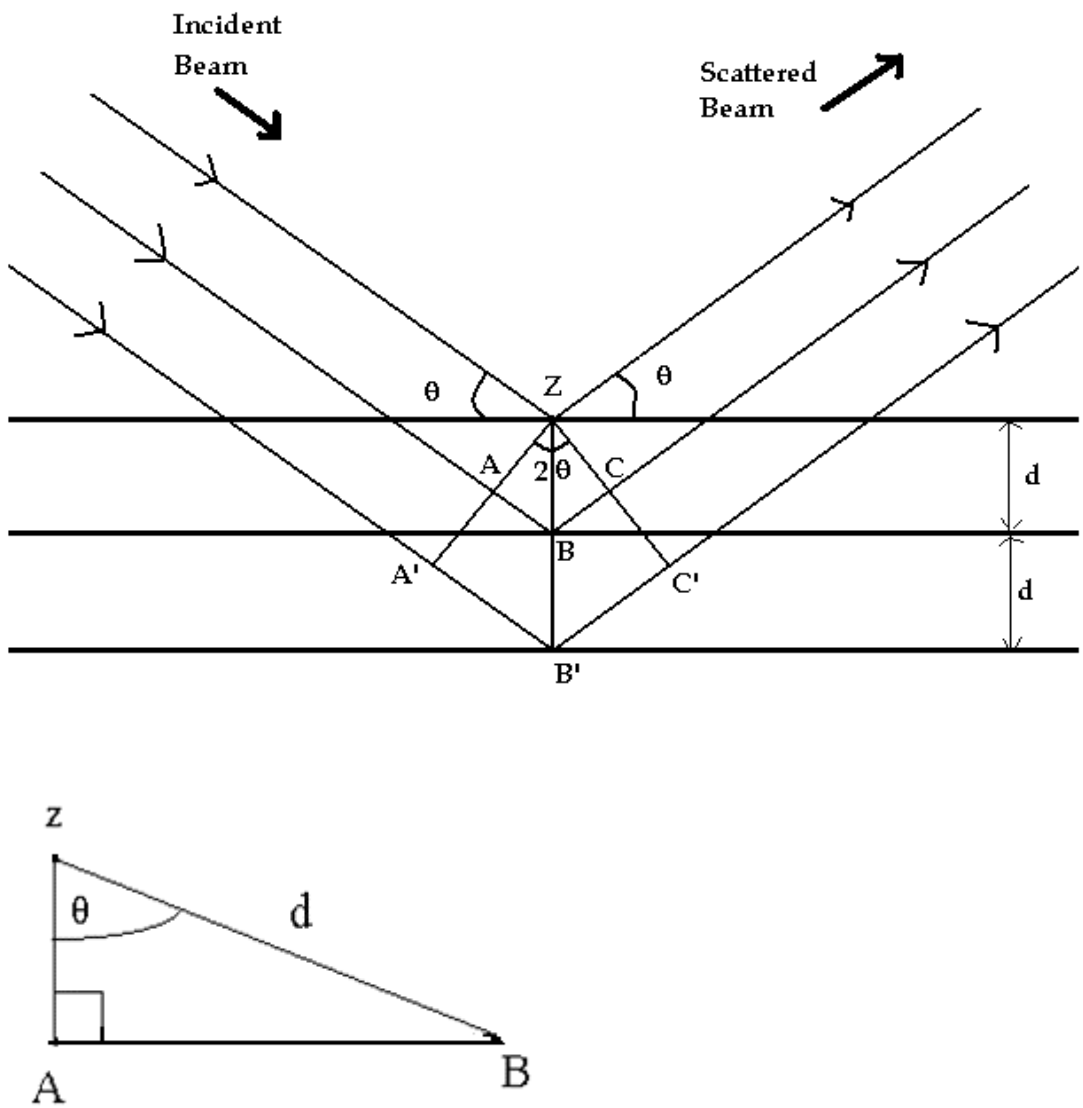

Figure 2-3: Schematic representation of X-ray diffraction

The rays of the incident beam are always in phase and parallel up to the point at which the top beam strikes the top layer at atom z (Figure 2-3). The second beam continues to the next layer where it is scattered by atom B. The second beam must travel the extra distance AB + BC if the two beams are to continue traveling adjacent and parallel. This

extra distance must be an integral (n) multiple of the wavelength (λ) for the phases of the two beams to be the same:

$$n\lambda = AB + BC \qquad (2.2).$$

As d the hypotenuse of the right triangle ABZ, using trigonometry d and θ can be related to the distance (AB + BC). The distance AB is opposite to angle θ so,

$$AB = d \sin\theta \qquad (2.3)$$

Where AB = BC hence eq. (2.2) becomes,

$$n\lambda = 2AB \qquad (2.4)$$

Substituting eq. (2.3) in eq. (2.4) Bragg's Law is derived as

$$n\lambda = 2\ d \sin\theta \qquad (2.1)$$

The XRD spectrum obtained as the scattering intensity versus 2θ provides distinct peaks. The shape and their position provide information on the structure of the diffracting species, which can be used as fingerprint (see Figure 2-4) to study the organoclay complexes. The scattering maximum of Na^+MMT (d_{00} of unmodified clay) is usually found in the range of 0.95-1.4 nm (9.5-14 Å), depending on both CEC and water content

of the sample. When Na^+ ions were replaced by organic cationic ion in the clay gallery, depending on the size and shape of the organic molecule and its arrangement type (Figure 2-2) inside the clay layer, the reflections broadened and shifted to lower angle. According to Bragg's law; the d-spacing is inversely proportional to the scattering angle. Therefore the shift of the peaks to lower scattering angles corresponds to larger d-spacing and hence larger distances between the silicate layers will be found [38].

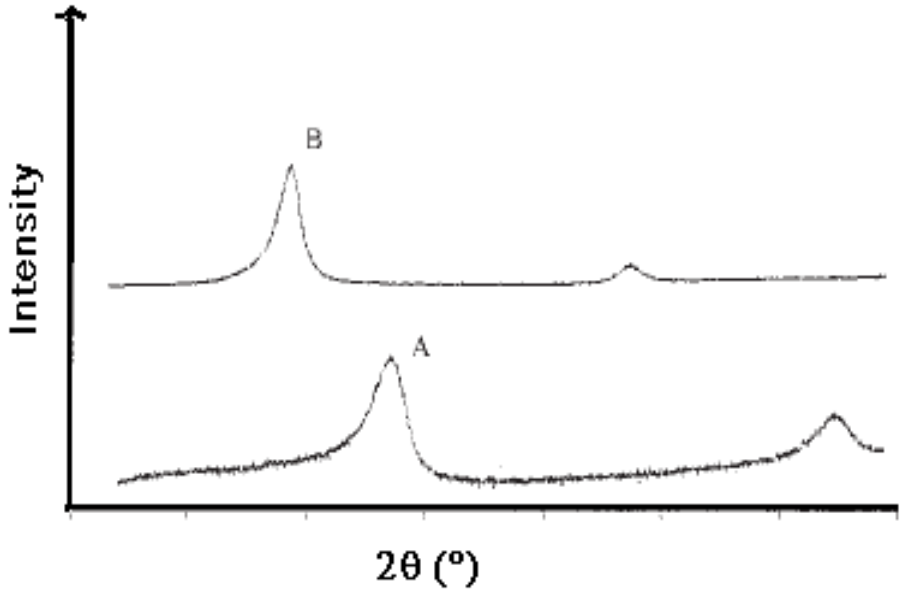

Figure 2-4: WAXS patterns of :(A) Unmodified clay, (B) Organo clay (After intercalation organic molecule)

2.6 Transmission Electron Microscopy (TEM)

Electron microscopy techniques have been the primary technique used to characterize nano particle size and shape [46, 47]. TEM uses electrons to illuminate a thin specimen. The electrons are high- energy matter that has wavelengths much smaller than that of light and this allows for the resolution of smaller objects. Since the electrons pass through the specimen, this technique gives information on the internal structure of a specimen [48]. Since the TEM has a better resolution of 0.2 nm, it is useful to qualitatively analyze the nano layer structure of the clay minerals through direct visualization. However TEM is time intensive and only gives qualitative information on the sample.

2.7 Energy Dispersive Spectroscopy (EDS)

Energy Dispersive Spectroscopy (EDS) is a standard procedure for identifying and quantifying elemental composition of sample areas as small as a few cubic micrometers. The technique utilizes x-rays that are emitted from the sample during bombardment by the electron beam to characterize the elemental composition of the analyzed volume. When the sample is bombarded by the electron beam (As shown in Figure 2-5) of the transmission electron microscopy (TEM), electrons are ejected from the atoms comprising the sample's surface. A resulting electron vacancy is filled by an

electron from a higher shell, and an x-ray is emitted to balance the energy difference between the two electrons [48]

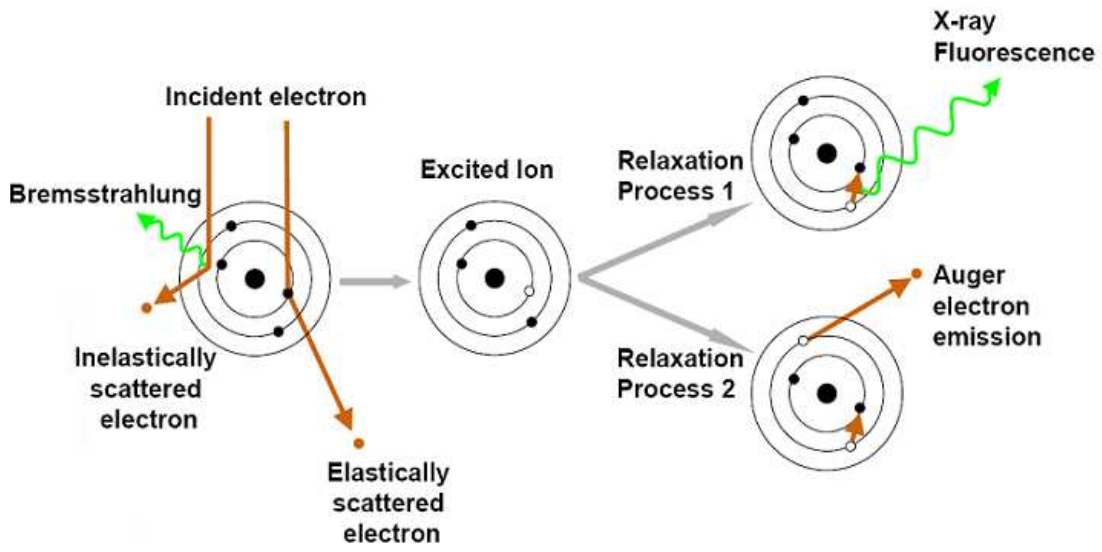

Figure 2-5: Scheme of Electron excitation of inner shell process

The EDS x-ray detector measures the number of emitted x-rays versus their energy. The energy of the x-ray is characteristic of the element from which the x-ray was emitted. A spectrum of the energy versus relative counts of the detected x-rays is obtained and evaluated for qualitative and quantitative determinations of the elements present in the sampled volume. Figure 2-6 shows a typical EDS spectrum of a Silica glass particle.

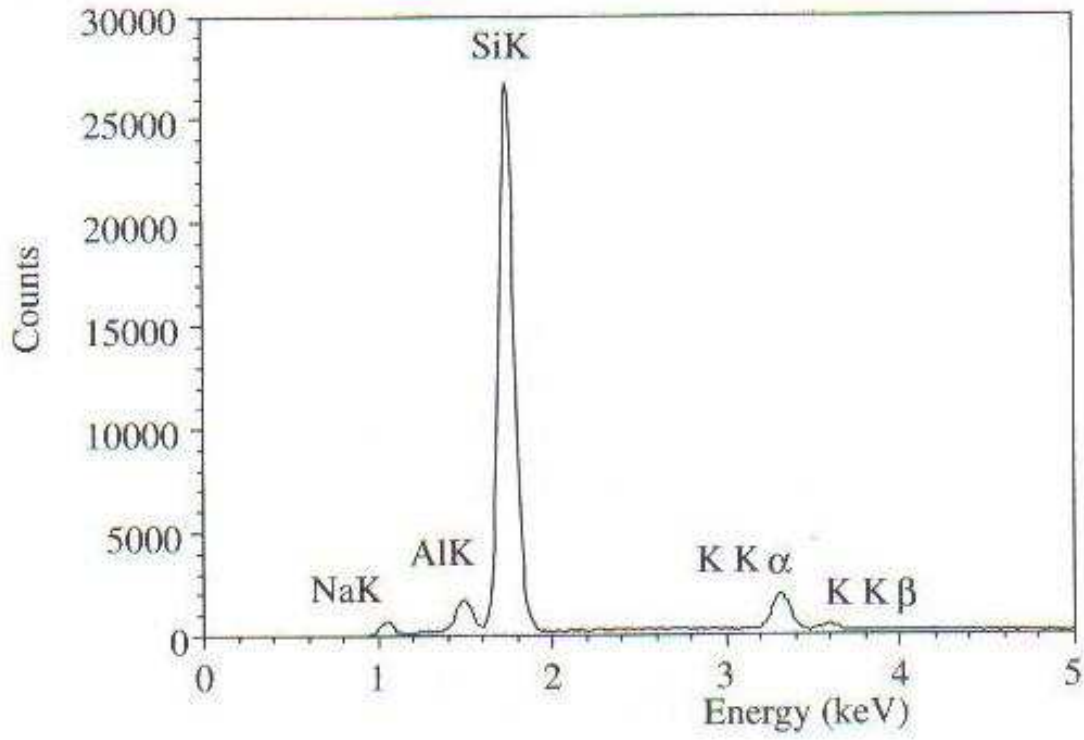

Figure 2-6: Typical EDS survey spectrum of Silica glass particle. Adopted from [49]

2.8 Thermo Analytical study of Organo-Clay Complex

In recent organo-clay study, three thermo analytical techniques predominate; which are thermogravimetric analysis (TGA), derivative thermogravimetry (DTG), and differential thermal analysis (DTA). Thermal analysis of clay minerals records the reactions taking place in the samples investigated on heating, such as dehydration, dehydroxylation and phase transition expressed by endothermic and exothermic DTA peaks and appropriate TG and DTG effects. In this study thermogravimetric analysis (TGA) along with derivative thermogravimetry (DTG) was employed to analyze thermal stability of clay dye pigment and its nanocomposites with polymers.

2.8.1 Thermo Gravimetric Analysis of Organo-Clay Complex

Organic compounds included in organo clay complexes can influence their thermal behavior to a much higher degree than clay components [15]. These differences in thermal behavior of organic and clay components of organo-clay complexes in comparison with that of individual organic compounds and clay minerals may serve as the basis for drawing conclusions regarding the character of the relation of organic matter and clay mineral in the sample investigated.

Thermal analysis may also be used for the differentiation between a simple mixture of clay mineral with an organic compound and an organo-clay complex i.e. for the establishment of some possible interaction between clay and organic matter. The procedure is based on the comparison of thermal curves obtained for each of these materials separately, with those obtained for them combined as a simple mixture. If the later curve differs from the sum of the thermal curves of the individual components, that evidences of some interaction during preparation[29].

Thermal studies of organo-clay complexes may also be applied to thermal characterization of adsorbed organic matter, for the determination of the nature of the associations of organic compounds with a clay mineral, with its exchangeable cations, adsorbed and interlayer water for detailed characterization of these complexes and for tracing the process occurring during contact between organic matter and clay. Clay minerals usually show two or three main stages of weight loss on TG curve. The low temperature weight loss occurs due to the evolution of adsorbed and interlayer water (between 250- 300 °C), and 2:1 minerals (smectite) show weight loss above 500 °C (between 500-800 °C) due to dehydroxylation effect [50-52]. The main reactions of organic matter take place at 200-500 °C [15]. The association of organic compounds with clay minerals influences the shape of thermal curves of the clay mineral in both low and high temperature weight losses. Typical TG-DTG curve of organo-clay (smectite) can be seen in Figure 2-7.

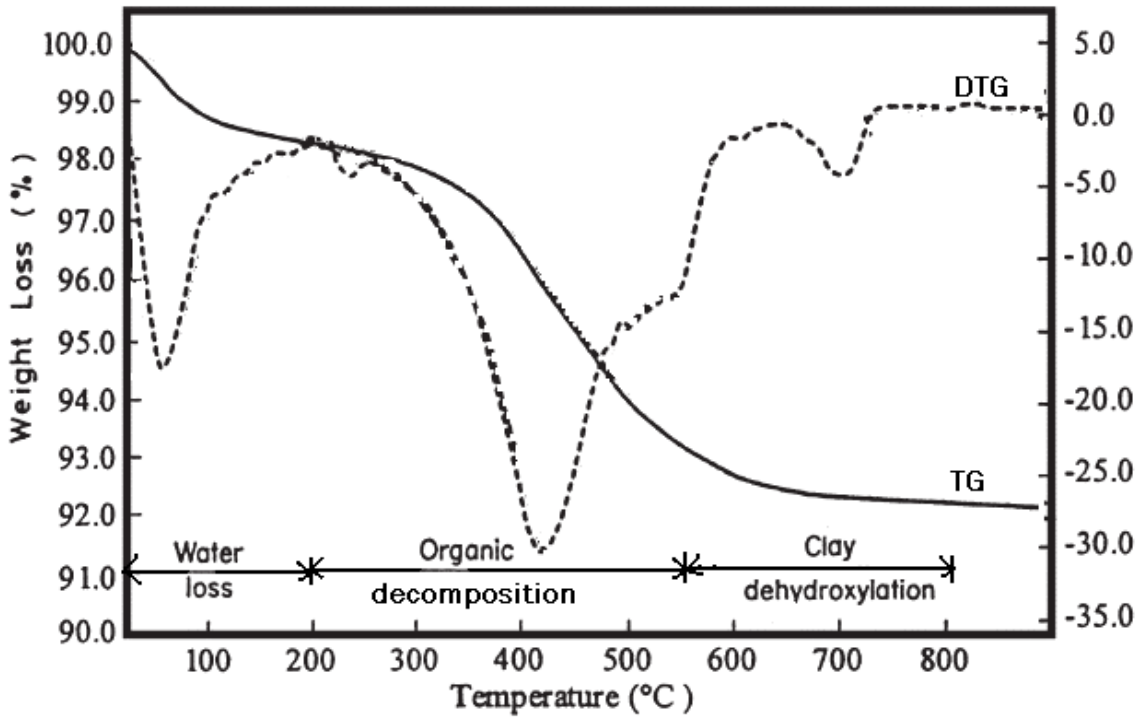

Figure 2-7: TG-DTG curve of organo-clay (smectite) complex.

Thermal behavior of organic matter that has entered into complexes with clay minerals differs from that shown by individual organic compounds, due to interaction with clay mineral. There may be a lack of some peaks or the peaks may occur at shifted temperatures and show different intensities than with the neat organic matter. Nevertheless, in many cases the thermal curves obtained cannot readily be interpreted in terms of reaction mechanisms or reaction products, and they can only be treated as "fingerprints" of the samples [53, 54].

2.8.2 Thermal Stability of Clay Dye Pigment- Polymer Nanocomposites

The stability of the clay-intercalent complex is essential to succeed melt exfoliation process. Experience shows that the lack of thermal stability complicates the production and the forming process of clay polymer nanocomposites (CPNC) not only for engineering and specialty resin (which require high processing temperature) but also for CPNC based on Polyolefins or Polystyrene (due to lack of polar group)[11].

Several researches reported that MMT intercalated with a long chain aliphatic quaternary ammonium cation is unstable at temperatures above 180 or 200 °C. Gilman et al.[55] reported that during extraction compounding of PS with dimethyl dioctadecyl ammonium chloride (2M2ODA) modified MMT at 185 °C the intercalent was thermally degraded. The authors pointed out two factors causing this unwanted effect; increase temperature and the presence of air and Hofmann elimination mechanism (quaternary ammonium react with oxygen to give peroxy radicals, which in turn attack the PS macromolecules)take place in the degradation. Tanoue et al [56] also reported similar observations for CPNC prepared by melt compounding PS with Cloisite 10A organo clay (MMT-2MBHTA).

During the last decades or so, the search for more thermally stable organoclays has intensified. The research on inorganic intercalants was a significant step in this direction, but owing to the complexity and associated costs so far this approach has not

gained industrial approval. Observations that readily interact with complex, aromatic salts resulted in repeated attempts to incorporate these, more thermally stable molecules as intercalants. Thus replacing ammonium salt by that of a cyclic tertiary amidine leads to greater thermal stability and more efficient intercalation of clay[57]. Since the complex, aromatic molecules are often either functional or coloured (conjugated double bonds), Eastman and TNO patented the use of dyes as intercalants [58, 59]

2.8.3 Role of Clay in Thermal stability of Clay Polymer Nanocomposites

It is known that the addition of very small amounts clay (≤ 5 wt %) brings about a large enhancement to the thermal and fire properties of polymers [60] [61]. Polystyrene nanocomposites gained interest in this research area, particularly since the reduction in the peak heat release rate is very large, typically about 60 % reduction was observed for well dispersed clays in polystyrene [62, 63]. There have been two mechanisms suggested for the peak heat release rate reduction, barrier and paramagnetic radical trapping. The clay layers in the nanocomposites act as a barrier, which can inhibit the heat and mass transfer of degrading polymer to the vapor phase and it will also serve to insulate the underlying polymer from the radiation and both of these would serve to enhance the thermal stability of the polymer [55]. The second pathway for thermal degradation reduction of polystyrene, radical trapping appears to only be important when the clay loading is quite low and the amount is insufficient to produce a good barrier. At the

normal clay loading of 3-5 %, the barrier formation is the accepted mechanism for the reduction of thermal degradation [64]. Jang et al [65] studied the thermal stability of polystyrene nanocomposites and they proposed that radical recombination reaction, which occur because of the presence of the clay cause the retention of the degradation products for longer period of time thus spreading out the degradation in time and reduce PS degradation.

2.9 Ultra Violet (UV) stabilization of Pigmented Polymer Nanocomposites

The thermal and UV stability of the dye are considered as an important property when it is used as a colorant for plastics. Plastics and organic coatings used outdoors are exposed to ultraviolet (UV) radiation in the range of 295 to 400 nm which is often the primary cause of degradation and weathering [66]. UV absorbers are commonly used in these applications to prevent UV radiation from reaching the bulk of the polymer or from penetrating the coating and reaching a UV-sensitive substrate. According to Hirt ea al. [67] The protective absorbers are not everlasting; they do photo decompose, but at a much slower rate than the materials which they are designed to protect. The photodecomposition was found to be dependent on a number of factors including the substrate in which the absorber is dispersed and the wavelength of irradiation.

2.9.1 Role of Clay in Photostabilization of Organo- Clay complex

Margulies et al [13] studied the use of cationic chromophores modified clay on photo stabilization of clay-organo (pesticides) complex. They proposed a mechanism for the photo stabilization. Figure 2-8 shows the schematic representation of a clay-organic complex and Figure 2-9 shows deactivation pathways for a molecule D which has been raised to an excited electronic state upon absorption of a photon. The actual pathway by which the excited molecule, D*, will release its excess of energy and return to the ground state will depend on the relative values of the rate constants $\mathbf{k_i}$ for all the different competing processes. In the case of a photo labile molecule, $\mathbf{k_1}$ is larger than $\mathbf{k_2}$ and $\mathbf{k_3}$ and the molecule undergoes a photochemical reaction before the energy is released as heat (internal conversion) or as light (luminescence). But in the presence of chromophores **A,** the energy can be transferred from **D*** to **A,** ending with **D** in its ground state and **A** in an excited state:

$$\mathbf{D^* + A \quad D + A^*}$$

It has been well established that the efficiency of an energy transfer process depends on the matching of energy levels of **D** and **A** chromophores, on the distance between them, and on their relative orientations

If the rate constant k_4 of this process is much larger than that of the photochemical reaction **(k_1),** the occurrence of the latter will be significantly reduced and **D** will be photo stabilized. Energy transfer between two different organic chromophores adsorbed on clay surfaces has been reported [68-70]**.** It is believed that stabilization occurs due to specific intermolecular interactions of cationic chromophores at the clay surface. The role of the clay is to keep the neutral organic molecule acting as energy donor (**D**) and the chromophores as an energy acceptor (**A**) at optimal distances of separation and orientation for efficient energy transfer.

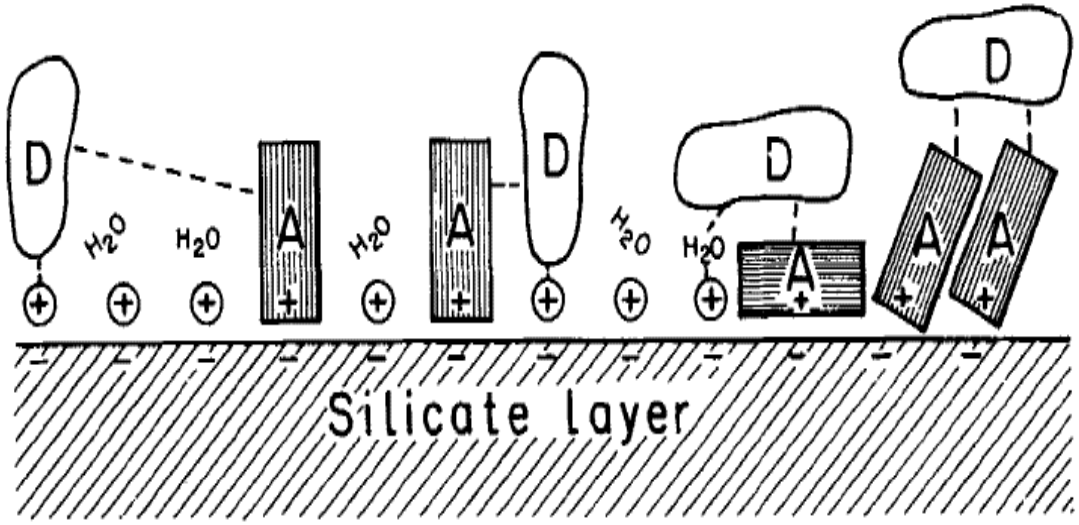

Figure 2-8: Schematic representation of adsorption of cationic chromophores (A) and neutral organic molecules (D) on the surface of a clay. (The organic cation A is shown to displace the inorganic cations). Adopted from [13]

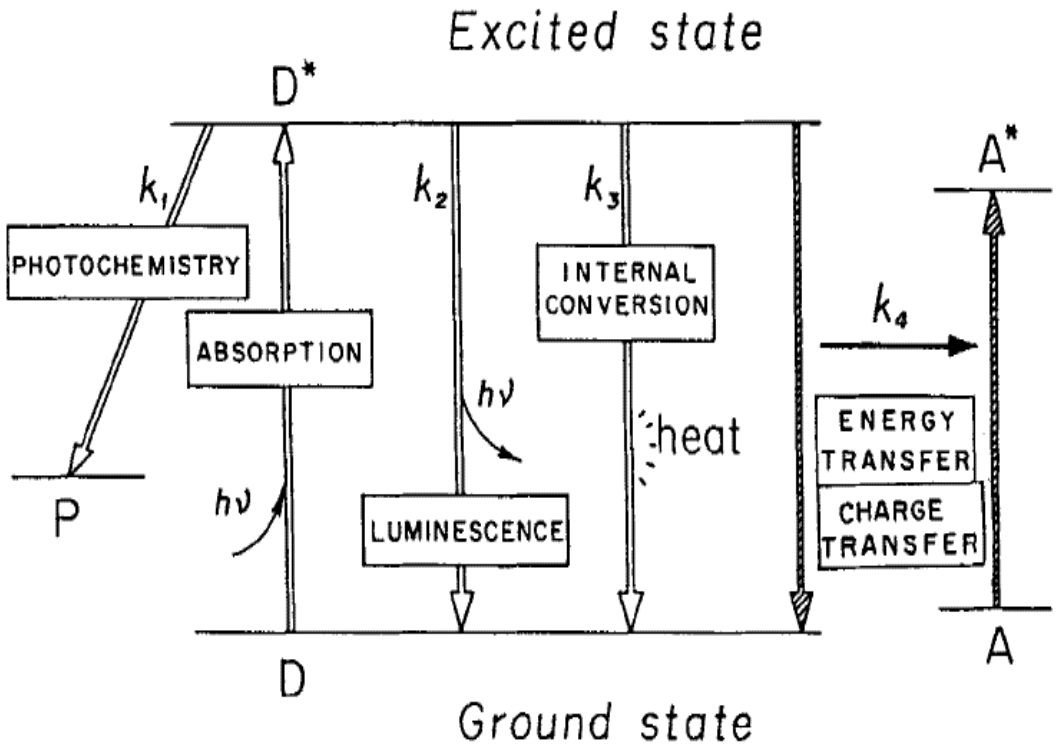

Figure 2-9: Schematic representation of the different deactivation pathways of a molecule D following excitation from the ground state to an electronically excited state (indicated by *) by absorption of energy (photon). Adopted from [13]

Same principles may apply for the enhanced UV stability of pigmented clay-polymer nanocomposites. The energy of the UV-radiation transmitted immediately on to the surface of the clay sheet via π interaction of cationic dye, which thus prevents the high energy load to the organic dye molecules and the energy absorbed by polymer molecule may also transferred be to dye molecule due to intermolecular interactions between organic dye and polymer and then transmitted to the clay layer.

CHAPTER 3: Materials, Experimental equipment and Procedures

Introduction

This chapter describes the raw material acquisition, sample preparation of clay-dye pigment & clay-dye pigmented polymer nanocomposites and experimental equipment and procedures that were used to prepare samples and to characterize the samples throughout the study.

3.1 Materials

The materials used in the preparation of clay-dye pigment were two different types of commercially available clays (Unmodified & Modified clay), hydrophilic organic dye, and an organophilic organic dye. Water was used as an intercalation medium for hydrophilic dye and organic solvent (Dichloromethane [DCM]) was used as an intercalation medium for organophilic dye. Polystyrene was used to prepare clay-dye pigmented polymer nanocomposite samples.

3.1.1 Clay

For this study unmodified Sodium-montmorillonite (NaMMT) clay received from UNIMIN Australia Limited and modified Montmorillonite clay (modified with quaternary ammonium salt) under the trade name of Cloisite® 15A which was obtained from Southern Clay Products were used. The properties of both clays are summarized in Table 3-1 below.

Table 3-1: Properties of clay used in this project. Information was obtained from Supplier's physical property data bulletin.

Clay Trade Name	Interlayer Cation	Cation exchange Capacity (CEC)/ Modifier Concentration	d-spacing (Å)
Na Bentonite	Na^+	97meq/100g	12.61
Cloisite® 15A	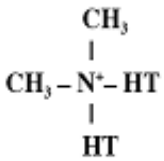	125 meq/100g	31.5

Where HT is Hydrogenated Tallow (~65% C18; ~30% C16; ~5% C14)

3.1.2 Organic Dyes

Organic dyes were chosen based on their ionic nature. Selection criterion was to have dye with cationic ion in order to allow ion exchange reaction between the clay cation (sodium ion or quaternary ammonium ion) that is present between the interlayer of the clay.

3.1.2.1 Hydrophilic dye

Rhodamine B red obtained from Ascher Color Services, Melbourne; was used to prepare clay-dye pigment in aqueous medium. The molecular structure of Rhodamine dye is (Rhod B) depicted below (Figure 3-1) and the properties are shown in Table 3-2;

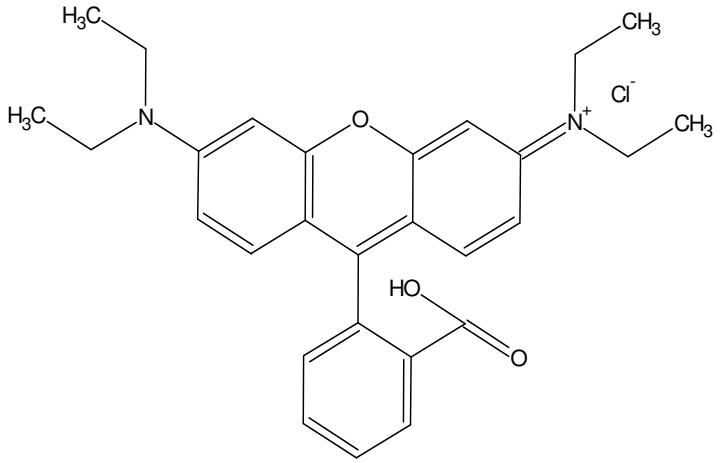

Figure 3-1: Molecular structure of Rhodamine B (Rhod B)

3.1.2.2 Organophilic Dye

Solvent dye was obtained from Allied color & Additives Pty Ltd. and modified to prepare samples in nonaqueous medium. Molecular structure of Solvent dye (SD) is shown in Figure 3-2. Modification of Solvent dye (form organophilic to hydrophilic form) was carried out within the Rheology and Materials Processing centre, RMIT University. Due to confidentiality agreement the molecular structure of modified Solvent dye and its details are unavailable for publication in this thesis.

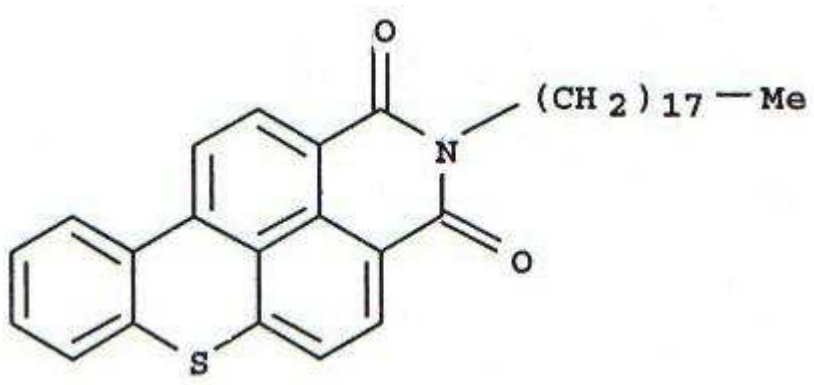

Figure 3-2: Molecular structure of Solvent Dye (SD)

Table 3-2: Specification of Organic Dyes

Name of Dye	Molecular Formula	M/W (AMU)	Color Index	CAS No
Rhodamine B red	$C_{28}H_{31}ClN_2O_3$	478.5	45170	81-88-9
Solvent Dye	$C_{36}H_{45}NO_2S$	555.81	-	-

3.1.3 Organic solvent

Organic solvent used as nonaqueous medium were Dichloromethane laboratory grade obtained from Biolab Scientific Pty Ltd and Laboratory grade Acetone from APS chemicals.

3.1.4 Polymer

General purpose PS (grade Austrex 555) obtained from Huntsman (Victoria, Australia) was used in sample preparation for Thermal and UV stability study of clay dye pigment. Details of the properties are given in Table 3-3 with values found in suppliers' datasheets.

Table 3-3: Properties of Polystyrene

Properties	Polystyrene
Grade	Austrex 555
Molecular weight (M_w)	165,000
Polydispersity	6.8
MFI (g/ 10min) at 180 ° C	18
Melt density (g/cc) at 190 ° C	0.97

3.2 Sample Preparation Methods

3.2.1 Clay- Dye pigment preparation Methods

Clay-dye pigment samples were prepared by two different methods of intercalation. Schematic diagram of the preparation method is described in Figure 3-3. Method-1 describes clay-dye complex prepared with naturally occurring MMT (unmodified clay) in aqueous medium (Water). Here cation exchange occurs between organic dye and clay interlayer Na^+ cation. Method-2 describes the clay-dye complex preparation with commercially available organo clay (MMT modified with alkyl ammonium salt) in nonaqueous medium. Expected cation exchange reaction for this method is between organic dye and clay interlayer alkyl ammonium cation

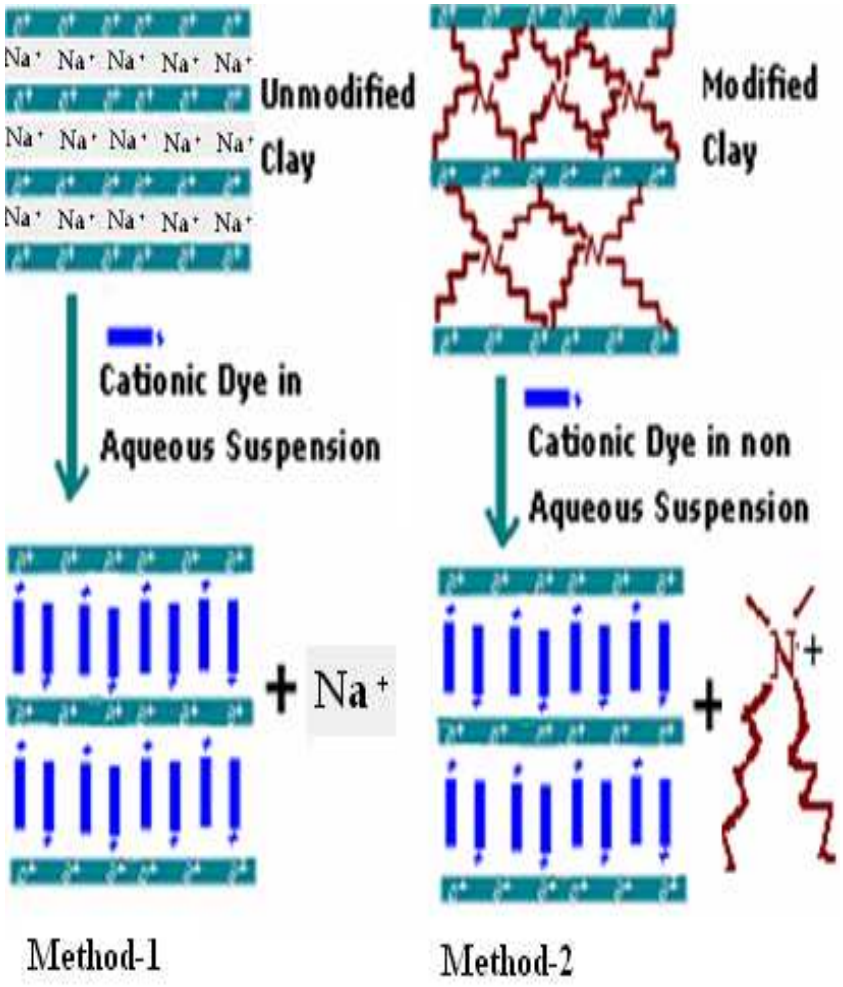

Figure 3-3: Scheme of preparation of clay-dye complex with unmodified clay & modified clay.

3.2.2 Cation Exchange Capacity (CEC) of the Clay and Dye loading

For successful intercalation the selected clay should have cation exchange capacity: CEC= 50- 200 meq/100 g clay. As mentioned earlier, organic cation can be adsorbed beyond the CEC of clay. The adsorption is irreversible until CEC is satisfied; but adsorption beyond CEC, the amount in excess of this level is readily desorbed[15]. According to Landau et al. [29]when the amount of dye is below 35 mmol (Rhodamine 6G) per 100 g clay in one of the principal associations the dye is located in the interlayer space and is able to form π bonds with the oxygen plane of the clay. But with higher amounts of dye the clay flocculates and the added dye is located in the interparticle space with no π interactions with the O-plane.

The CEC of the NaMMT clay that Landau et al. used was 74 meq/100 g clay (74mmol Na^+). Cationic Exchange Capacity (CEC) of the unmodified clay used in this study was 97 meq/100 g clay (97mmol Na^+); therefore the required dye loading is around ~ 46 mmol/ 100 g clay. Hence 50 mmol dye for 100 g clay basis was chosen for sample preparation with unmodified clay. Modifier concentration of modified clay Cloisite 15A is about 125 meq/100 g clay and same as the dye loading would be around ~60 mmol/ 100 g clay basis. The dye loading that was used for sample preparation with modified clay was 100 mmol/ 100 g dye basis, because here expected cation exchange reaction with modified clay is between alkyl ammonium cation and the dye. Therefore higher dye loading was chosen. (100 % ion exchange assumed and therefore actual amount of dye used was maintained in some excess.)

3.2.3 Clay-dye pigment Sample preparation in aqueous medium

Rhodamine B dye- NaMMT clay complex: 250 ml deionised water was added into beaker and then 5 g Na-MMT was added. Intensely stirred for 12 h at 60 rpm to disperse the clay evenly. 2.5 mmol (1.2 g) dye was dissolved in 100 ml water with 5ml of 1M HCl (for protonation). Then dissolved dye solution was added to the clay suspension. The two solutions were mixed and stirred for 24 hours using the magnetic stirrer at 60 rpm. Then the colored Na-MMT clay- dye solution was allowed to settle down for 24 hours.

Precipitates from the sample was centrifuged at 4400 rpm for 15 minutes and washed with 100 ml of deionised water for three times. Samples being washed and filtered were put into the oven for drying, at 95° C for 24 hrs. Dried samples of clay-dye pigment were crushed with agate mortar and pestle. Crushed samples were sieved using sieve tray with sieve size of 45µm.

Solvent Dye (SD) - NaMMT clay complex / Modified Solvent Dye (mod SD) - NaMMT clay complex: NaMMT clay suspensions prepared using same amount and method as mentioned above for Rhodamine dye. But dye solution was prepared by dissolving 2.5 mmol (SD =1.39 g and modified SD= 1.32 g) dye in 100 ml of Acetone with 10 ml of 1M HCl (for protonation). Then the dissolved dye solution was added to the clay suspension. The two solutions were mixed and stirred for 24 hours using the magnetic stirrer at 60 rpm. Then the colored Na-MMT clay- dye solution was allowed to settle down for 24 hours.

Precipitates from the sample was centrifuged at 4400 rpm for 15 minutes and washed with 100 ml of Acetone for three times. Samples being washed and filtered were put into the oven for drying, at 60° C for 24 hrs. Same procedure was followed for grinding and sieving (as above for Rhod B. dye).

3.2.4 Clay-dye pigment Sample preparation method in non-aqueous medium

About 2 gm of Cloisite 15A clay was dissolved in 200 ml of dichloromethane (DCM) solvent; then 2mmol (Rhod B = 0.957g, SY98 = 1.11g) of dye was added to the solution. 5ml of 70 % perchloric acid (for protonation) was added to clay-dye suspension and stirred at 60 rpm for 12 hour at room temperature. Then the colored clay- dye solution was allowed to settle down for 24 hours.

Precipitates from all the samples were centrifuged at 2000 rpm for 15 minutes and washed with 50 ml of DCM for three times. Samples being washed and filtered were air dried for 24 hrs. Dried samples of clay-dye pigment were crushed with agate mortar and pestle. Crushed samples were sieved using sieve tray with sieve size of 45µm.

3.2.5 Clay- dye polymer Nanocomposites Sample preparation method

50 g of Polystyrene was mixed with calculated amount of dye (as shown in Table 3-4) using HAAKE twin-rotor batch mixer (model: Rheomex with Haake software, Haake instruments, Germany) with 69 cm^3 capacity. Mixing was carried out at 180 °C and at 60 rpm for 10 minutes. At the end of the mixing, the material was recovered and was compression molded into 1.5 mm thick plaques at 180 °C.

Table 3-4: Amount of dye/ dye pigment (The amount clay-dye pigment that gives 100 mg dye) used in polymer nanocomposites preparation

Sample	Dye/ Clay-Dye Pigment (mg)
PS-Rhod B	100
PS-Rhod B+ NaMMT	518
PS-Rhod B+ Cloi 15A	309
PS-SD	100
PS-SD+NaMMT	460
PS-SD+Cloi 15 A	280

3.3 Instrumentation and Characterization

3.3.1 X-Ray Diffraction (XRD) Characterization

The typical distances between the silicate layers (d-spacing) and hence the extent of organic dye intercalation into the clay layers were determined using X-ray scattering techniques (WAXS & SAXS). As discussed before in section 2.5, the calculation of the *d*-spacing can be achieved with the use of Bragg's law [Eq. 2.1].

$$n\lambda = 2d \sin\theta \qquad (2.1)$$

Where, n is the order of diffraction, λ is the wave length, θ is the angle of diffraction, and d is inter planar distance

Clay-dye pigment samples prepared with unmodified clay were characterized by using WAXS. Experiments were conducted by using Philips diffracto- meter. Operational conditions were set to be 30 kV acceleration voltages and 30 mA current. Generated Cu K_α radiation was passed through 0.6 mm of tungsten (W) slit to collect the data. The measurements were conducted in step scanning mode, with a step size of 0.05° for 2θ and counting time of 5 seconds at each step. Data were collected from 2θ = 3° to 2θ = 10°.

SAXS measurements were carried out at room temperature using a Bruker NanoStar for samples prepared with modified clay. A ceramic fine-focus X-ray tube, powered with a Kristallflex K760 generator at 35 kV and 40 mA, has been used in point focus mode. The primary X-ray flux is collimated using cross-coupled Gobel mirrors and a pinhole of 0.1 mm in diameter providing a Cu K_{α} radiation beam with a full width at half-maximum of about 0.2 mm at the sample position. The scattering curve of the empty SAXS chamber was subtracted from the scattering curves of the clay-dye complex sample to get insight into the scattering behavior of the samples. Data were collected from $2\theta = 0.6°$ to $2\theta = 12°$.

3.3.2 TEM/ EDS Analysis

The TEM Images were produced using the JEOL 2010 model with a medium acceleration voltage of 200 kV and high vacuum. The point-to-point resolution of this TEM is 0.194 nm and its slow-scan charge-coupled diode (CCD) camera allows digital image recording. Dispersed clay-dye complex suspensions were deposited on collodion-coated Cu grids and air-dried prior to mound the sample in TEM. The samples were magnified to 100,000 X. The images produced were analyzed and interlayer space distances were measured using Digital Micrograph ™ software version 3.8.2.

Elemental analysis was performed using Link Analytical energy dispersive spectrometer (EDS) with an ultra thin windowed Si (Li) detector connected to the TEM. In order to limit irradiation damages, analyses were done using a probe spot 100 nm in diameter [71]. A minimum of three layer structure (i.e. at three different spots) were analyzed in order to get average element composition of the clay-dye complex. Software used to analyze the EDS spectrum was High Performance X-Ray Microanalysis, Version 4 from Thomson Scientific Instruments Pty. Ltd. The detector used in this study has the limitation for small elements. Elements below Sodium in the periodic table can not be detected.

3.3.3 Principles of Operation of EDS

When an x-ray photon enters the body of the detector, it is absorbed to create a high energy photoelectron. This electron strikes other near by atoms in the sample, it looses energy itself but ionizes other atoms and free more electrons. When electrons ionize atom, the emitted characteristic x-ray energy is unique to the ionized atom. When the electrons are slowed by interaction with the nucleus, they produce a continuum of bremsstrahlung X-rays. The characteristic x-rays appear as Gaussian-shaped peaks superimposed on a background of bremsstrahlung X-rays.

EDS system interfaced to TEM consists of three parts, the detector, the processing electronics (pulse processor) and multi channel analyzer (CMA) display. All three parts are controlled be computer (Figure 3-4). The detector generates a charge pulse

proportional to the X-ray energy. This pulse is first converted to a voltage. Then the signal is amplified through a field effect transistor (FET), isolated from other pulses, further amplified, and then identified electronically as resulting from an X-ray of specific energy. Finally, digitized signal is stored in a channel assigned to that energy in the multi channel analyzer (CMA)

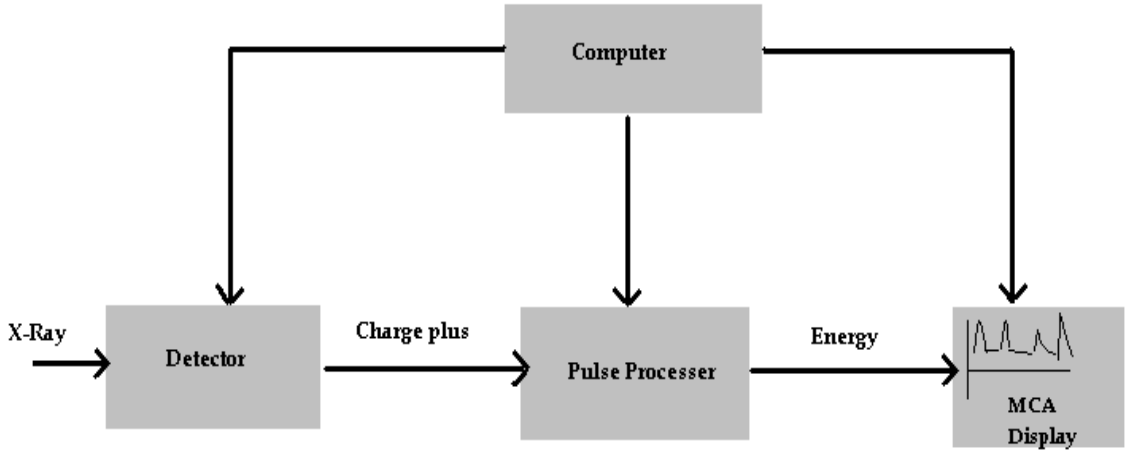

Figure 3-4: Scheme of EDS system with computer control. (Re produced from [49])

3.3.4 Thermo-gravimetric Analysis (TGA)

Thermal gravimetric analysis (TGA) shows the changes in mass of a sample as the temperature increases linearly. Data form the thermal analyses of clay-organic complexes provides the valuable information about the water content (hydrophilic to hydrophobic nature of such complexes), organic content, and clay mineral dehydroxylation phase changes.

Thermal stability of clay-dye pigment was investigated using a Perkin Elmer TG analyzer (TGA7/TAC7DX). 5-10 mg of clay-dye pigment were carefully loaded into a pan and subjected to a constant heating rate of 10 °C/min from 50-800 °C in an inert atmosphere (N_2) and the weight loss against temperature was recorded. The fractional weight loss between the two given temperatures was found graphically. Perkin-Elmer TGA instrument was calibrated to get to the starting temperature 50 °C and was hold for one minute.

3.3.5 Ultra Violet (UV) Stability Study.

Test method followed to study the UV stability of clay-dye polymer nanocomposites was similar to ASTM **D 4674-89** standard test method for Accelerated Testing for Color Stability of Plastics Exposed to indoor Fluorescent Lighting and Window- Filtered Daylight.

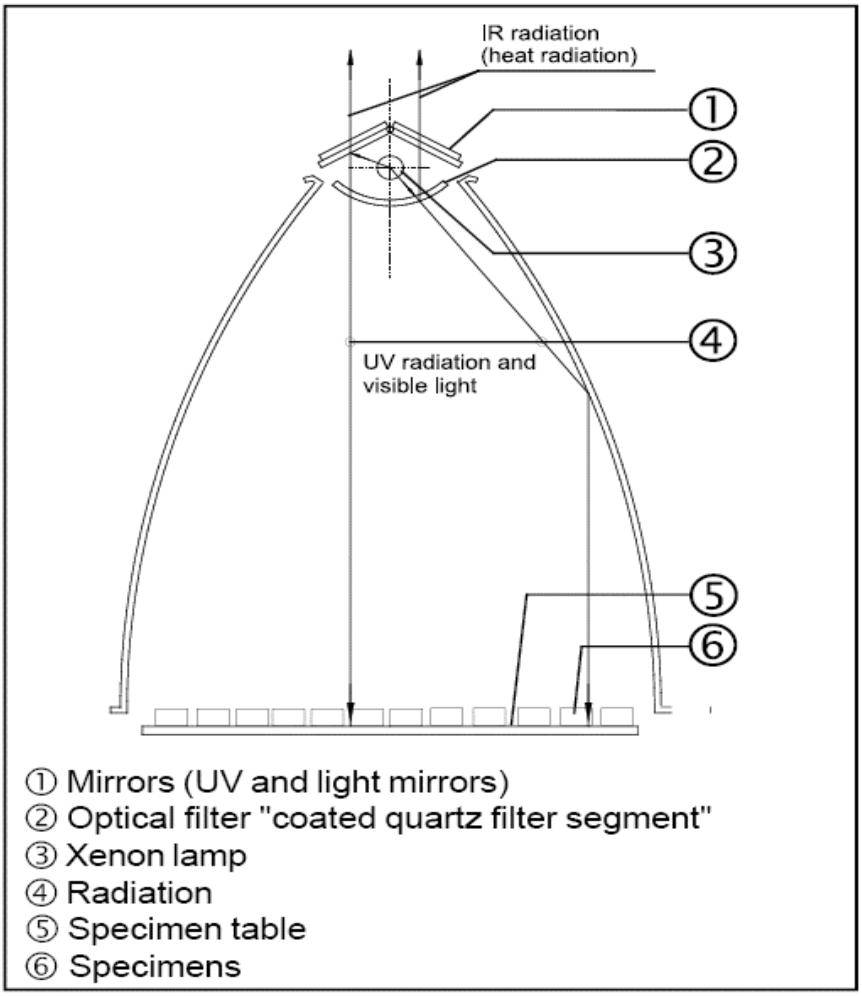

Figure 3-5: Irradiation chamber of Suntest CPS/CPS+. Adopted from SUNTEST CPS/CPS+ Operating manual.

The equipment used for this test was SUNTEST CPS / CPS+ manufactured by Atlas Materials Testing Solutions, Germany. The test chamber of this equipment with its components is shown in Figure 3-5. Spectral distribution of Suntest CPS/CPS+ irradiation lamp with additional filter can be seen in figure A.1 (Appendix A) and it can be compared with daylight irradiation spectral distribution which is shown in figure A.2 (Appendix A)

Compression molded rectangular flat specimen, 1.5 mm thick was used for UV exposure. Samples were arranged in sample tray and half part of the sample were masked with metal bar then left inside the irradiation chamber of Suntest CPS/CPS+ instrument. Xenon lamp was turned on to irradiate the samples. This irradiation was continued for several hours until the sample shows visible colour change. Color change was monitored every 2 hrs. The intensity of the lamp was 765 W/m^2 (300-800nm wave length) Results were compared based on visual observation of color change

CHAPTER 4: RESULTS AND DISCUSSIONS

Introduction

This chapter describes in detail analysis of the results of the experimental work carried out during the course of the research. The study of clay intercalation with organic dye described under the following major topics; XRD & TEM/EDS characterization of organic dye–clay complex, Thermogravimetric analysis of organic dye–clay complex and Thermal & UV stability of clay-dye pigment polymer nanocomposites

4.1 X-Ray Diffraction Characterization of Clay-Dye Complex

The extent of intercalation of organic dye into the clay mineral was studied by using X-ray diffraction technique as described in section 2.5. WAXS experiments were conducted for clay dye pigment samples that were prepared with unmodified clay. The modified clay Cloisite 15 A, was found to have the peak at low incidence angle (2θ) range (2θ = 0.5°- 3°). Therefore to obtain better results SAXS experiments were carried out for clay dye pigment samples that were prepared with modified clay. In the following the changes of d-spacing will be discussed with respect to the intercalation medium and chemical structure of the organic dye as well as the organo compound (Alkyl ammonium cation) that was present in the modified clay.

4.1.1 WAXS analysis of unmodified clay based dye-pigment

Figure 4-1& Figure 4-2 illustrate the WAXS curves of clay-dye pigment that was prepared using unmodified clay (in aqueous medium) with hydrophilic dye (Rhodamine B[Rhod B]) and organophilic dye (Solvent Dye[SD]) respectively and compares with WAXS curve of the neat unmodified clay. The scattering maximum of Na^+MMT (the 001 reflection) is usually found in the range of 0.95-1.4 nm (9.5-14 Å), depending on both CEC and water content of the sample. When Na+ ions were replaced by organic cationic ion in the clay gallery, the reflections broadened and shifted to lower angles, i.e. larger d-spacing and hence larger distances between the silicate layers will be found. [38].

The actual unmodified clay used in this study showed a d-spacing of 1.26 nm (12.61 Å). It can be seen that the interlayer distances (d_{00}) of both clay-dye complexes were increased (Figure 4-1& Figure 4-2). In the case of hydrophilic dye (Rhod B) the increase of d-spacing (1.26 to 1.92 nm) is larger, where as organophilic dye (SD) shows slight increase in d-spacing (1.26 to 13.2 nm). According to Yariv [15] a basal spacing of less than 1.4 nm does not permit any kind of aggregation of the dye cation to take place inside the interlayer space. The adsorbed dye cations probably form monolayers of monomeric species in the interlayers, with aromatic rings lying parallel to the silicate layer or almost parallel with the very small tilting. Parallel orientation should be facilitated by π interactions between the organic dyes and O-planes of the smectites.

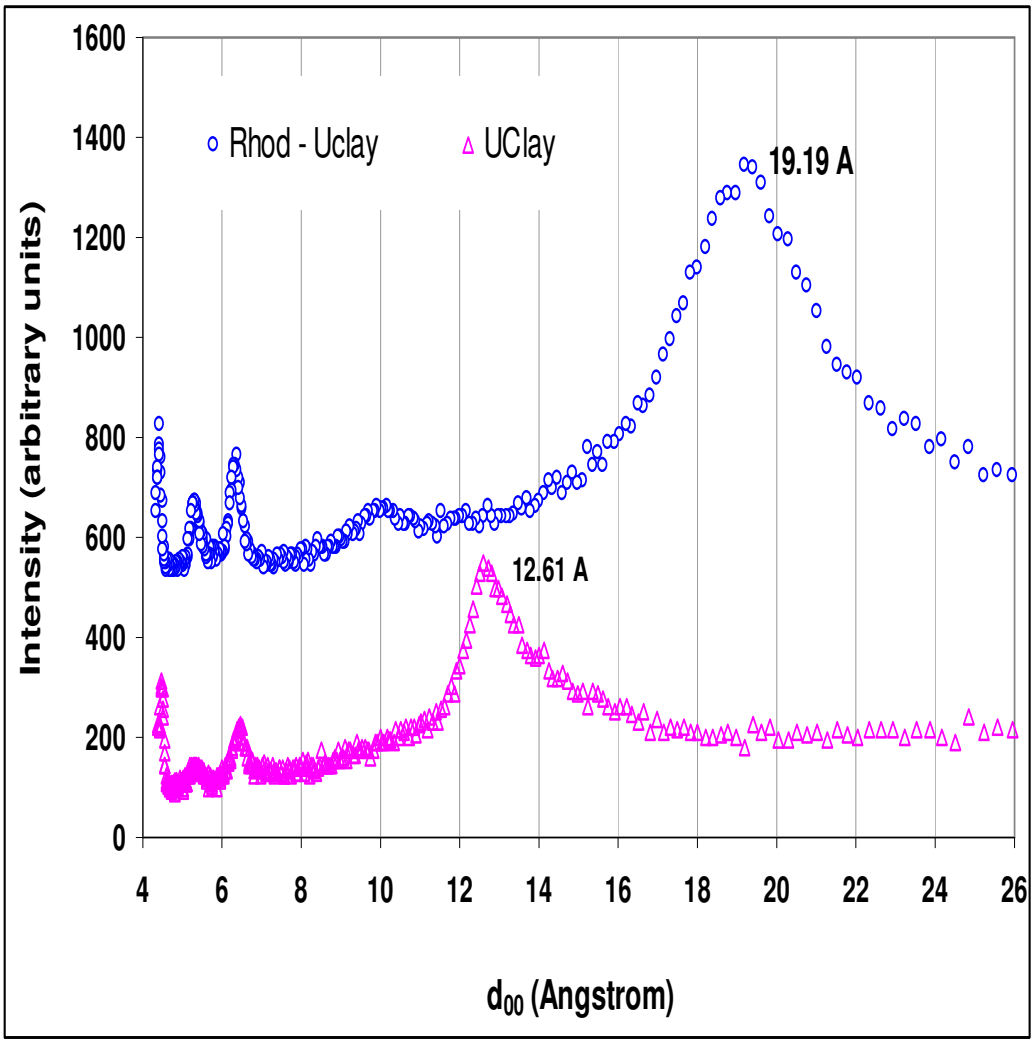

Figure 4-1: WAXS curves (Intensity versus d-spacing) of Rhodamine- NaMMT Clay complex prepared in aqueous medium and unmodified clay (U Clay).

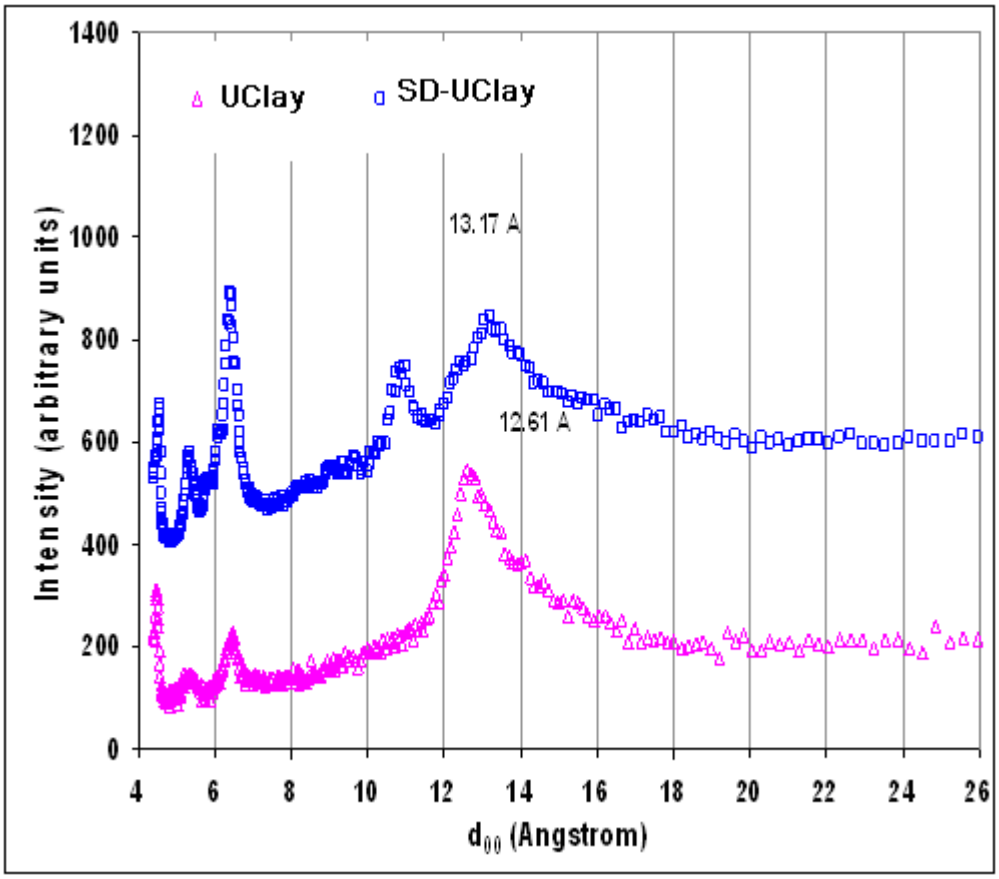

Figure 4-2: WAXS curves (Intensity versus d-spacing) of Solvent Dye- NaMMT Clay complex prepared in aqueous medium and unmodified clay (U Clay).

Solvent dye shows very slight increase in d-spacing (d_{00} = 13.17, Δd= 0.57 Å). Considering the molecular structure of Solvent dye (see section 3.1.2) even though the aromatic rings may be lying parallel to the silicate layer it is expected to have a large space distance; because of the long alkyl chain (-$(CH_2)_{17}$-Me) attachment to the aromatic ring. Hence XRD results reveal that Solvent dye molecules did not penetrate into the interlayer space and possibly the dye adsorption must have taken place on external

surface of the clay by weaker hydrogen bonds or Van der Waals interactions between dye molecule and the O-plane of outer surface of the clay layer.

The cationic dye Rhodamine B consist of a xanthene moiety, which is responsible for their characteristic $\pi \quad \pi^*$ transition. In addition this cation possess a phenyl ring, the plane of which is perpendicular to that of the three xanthene rings, and consequently has only a small effect on the $\pi \quad \pi^*$ transition. This dye is a metachromic and form dimeric species in aqueous solutions ([15]). In the case of Rhodamine B dye a large increase in d-spacing was obtained (Δd= 6.58 Å). This indicates that Rhodamine B dye molecules penetrated inside the clay layer and possibly located inside the clay layer in the form of dimers (Figure 4-3 A-bilayer structure). However from the characterization methods available, the arrangement of the molecules cannot be directly deduced.

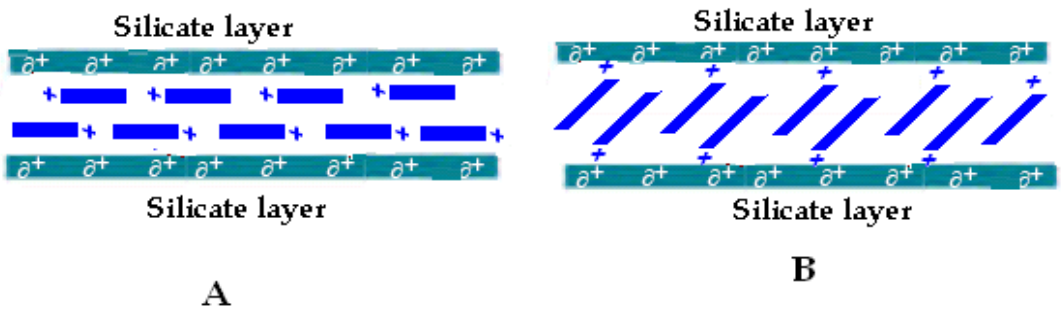

Figure 4-3: Proposed structures of the intercalation compounds. (A) Bilayer model; (B) Tilted model as illustrated in Lagaly [72].

Rhodamine consists of quaternary ammonium cation where Solvent dye has dicarboximide form of ion. The interaction between amides and montmorillonite saturated with different cations was investigated by Tahoun & Mortland [73] [74]. When amides are adsorbed by montmorillonite, they can be protonated. The extent of protonation depends on the acid strength of the exchangeable cation. The carbonyl group oxygen is being the protonation site, rather than the NH_2 group.

Stutzmann et al. [75] studied the adsorption mechanism of acetamide and polyacrylamide by montmorillonite and Kaolinite using IR spectroscopy. They concluded that amide adsorption takes place on the external surface of the clay particles. The organic molecules are protonated on the surface and adsorbed by electrostatic forces. They proposed two possible adsorption mechanisms; (1) a strong, irreversible adsorption, which corresponds to the formation of a monolayer of chemisorbed molecules, and (2) a more important adsorption of molecules retained by hydrogen bonds, which can be eliminated by heating at low temperatures.

Therefore it is more likely that the Rhodamine B dye molecules penetrated inside the clay layer and participated in cation exchange reaction with interlayer Na^+ cation, where Solvent dye molecules are possibly adsorbed onto the outer surface O-plane of the TOT layers by strong irreversible adsorption or hydrogen bonding due to carbonyl group oxygen domination in protonation site, rather than the NH_2 group.

4.1.2 SAXS analysis of modified clay based dye-pigment

As shown in Figure 4-4 & Figure 4-5, the clay-dye complex prepared in non aqueous medium (DCM Solvent) show interlayer space decreases for both dyes (Rhodamine B & Solvent dye). Dye molecules have necessarily a rather flat shape because of the conjugated π-system [38]. Therefore, a flat arrangement of these molecules within the silicate layers after dye modification was assumed, resulting in rather small interlayer distances after replacement of alkyl ammonium molecule by a dye molecule.

Actual d-spacing of modified clay was found to be d_{00}= 31.5 Å. Rhod B dye shifted to d_{00}= 24.1 Å where Solvent dye shifted to d_{00}= 25.2 Å. This decrease of d-spacing shows some interaction of dye molecule with the bulky alkyl ammonium molecule that was present in the interlayer of the modified clay.

K. Ito et al. [36] studied cation exchange mechanism of the cationic dye by alkylammonium modified montmorillonite. They noted that the structure of the alkyl ammonium ions present in the clay layer markedly affects the ion exchange of the cationic dye depending on the size and number of the alkyl chain. They observed that the most effective ion exchange reaction of cationic dye takes place with bulky tetra alkyl ammonium ion substituted clay. They reported interlayer space decrease of 23.6 Å to 20-22 Å in their study of intercalating water insoluble fluoran dye into the alkylammonium

ion [$(C_{10}H_{21})_4N^+$] modified clay by exchange reaction between cationic dye and alkylammonium ion in non –aqueous medium (Acetone).

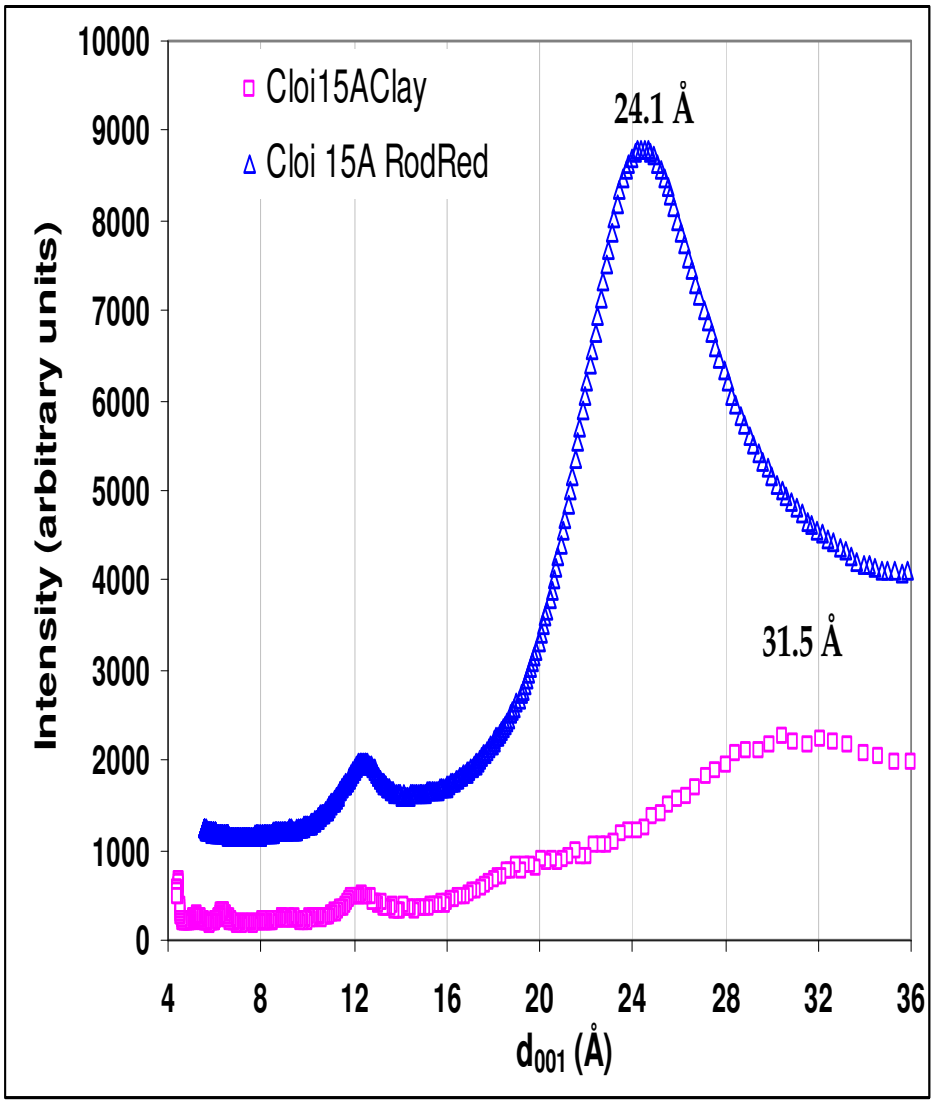

Figure 4-4: SAXS curves (Intensity versus d-spacing) of Rhodamine dye - Cloisite 15A Clay complex prepared in non-aqueous medium and neat modified clay (Cloisite 15A).

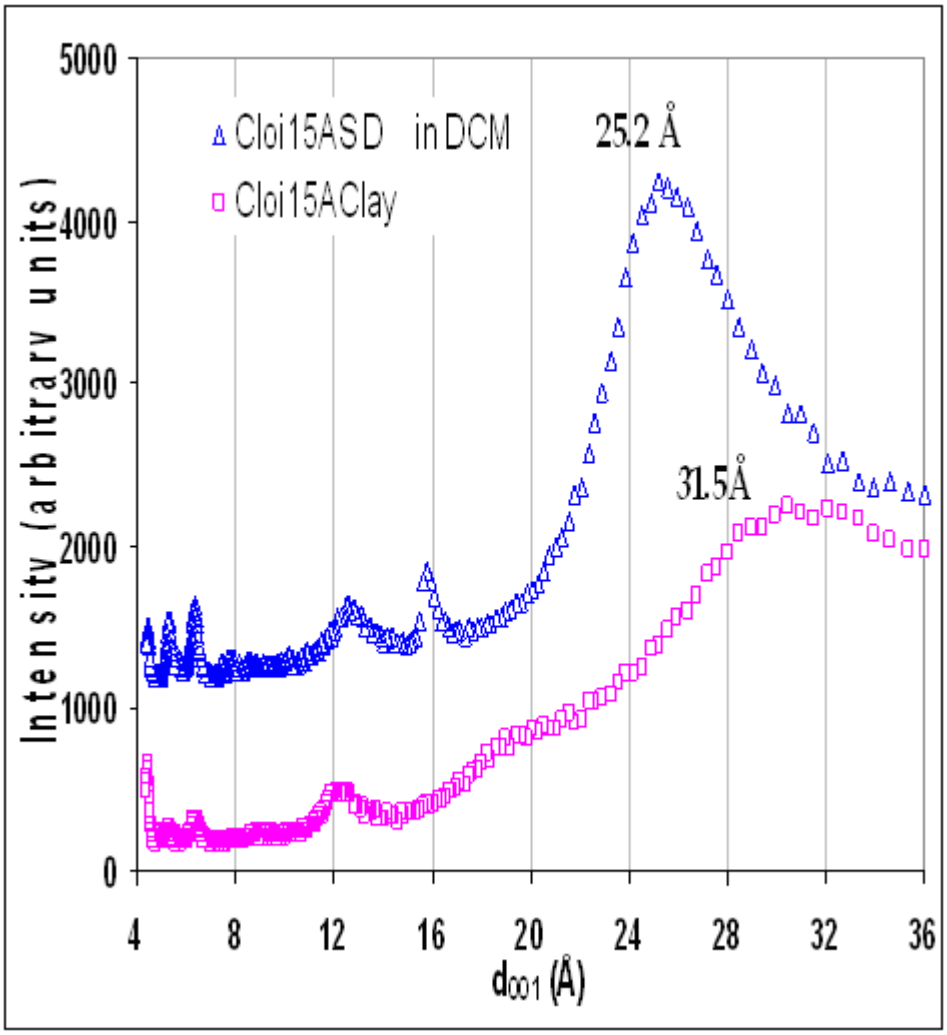

Figure 4-5: SAXS curves (Intensity versus d-spacing) of Solvent dye (SD)- Cloisite 15A Clay complex prepared in non-aqueous medium and neat modified clay (Cloisite 15A).

The actual alkylammonium ion used in the modified clay (Cloisite 15A), is dimethyl dihydrogenated tallow quaternary ammonium ion (Figure 4-6). According to technical data sheet from Southern Clay Products (See Appendix B1& B2), both Cloisite

15A & Cloisite 20A clays are product of natural montmorillonite modified with the same dimethyl dihydrogenated tallow quaternary ammonium salt. But they differ in the d-spacing; Cloisite 15A has a d-spacing of 31.5 Å; where as d-spacing of Cloisite 20A is 24.2 Å; this attributed from modifier concentration. Cation exchange capacity (CEC) of Cloisite 15A & Cloisite 20A are 125 meq/100g clay and 95, meq/100g clay respectively. The d-spacing of Rhod B dye (which is nearly similar to Cloisite 20 A) and Solvent dye shifted to 24.1 Å, 25.2 Å respectively. This decrease of d-spacing indicates the reduction of modifier concentration of the clay by dye molecule and hence confirms partial removal of alkylammonium molecule from the clay interlayer.

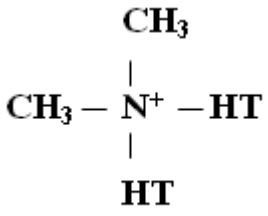

Figure 4-6: Quaternary ammonium ion present in Cloisite 15 A clay. Where HT is Hydrogenated Tallow (~65% C18; ~30% C16; ~5% C14)

When comparing the clay- dye complex of Rhod B dye and Solvent dye, the small difference in d-spacing may be the cause of organic dye molecular structure on removal of alkylammonium molecule from clay layer in non aqueous medium. The strength of the cationic ion greatly influences the ion exchange reaction as mentioned earlier [22].

Another possible explanation for this d-space decrease could be the formation of quaternary ammonium-organic dye complex inside the clay layer due to H-bonding or Van der Waals interactions that cause changes in orientation of two long alkyl chain (HT) of quaternary ammonium molecule abruptly from horizontal to roughly vertical or with a small tilting. It is observed that the intensity peak of modified clay (Cloisite 15A) changed form broad peak to a narrow sharp peak after being treated with organic dye.

It was found that the d-space of Rhod B dye-clay complex prepared with unmodified clay in aqueous medium (19.19 Å) differ from those prepared with modified clay in non aqueous medium (24.1 Å), which is confirming the presence of some bulky organic molecule inside the clay layer (Δd= 4.91 Å). This could be the cause of incomplete exchange reaction due to insufficient reaction time. This observation also shows that selected intercalation medium greatly influenced the clay intercalation process of organic dye.

SAXS results show some evidence for desorption of alkyl ammonium cation from organically modified montmorillonite clay (Cloisite 15A). However the replacement of organic dye molecule to the interlayer clay surface cannot be directly verified from the characterization methods available.

4.2 Transmission Electron Microscopy (TEM) and Energy Dispersive Spectroscopy (EDS) Study of Clay-Dye complex

Transmission electro microscopy (TEM) in conjunction with energy dispersive spectroscopy (EDS) was used to qualitatively analyse the nano-layer structure of the clay-dye complex and to identify and quantify the elemental composition of the clay-dye pigment samples.

4.2.1 TEM Study

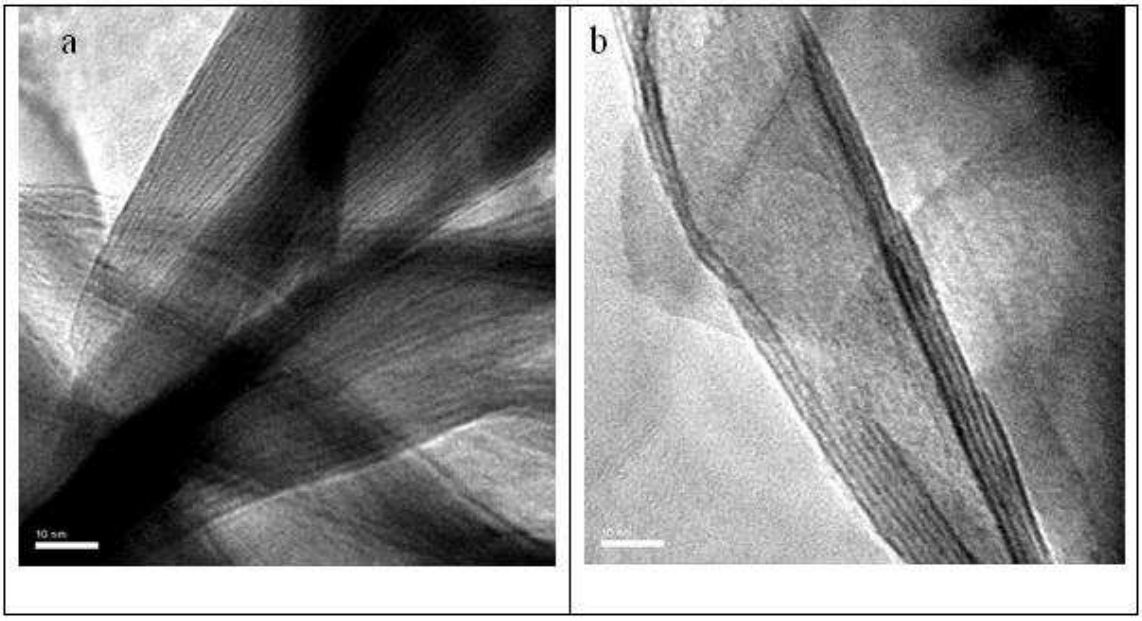

Figure 4-7: TEM images of Rhodamine Dye-Na montmorillonite clay complex

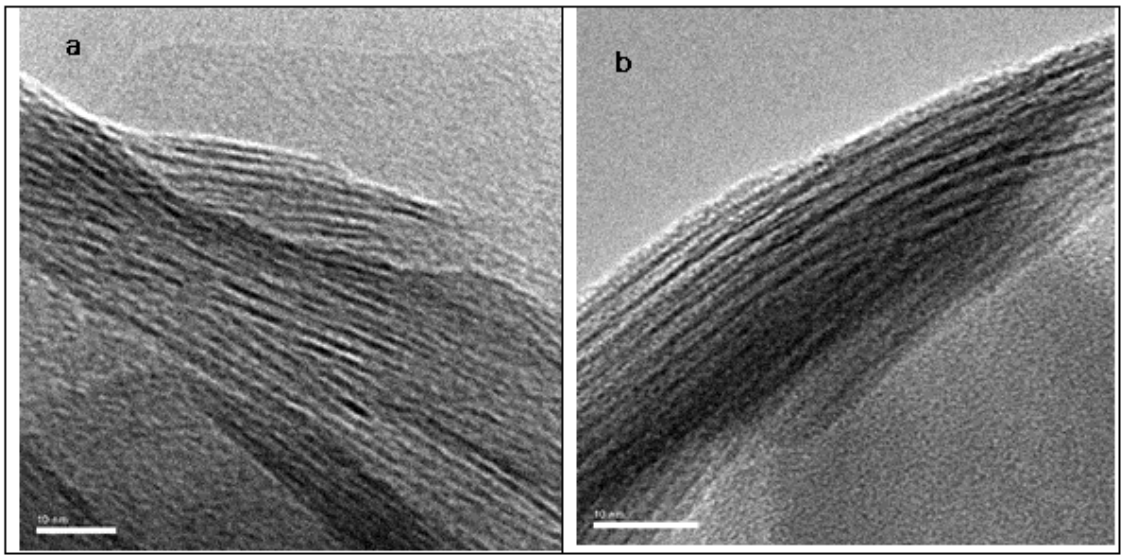

Figure 4-8: TEM images of Solvent Dye- Cloisite 15A clay complex

Figure 4-7 a & b and Figure 4-8 a & b illustrate TEM micrographs of Rhodamine dye – unmodified clay (NaMMT) complex and Solvent dye-modified clay (Cloisite 15 A) complex respectively. These images visually confirm the existence of layer structure after dye molecular intercalation and the changes of the interlayer space distance. Rhodamine B dye intercalated NaMMT clay shows d-spacing in the range of 1.75-1.83 nm at various points of layer focus. Solvent dye- modified clay complex found to have d-spacing range of 2.2- 2.4 nm. It can be seen from Table 4-1 that d-spacing estimated from TEM of the same sample varies from XRD d-spacing measurements. The possible reason for this variation arises from the imaging angle. If the TEM image was not taken through the perpendicular direction of clay layer stack (i.e. imaged through a different angle of clay stack), the measured space distance would be smaller than the actual distance.

Table 4-1: Interlayer space distance comparison from XRD results with TEM

Clay -Dye Pigment	Interlayer d-spacing from XRD d_{00} (nm)	Change of d-spacing from Neat Clay* Δd (nm)	Interlayer d-spacing from TEM d_{00} (nm)
NaMMT-Rhodamine B dye	1.92	0.67 ↑	1.75- 1.83
Cloisite 15A-Solvent dye	2.52	0.63 ↓	2.2- 2.4

* Where interlayer d-spacing of neat NaMMT is 1.26 and neat Cloisite 15A is 3.15

4.2.2 Energy Dispersive Spectroscopy study

Energy dispersive spectroscopy is useful to quantitatively characterize the elemental composition of samples with the size of 0.1- 2 μm. The EDS measurement device that was used along with JEOL 2010 TEM in this study has the detection limitation; elements smaller than sodium can not be detected. Hence considering the elements present in Rhodamine dye, which are below the detection limit; the amount of Rhod B dye present in Rhod B dye- NaMMT clay complex can not be verified. But the Solvent dye molecules itself have sulfur and modified clay Cloisite 15A does not have any sulfur present in it. This enables to use EDS analysis to study intercalation of Solvent dye into the modified clay. The spectroscopy of Solvent dye-Cloisite 15 A clay complexes can be found in Appendix- C.

To study the elemental composition of clay-dye complex, EDS analysis was made on lateral resolution of clay layer of 0.1-0.2µm. For the validity of the results first the ratio of Silica (Si) to Aluminum (Al) was studied. The weight ratio of Si: Al from chemical composition of the typical natural montmorillonite $[[Al_{1.67}Mg_{0.33}(Na_{0.33})]Si_4O_{10}(OH)_2]$[11] is 2.48:1 (where CEC= 90 meq/100g clay) and the ratio found from EDS study was 2.78:1 (where CEC= 97 meq/100g clay) which is nearly similar to the composition ratio (see Table 4-2)

Table 4-2: weight ratio of Silica to Aluminum comparison from chemical composition and from EDS; where atomic weight of Si- 28 & Al- 26.98

	Si	**Al**
Chemical composition	4 x 28 = 112 **2.48**	1.67 x 26.98 = 45.1 **1**
Composition from EDS	**2.78**	**1**

Table 4-3: weight ratio of Silica to Sulfur comparison from Stoichiometric ratio and from EDS; where atomic weight of Si - 28 & S - 40

	Si	**S**
From Stoichiometric ratio	4 x 28 = 112 **8.48**	0.33 x 40 **1**
Composition from EDS	**12.2**	**1**

Typical Sodium montmorillonite Chemical Composition is shown below;

$$[Al_{1.67}Mg_{0.33}(Na_{0.33})]Si_4O_{10}(OH)_2$$

According to the formula above, available exchangeable cation is 0.33 mole Na per 1 mol of clay. Solvent dye molecule consists only one sulfur atom; therefore if we assume 100 % adsorption the stoichiometric ratio of silica to sulfur would be 8.48: 1. CEC of typical NaMMT = 90 meq/100g clay and the modifier concentration of Cloisite 15 A is 125 meq/100 g clay; hence expected Silica to sulfur ratio for Solvent dye-Cloisite 15A complex would be 11. 78: 1 and the ratio found from EDS were 12.2:1 (See Table 4-3). This suggests that expanded layer structure of the modified clay enabled the Solvent dye to penetrate inside the clay layer and evenly located inside the clay layer. Penetrated dye molecules may be weakly bonded by weaker hydrogen bonds or Van der Waals interactions either with the O-plane of interlayer surface of the clay layer or with the alkyl ammonium cation present inside the clay layer.

4.3 Thermo gravimetric Analysis of Clay- Dye Complex

As mentioned earlier (section 2.8) Clay minerals usually show two or three main stages of weight loss on TG-DTG curve. The low temperature weight loss occurs due to the evolution of adsorbed and interlayer water, which occurs in the temperature range from ambient temperature to 250 °C. The 2:1 minerals (smectite) show weight loss due to dehydroxylation effect in the temperature of above 500 °C (between 500-800 °C). The association of organic compounds with clay minerals influences the shape of thermal curves of the mineral constituent in both low and high temperature (dehydroxylation) weight losses, although the main reactions of organic matter take place at 200-500 °C [15, 50-52]

4.3.1 Thermo gravimetric study of Clay- Dye Complex with Unmodified Clay

The TG curve of unmodified clay (NaMMT) is depicted in Figure 4-9. TG curve shows two stages of mass loss. First stage of mass loss occurs below 150 °C which is about 6.5 % weight loss due to dehydration and second stage of further 3.5 % weight loss takes place in the temperature range 150- 800°C which occurs because of dehydroxylation of clay minerals. DTG curve shows two peaks, one at 79°C (low temperature dehydration peak of evolved water) and the other one at 650°C (High temperature dehydroxylation peak of clay mineral).

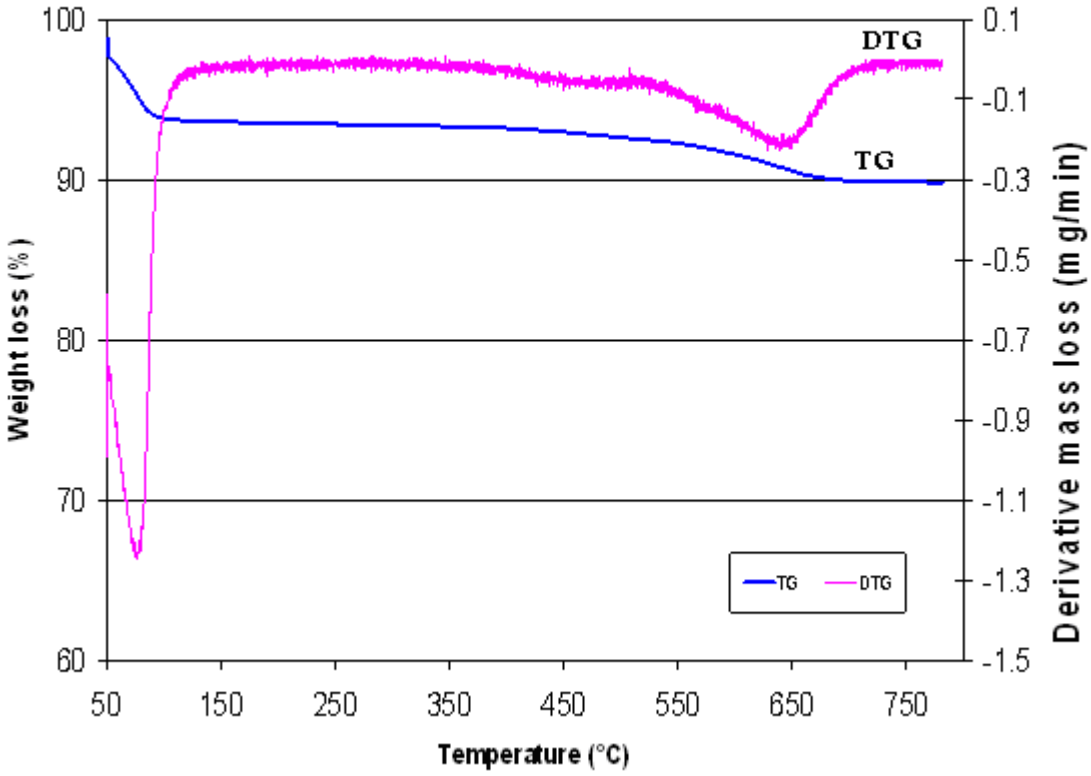

Figure 4-9: TG-DTG curve of Unmodified Clay (NaMMT)

TG-DTG curves of Rhodamine B dye- NaMMT complex and Solvent dye-NaMMT complex are depicted in Figure 4-11& Figure 4-13 respectively. Table 4-4 summarizes the weight loss and DTG peaks of two different clay-dye complexes at different temperatures and compares with their neat dye and unmodified clay. Rhodamine B dye shows the following stages of mass loss(See Figure 4-10): Up to 200 °C the dehydration of dye gives < 1 % weight loss, between 200 °C to 500 °C and about 76 % weight loss due to decomposition of organic dye. In this temperature range DTG curve shows four peaks at 216, 260, 380 & 454 °C. Further 5 % weight loss is found in the

temperature range of 500 to 800 °C. In the case of Rhod B-NaMMT complex, TG curve shows (Figure 4-11) only 3 % mass loss up to 200 °C due to dehydration; 7 % weight loss in the temperature range of 200-500 °C from decomposition of organic dye and further 3 % weight loss possibly due to dehydroxylation of clay.

Low temperature weight loss of unmodified clay is reduced from 7% to 3 % in the TG curve of Rhodamine B-clay complex. This change indicates the formation of dye-clay complex which is hydrophobic due to the adsorption of dye by the clay surface. According to Yariv [53] the presence of organic molecules adsorbed on to the clay surface imparts a hydrophobic character. The small DTG peaks of neat Rhod B dye in the temperature range of 200 °C to 500 °C disappeared (216 °C, 260 °C & 455 °C) and the main peak shifted from 380 °C to 405 °C. This evidences some interaction between organic dye and clay minerals.

Landau et al. [29] postulated that the organic dye adsorbed into clay layer formed π- bonds with the clay and their oxidation continued up to 800 °C. The organic dye adsorption took place on the external surface of the clay which did not form any bond with the clay and hence the oxidation of the organic matter was completed already below 550 °C. In this study the Rhodamine B-clay complex shows the second stage of weight loss of only 7 % in the temperature range of 200-500 °C and the weight loss continued above 550 °C, which indicates that Rhodamine B dye molecules penetrated the interlayer and located inside the clay layer. It is also noted that the high temperature DTG peak at 650 °C of NaMMT disappeared or shifted to 550 °C in the DTG curve of Rhodamine B-clay complex.

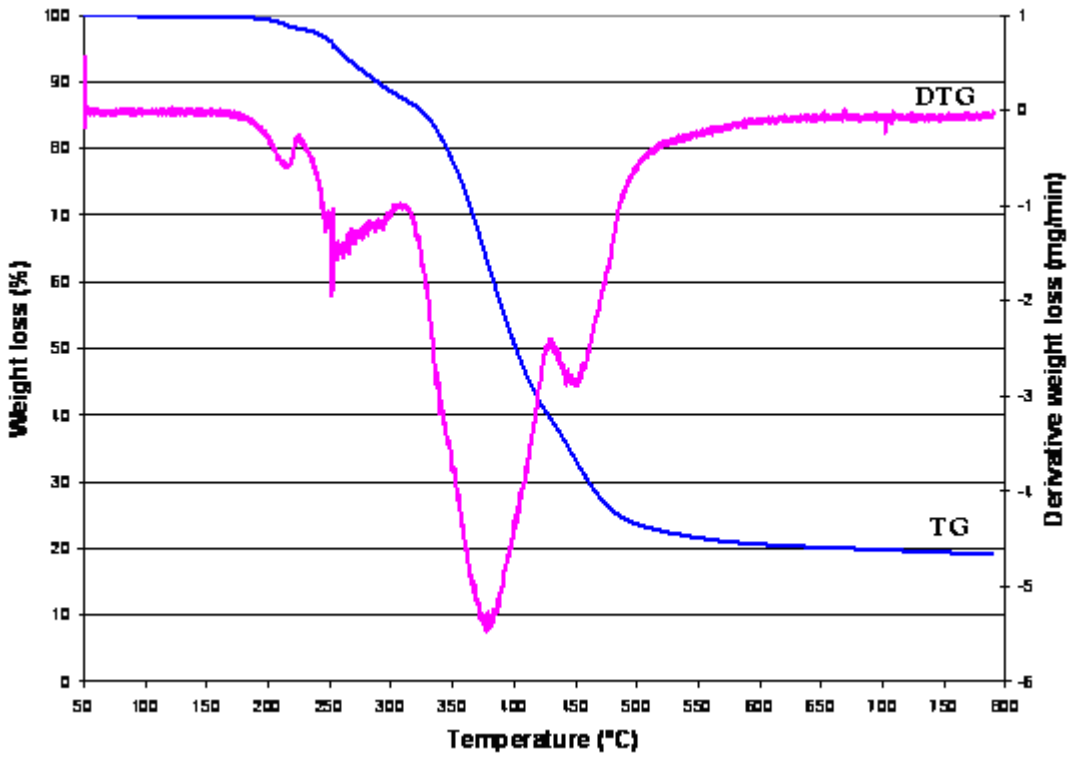

Figure 4-10: TG-DTG curve of neat Rhodamine Dye

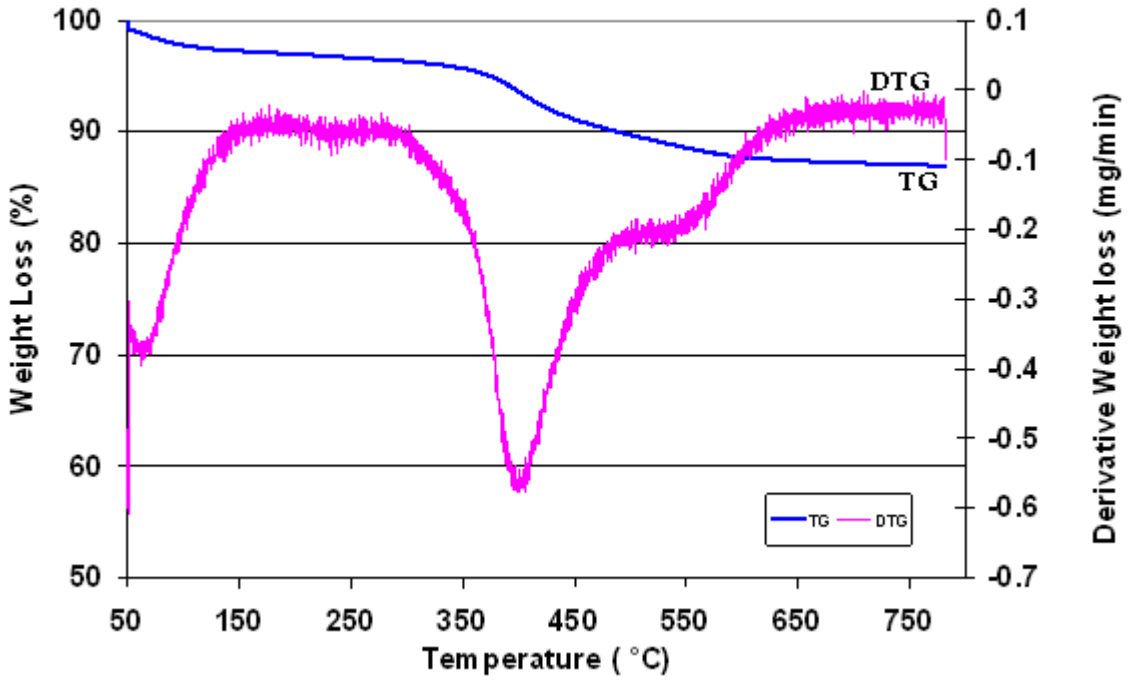

Figure 4-11: TG-DTG curve of Rhodamine dye- unmodified (NaMMT) Clay complex

The TG curve of Solvent dye (Figure 4-12) does not show any considerable weight loss at low temperature range (50- 200 °C) due to hydrophobic nature of the dye. In the second stage of weight loss (200-500 °C) it shows nearly complete decomposition at about 425 °C. DTG curve of Solvent dye-NaMMT complex shows two peaks, one at low temperature (80 °C) and the other at high temperature (650 °C) to that of neat NaMMT clay (Which is similar to unmodified clay; where as this is not the case for Rhodamine B-NaMMT clay complex as shown in Figure 4-11). Only 4% weight loss was

found within the temperature range of 200-500 °C and a DTG peak at about 370 °C (with small peak intensity) was obtained. This observation indicates that there is no interaction between Solvent dye and interlayer cation of the clay minerals as depicted by WAXS characterization. Dye molecules did not penetrate the clay interlayer and the adsorption must have taken place on outer surface O-plane by hydrogen bonds, which can be eliminated by heating at low temperatures.

Yariv et al postulated from their thermal studies of the adsorption of crystal violet by Wyoming montmorillonite[76, 77] and Laponite[78], that the π interactions between aromatic cations and the oxygen plane of the aluminosilicate layer of montmorillonite increase the thermal stability of the dye cation. From this study it was noted that in the organic matter decomposition temperature range (200-500 °C), the main DTG peak of Rhodamine B dye-NaMMT clay complex shifted to higher temperature from that of neat Rhodamine dye, where for Solvent dye- clay complex, the peak lowered from 425 °C to 370 °C. Hence Rhodamine B dye must have participated in π interactions with the oxygen plane of the aluminosilicate layer, conversely Solvent dye does not form any π interaction.

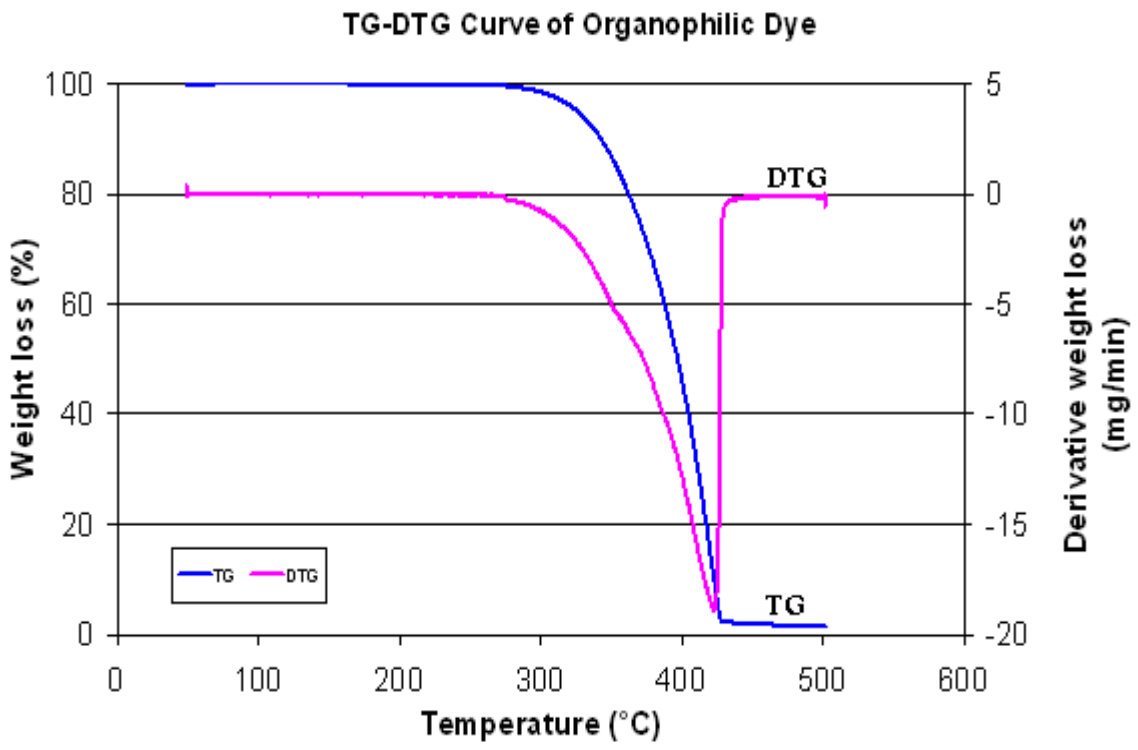

Figure 4-12: TG-DTG curve of Solvent Dye

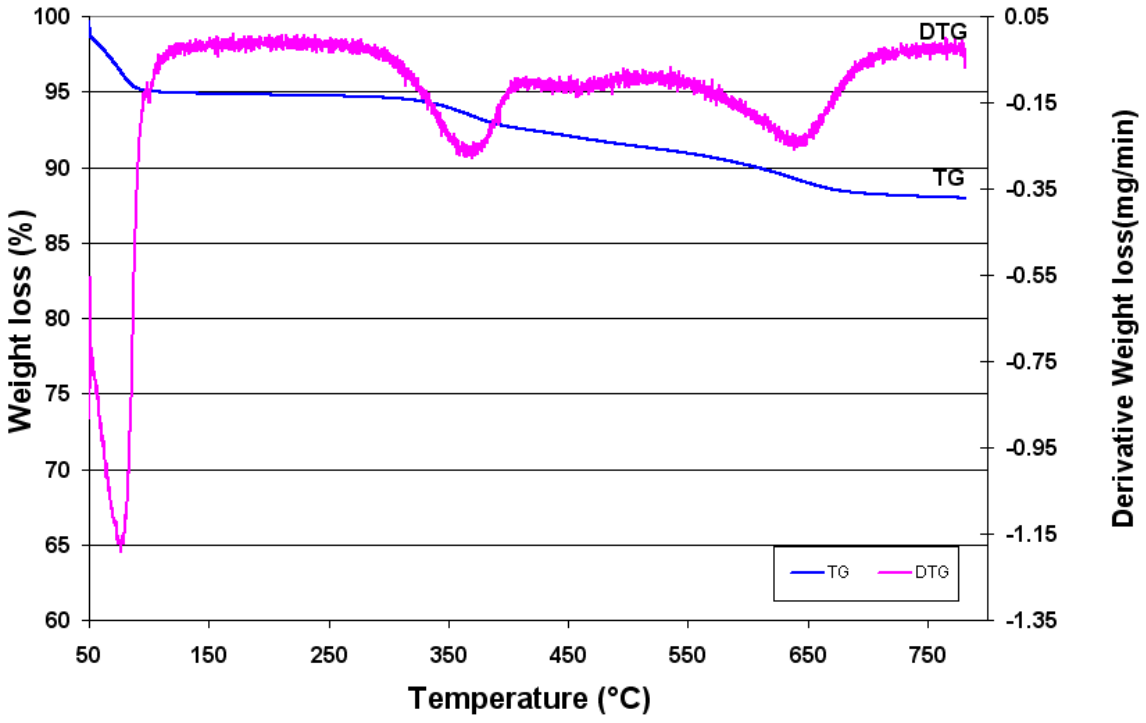

Figure 4-13: TG-DTG curve of Solvent dye-NaMMT Clay complex (SD-NaMMT)

Compound	Clay Content (Wt %)	Organic Dye Content (Wt %)	Temperature Range (°C)	Weight loss (%)	DTG Peaks Temperature(°C)
NaMMT	100	0	50-200	7	80
			200- 500	1	-
			500- 800	3	650
Rhod B Dye	0	100	50-200	0.7	-
			200- 500	76	215, 260, 380,455
			500- 800	5	-
Rhod B-NaMMT Complex	81	19	50-200	3	65
			200- 500	7	405
			500- 800	3	550
Solvent Dye	0	100	50-200	0	-
			200- 500	99	425
			500- 800	0	-
Solvent - NaMMT Complex	79	21	50-200	5	80
			200- 500	4	370
			500- 800	3	650

Table 4-4: Weight loss comparison of unmodified clay-dye complex (& their neat clay and dye) at three stages (dehydration, organic matter decomposition & clay dehydroxylation) with DTG peaks and sample composition of clay and organic dye.

4.3.2 Thermo gravimetric study of Clay- Dye Complex with modified Clay

TG- DTG curve of organoclay (Cloisite 15A) used in this study is shown in Figure 4-14. There was no DTG peak in low temperature range and the TG curve shows less than 1 % weight loss because of the hydrophobic nature of the clay. Decomposition of organic matter begins at 230 °C and it shows about 40 % weight loss between the temperature ranges of 200- 500 °C.

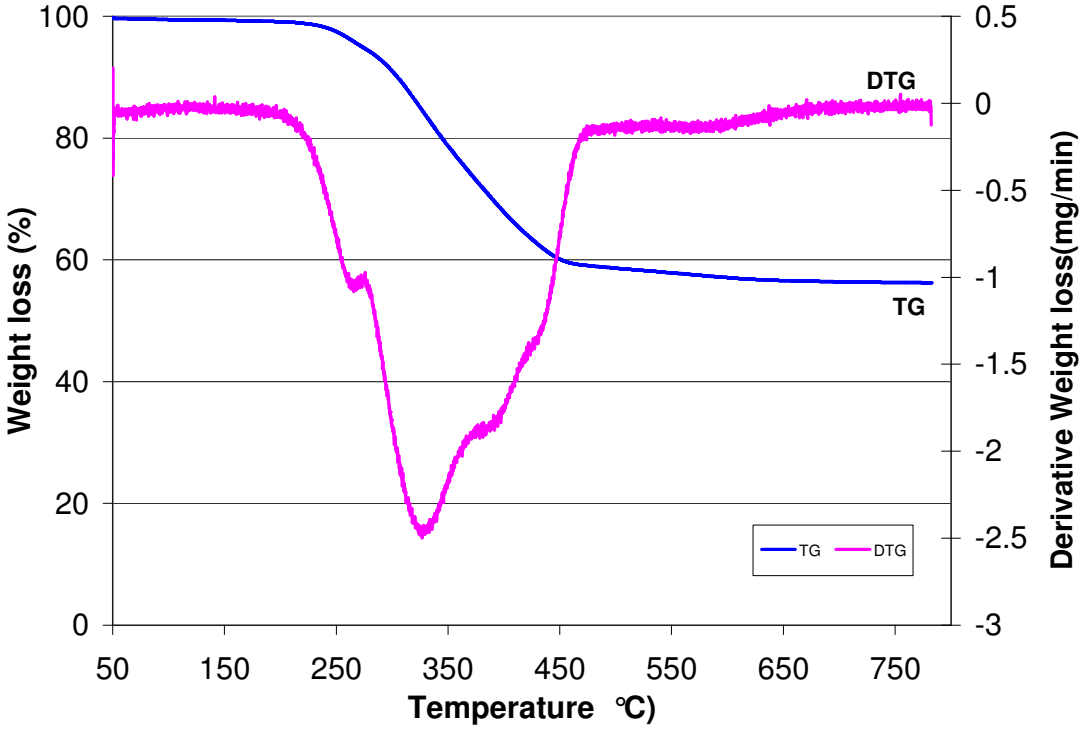

Figure 4-14: TG-DTG curve of neat modified Clay (Cloisite 15A)

TG- DTG curve of Solvent dye- Cloisite 15A clay complex and Rhodamine B dye-Cloisite 15A clay complex were depicted in Figure 4-15 & Figure 4-16respectively. DTG peak of Rhodamine B dye- Cloisite 15 A complex, in the temperature range of 200°C to 500 °C was found identical to that of neat organo clay DTG peak for the same temperature range, but the main peak shifted from 330 °C to 365 °C. On the contrary DTG curve of Solvent dye-Cloisite15A clay complex shows some changes to the DTG peak in that same temperature range. The main peak narrowed and small peak at 270 °C & 395 °C disappeared. This indicates the existence of some interactions between Solvent dye and interlayer alkylammonium cation or with interlayer O-plane.

Expanded layer structure of modified clay (Cloisite 15A, d_{oo}- 3.15 nm) must have enabled the dye molecule to penetrate inside the clay layer. According to Barrer [20] ammonium cations in the organo-clays play the role of a pillar, holding the layers permanently apart without filling all the interlayer space, thus preserving the distance between the layers. When secondary adsorption takes place in organo clays, the nonpolar molecules penetrate into the expanded space between the pillars and the sorption capacity is greatly enhanced. These nonpolar molecules are not intercalated in the parent montmorillonite. Barrer suggested that the secondary adsorption isotherms are of the Langmuir type, indicating that the secondary adsorbed molecule lie parallel to the surface, covering that part of the oxygen plane that is not covered by the ammonium cations, confirming that the nonpolar molecules are bound directly to the oxygen plane.

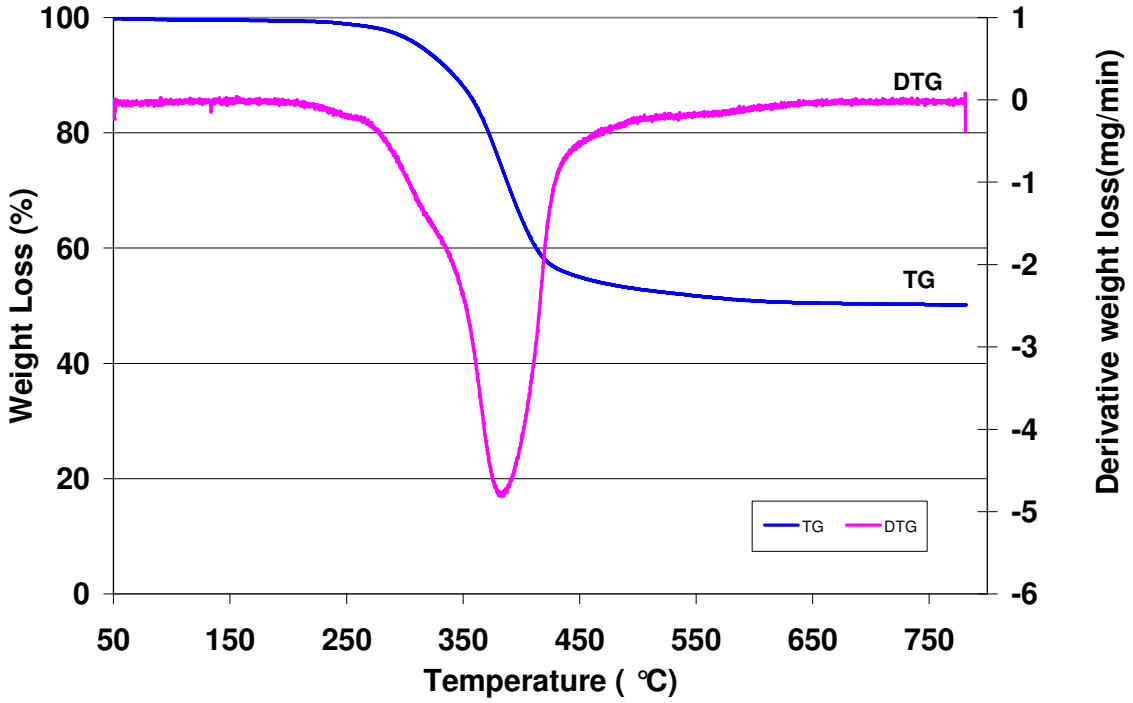

Figure 4-15: TG-DTG curve of Solvent dye-modified Clay (Cloisite 15A) complex

In the case of Solvent dye because of nonpolar nature, it could be possible that secondary adsorption dominates the dye adsorption process of organo-clay rather than cation exchange process between dye molecules and organo cation of the dye. The long alkyl chain part of the dye may bond to the clay interlayer O-plane as Barrer suggested. Oxygen atom of dicarboximide could also form hydrogen bond to long alkyl chain of the quaternary ammonium cation (pillars). TG curve shows that the onset temperature of decomposition of the organoclay-dye complex decreased from that of neat dye decomposition temperature. Decomposition of Solvent dye begins at 285 °C (Figure

4-12), where as Solvent dye- Cloisite 15A complex decomposition starts at 240 °C (Figure 4-15). This negative influence on the thermal stability evidences the presence of alkylammonium cation in organoclay-dye complex. It can be seen in Figure 4-14 that neat organoclay begins to decompose at 230 °C; hence the presence of organic matter from clay lowered the onset of organoclay-Solvent dye complex. As mentioned earlier EDS analysis of Solvent dye-Cloisite 15A complex also confirms the presences of large amount of Solvent dye inside the clay layer.

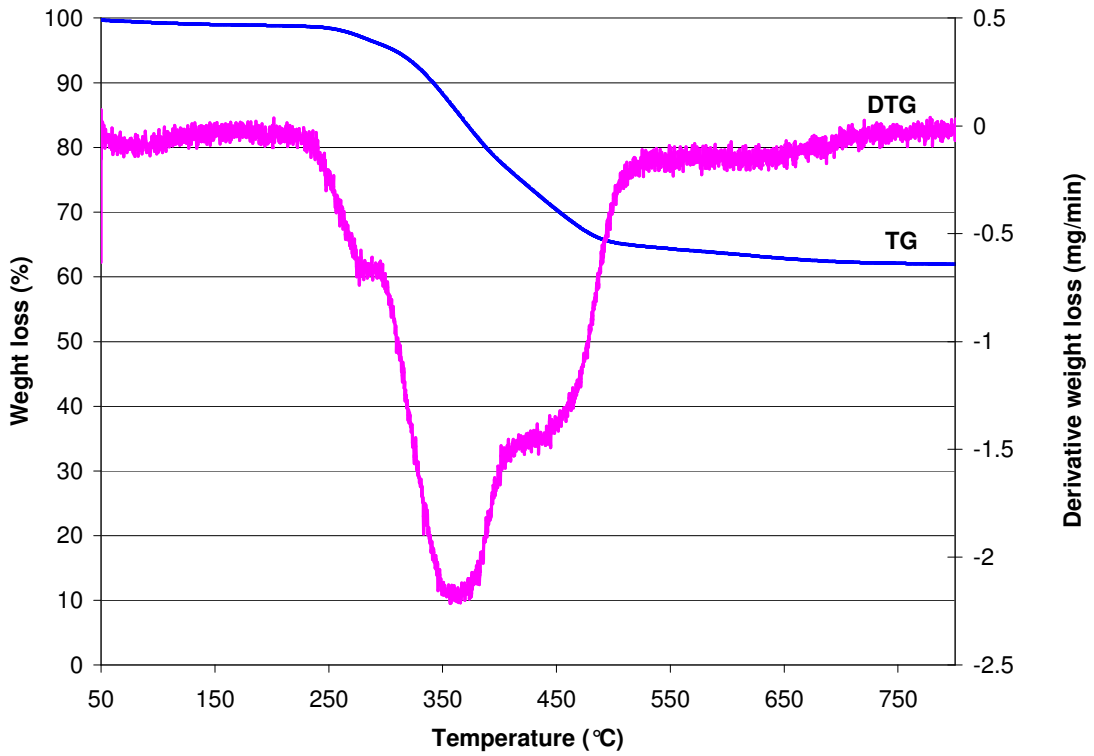

Figure 4-16: TG-DTG curve of Rhodamine dye-modified Clay (Cloisite 15A) complex

Rhodamine dye molecular structure only consists of aromatic rings. In addition the quaternary ammonium cation does not form H-bonds either with proton donors or with acceptors [15]. Therefore there is no interaction between Rhodamine B dye and the inter layer O-plane of the modified clay. However as indicated by WAXS results if some of the alkyl ammonium cation was removed by the influence of nonpolar organic solvent (DCM) and the dye, it will allow small amount of Rhodamine B dye molecule to replace the O-plane that was previously occupied by alkyl ammonium cation.

Organic matter decomposition onset temperature of Rhodamine B dye- Cloisite 15A clay complex was found to be 230 °C (Figure 4-16) where decomposition onset of neat Rhodamine B dye was 230 °C and Rhodamine B dye- clay complex that was prepared with unmodified clay shows onset temperature of 280 °C. This suggests that organo matter of the clay dominates the decomposition rather than the Rhodamine dye.

Compound	Clay Content (Wt %)	Alkyl ammonium Content (Wt %)	Organic Dye Content (Wt %)	Temperature Range (°C)	Weight loss (%)	DTG Peaks Temperature(°C)
Cloisite 15A	60	40	0	50-200	1	-
				200- 500	40	270,330,395
				500- 800	2	-
Rhod B Dye	0	0	100	50-200	0.7	-
				200- 500	76	215, 260, 380,455
				500- 800	5	-
Rhod B-Cloisite15A Complex	40.8	27.2	32	50-200	1	85
				200- 500	34	280, 365. 450
				500- 800	3	550
Solvent Dye	0	0	100	50-200	0	-
				200- 500	99	425
				500- 800	0	-
Solvent Dye-Cloisite 15 A Complex	38.4	25.6	36	50-200	0.6	-
				200- 500	48	385
				500- 800	2	-

Table 4-5: The weight loss comparison of modified clay-dye complex (& their neat clay and dye) at three stages (dehydration, organic matter decomposition & clay dehydroxylation) with DTG peaks and sample composition of clay and organic dye.

Table 4-5 summarizes the weight loss of organoclay-dye complex and their neat clay, dye at three stages (dehydration of water, organic matter decomposition & clay mineral dehydroxylation) with DTG peaks and sample composition of clay mineral, organo content of the clay and organic dye. From Southern Clay products Technical data sheet of Cloisite 15A, it is noted that clay consist about 40 % alkyl ammonium compound by weight and it shows nearly 40 % weight loss in the organic matter decomposition temperature range(200- 500 °C). According to clay : dye ratio used to prepare the sample, the organo content of Rhodamine B-Cloisite 15A complex is about 59.2 % organic matter(alkyl ammonium compound + Rhodamine B dye) and its TG curve shows about 34 % weight loss in the organic matter decomposition temperature range. Similarly as Solvent dye-Cloisite 15A complex consists of 61.6 % organic matter (alkyl ammonium compound + Solvent dye) and TG curve gives around 48 % weight loss. This indicates the presence of both (dye & alkyl ammonium cation) in the sample. According to Stoichiometric ratio organic content of both Rhodamine B dye- organoclay complex and Solvent dye organo clay complex samples slightly varies (59.2 % & 61.6 %) but Solvent dye-organoclay complexes shows quite large (48 %) weight loss in organic matter decomposition temperature than Rhodamine B dye- organoclay complex (34 %); suggesting large amount of Solvent dye adsorbed by modified clay. However it is difficult to verify the actual dye: alkyl ammonium compound ratio that was present in the sample and the form of attachment/ or interaction to the clay minerals, with this TGA analysis method.

4.4 Intercalation Study with modified Solvent Dye and Unmodified Clay

In the process of chemical dye modification solvent dye was modified from organophilic form to hydrophilic form of dye. The long alkyl group was removed and replaced by a short alkyl quaternary ammonium ion. Therefore with modified Solvent dye it was expected cation exchange reaction to occur between quaternary ammonium cation and clay interlayer O-plane.

4.4.1 XRD Characterization

Figure 4-17 compares interlayer space expansion of modified Solvent dye intercalated NaMMT with neat NaMMT. It shows d-space increased from 1.24 nm to 1.4 nm. This suggests aromatic entities of dye molecule lie parallel to the silicate layers. The possible type of dye-smectite association would be B2 type as designated in figure 2.2 (section 2.4.7) According to Yariv[15] a basal spacing of less than 1.4 nm does not permit any kind of aggregation of the dye cation to take place inside the interlayer space. The adsorbed dye cation probably forms monolayers of monomeric species in the interlayers, with aromatic rings lying parallel to the silicate layer.

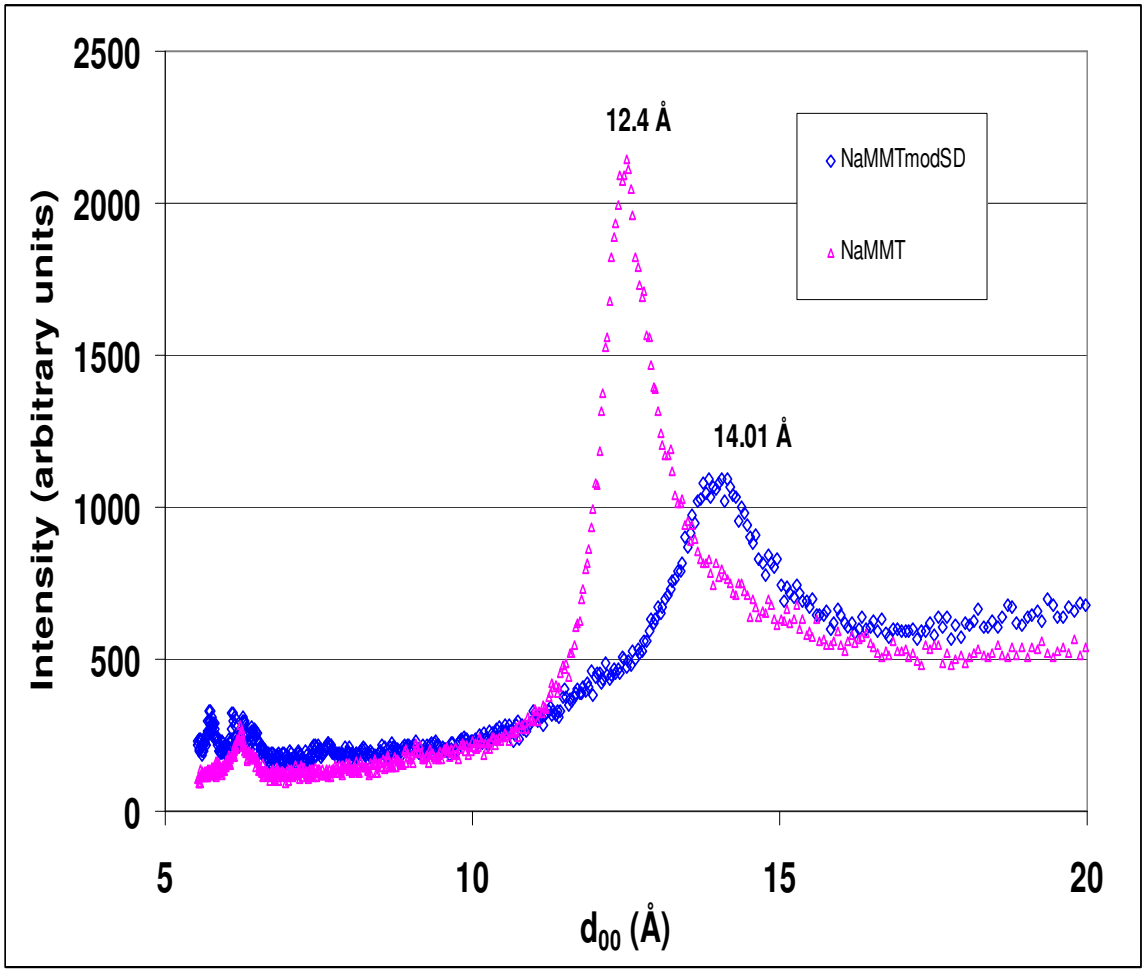

Figure 4-17: WAXS curves (Intensity versus d-spacing) of modified Solvent dye (SD) - NaMMT Clay complex comparison with neat NaMMT.

4.4.2 Thermogravimetric Analysis of Modified Solvent dye- NaMMT complex

TG-DTG curve of neat modified Solvent dye and modified Solvent dye- NaMMT complex are depicted in Figure 4-18 & Figure 4-19 respectively. When we compare modified Solvent dye TGA/ DTG results with Rhodamine dye it can be seen that type of cation greatly influences the interaction between clay interlayer O-plane and dye cation. In the case of Rhodamine B dye main DTG peak in organic matter decomposition temperature range (200- 500 °C) shifted to higher temperature (from 380 to 405 °C); where for modified Solvent dye this DTG peak shifted to lower temperature (see Table 4-6 first peak shifted from 320 to 305 and 2nd peak shifted from 450 to 415 °C). Also it can be seen in Table 4-6 that low temperature weight loss for Rhodamine B-NaMMT complex reduced from 7% to 3 % compared to that of neat NaMMT and clay mineral dehydroxylation DTG peak (650 °C for neat NaMMT) disappeared or shifted to very low temperature and overlapped with organic matter decomposition DTG peak, on the contrary for Solvent dye- NaMMT complex shows same amount of weight loss in the low temperature range due to dehydration and high temperature (clay mineral dehydroxylation). This is clearly visible at 570 °C in the DTG peak, which shifted from 650 to 570 °C. This suggests that the position of the quaternary ammonium ion in the cationic dye molecule affects the specific π interaction between oxygen planes of silicate layer cationic dye that facilitate thermal stability. In the Rhodamine B dye structure, quaternary ammonium ion directly attached to the carbon atom of the aromatic ring

where as in the case of modified Solvent dye quaternary ammonium ion attached to the nitrogen atom of the aromatic ring by a short alkyl chain.

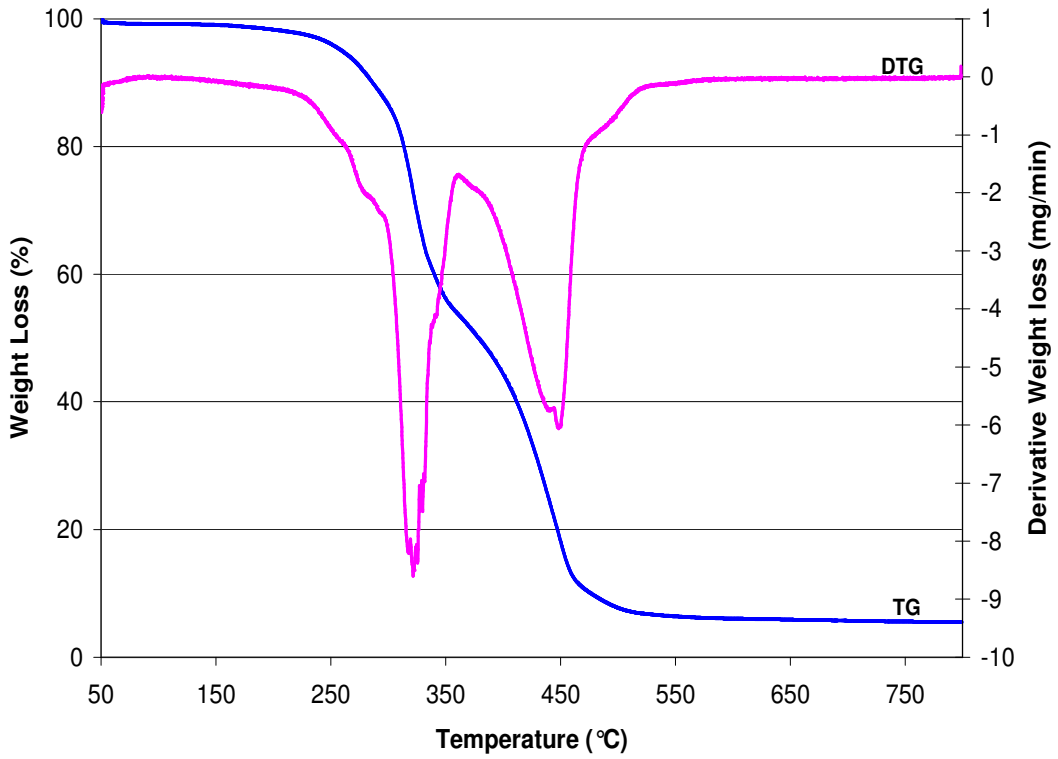

Figure 4-18: TG-DTG curve of modified Solvent dye

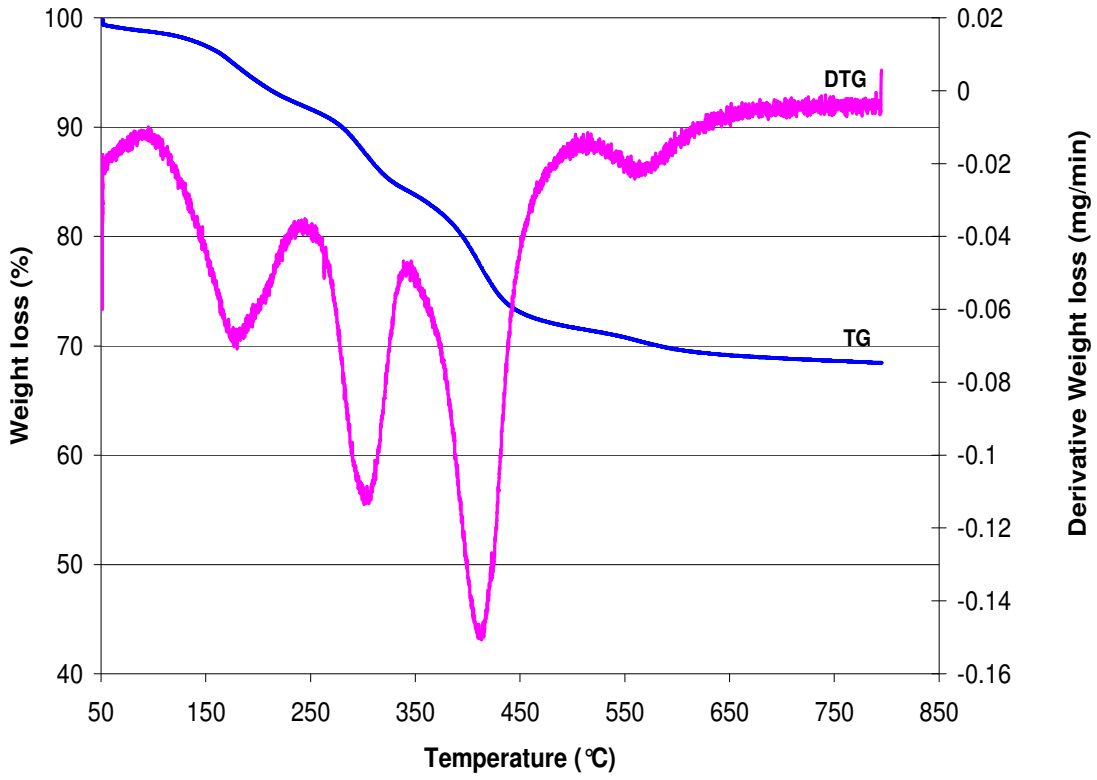

Figure 4-19: TG-DTG curve of modified Solvent dye with NaMMT Clay

Table 4-6: The weight loss comparison of modified Solvent dye-NaMMT complex (& their neat clay and dye) at three stages (dehydration, organic matter decomposition & clay mineral dehydroxylation) with DTG peaks

Compound	Temperature Range (°C)	Weight loss (%)	DTG Peaks Temperature(°C)
NaMMT	50-200	7	79
	200- 500	1	-
	500- 800	3	650
Modified Solvent dye	50-200	2	-
	200- 500	91	320, 450
	500- 800	2	-
Modified Solvent dye-NaMMT Complex	50-200	7	180
	200- 500	22	305, 415
	500- 800	3	570

4.5 Thermal Stability Study of Pigmented polymer Nanocomposites

The thermal stability of clay polymer nanocomposites (CPNC) very much depends on the relative flammability, the amount of the matrix polymer and the organoclay intercalant [60]. Thermogravimetric analysis (TGA) is often carried out to measure high temperature stability of CPNC. The TGA results are usually presented in the form of three parameters: T_{10} (°C), T_{50} (°C) and char content (wt %). The first two indicating the temperature at which 10 or 50 % weight loss was recorded, and the last represents the fraction of material which remains at 600 °C.

4.5.1 Thermal Stability of unmodified clay based Dye Pigment Polymer Nanocomposites

TG-DTG curve of unmodified clay based dye Pigment Polymer Nanocomposites of Rhodamine B and Solvent dye are shown in Figure 4-20 and Figure 4-21 respectively. The temperature of 10 %, 50 % weight loss and char content at 600 °C for neat dye and unmodified clay dye pigment and modified clay dye pigment are summarized in Table 4-7 & Table 4-8. In the case of Rhodamine B-NaMMT-PS composite, with the clay content of ~0.9 % it shows significant improvement in thermal stability. 10 % and 50 % weight loss temperature increased by 4 °C and 20 °C respectively from that of neat Rhodamine B dye- PS composite. DTG peak shifted from 428 °C to 450 °C. On the contrary for Solvent dye- NaMMT -PS nanocomposites with the clay content of ~0.8 % it

does not show any significant change in thermal stability. 10 % & 50 % weight loss temperature decreased by 1 °C from that of neat Solvent dye –PS composites.

This suggests that some specific interactions between organic cationic dye and clay layer should be the cause for the thermal stability enhancement. Rhodamine B dye is more likely to have some interactions with the clay layer where as Solvent dye has no interactions between clay layer, thus there is no improvement in thermal stability.

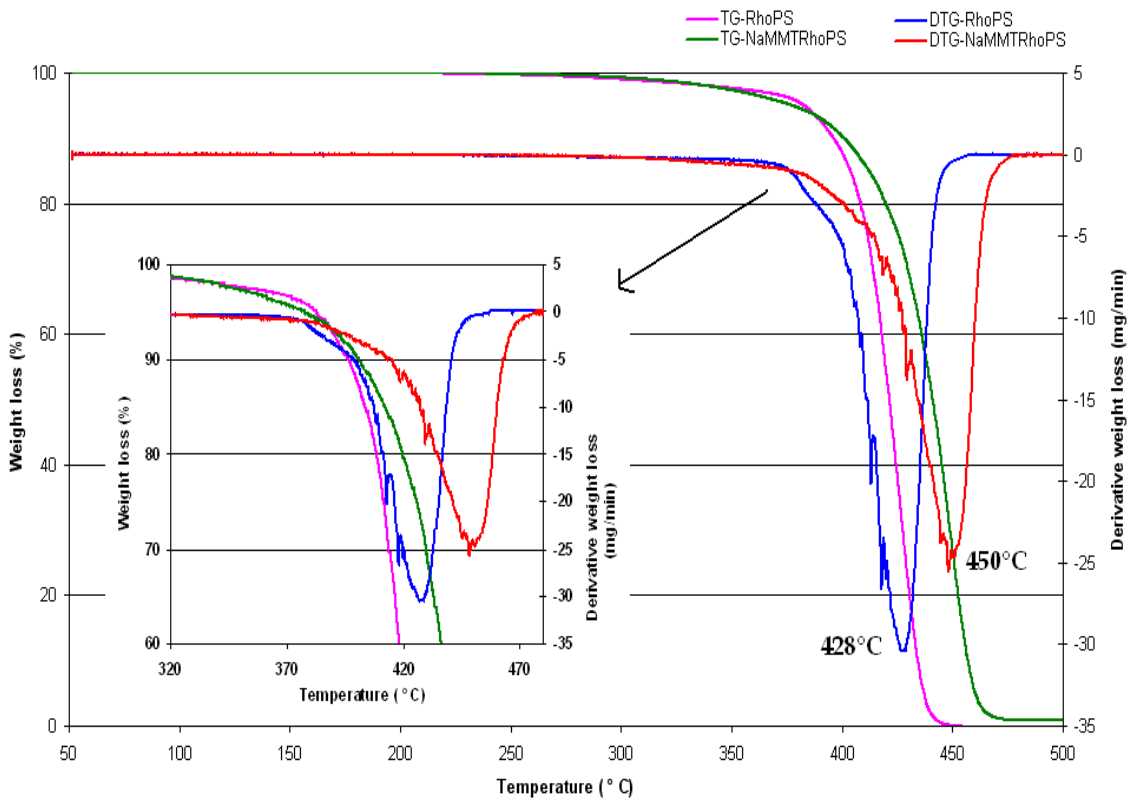

Figure 4-20: TG-DTG curve of unmodified clay based Rhodamine B dye pigment polymer nanocomposites (Rhod B-NaMMT-PS)

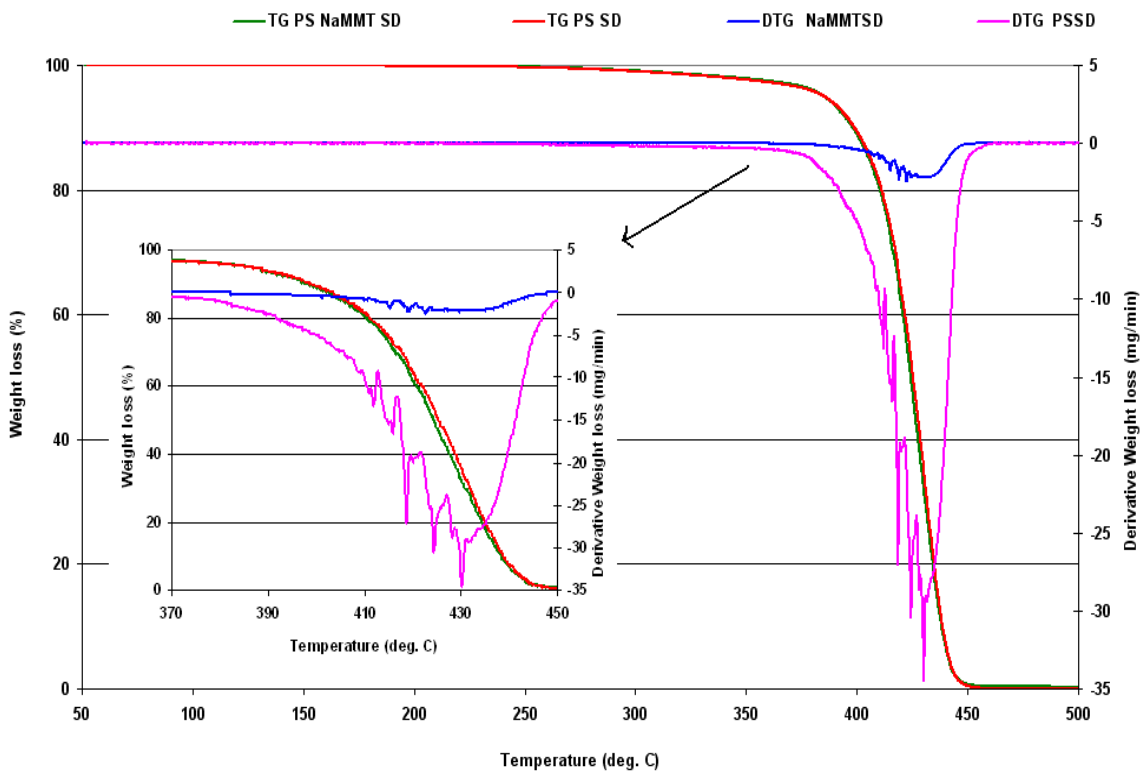

Figure 4-21: TG-DTG curve of unmodified clay based Solvent dye pigment polymer nanocomposites (PS -NaMMT- SD)

Table 4-7: The temperature of 10 %, 50 % weight loss and char content at 600 °C for neat Rhodamine B dye and its clay dye pigment

	PS-Rhod B	PS-Rhod B NaMMT	PS-Rhod B Cloi 15A
Clay (mineral only) content (%)	0	~0.9	~0.4
T_{10} (℃)	396	400	393
T_{50} (℃)	421	441	425
Char Content at 600℃ (%)	0	0.66	0.36

Table 4-8: The temperature of 10 %, 50 % weight loss and char content at 600 °C for neat solvent dye and its clay dye pigment

	PS-SD	PS-SD NaMMT	PS-SD Cloi 15A
Clay (mineral only) content (%)	0	~0.8	~0.3
T_{10} (℃)	399	398	399
T_{50} (℃)	425	424	426
Char Content at 600℃ (%)	0	0.25	0.28

4.5.2 Thermal Stability of modified clay based Dye Pigment Polymer Nanocomposites

TG-DTG curve of modified clay (Cloisite15A) based Pigmented Polymer Nanocomposites of Rhodamine dye and Solvent dye are depicted in Figure 4-22 & Figure 4-23 respectively. Rhodamine B-Cloisite 15A clay-PS composites consist of about 0.4 % clay mineral. It shows that 10 % weight loss temperature decreases from 396 °C to 393 °C for that of neat Rhodamine B-PS composites. This may be attributed due to the presence of alkyl ammonium molecule. Several researches reported that MMT intercalated with a long chain aliphatic quaternary ammonium cation is unstable at temperatures above 180 or 200 °C [55]. It is also noted that 50 % weight loss temperature increased by 4 °C. This indicates the possibility that some Rhodamine B dye

molecules are attached to the clay inter layer surface (i.e. partial replacement of alkyl ammonium by Rhodamine B cation). Solvent dye-Cloisite 15A- PS composites do not show any considerable change in thermal stability.

Therefore cationic dye interaction with the clay interlayer surface enhances the thermal stability of polymer clay nanocomposites. The level of clay content greatly influences the thermal stability. The presence of long chain aliphatic quaternary ammonium cation lowers the thermal stability of polymer clay nanocomposites

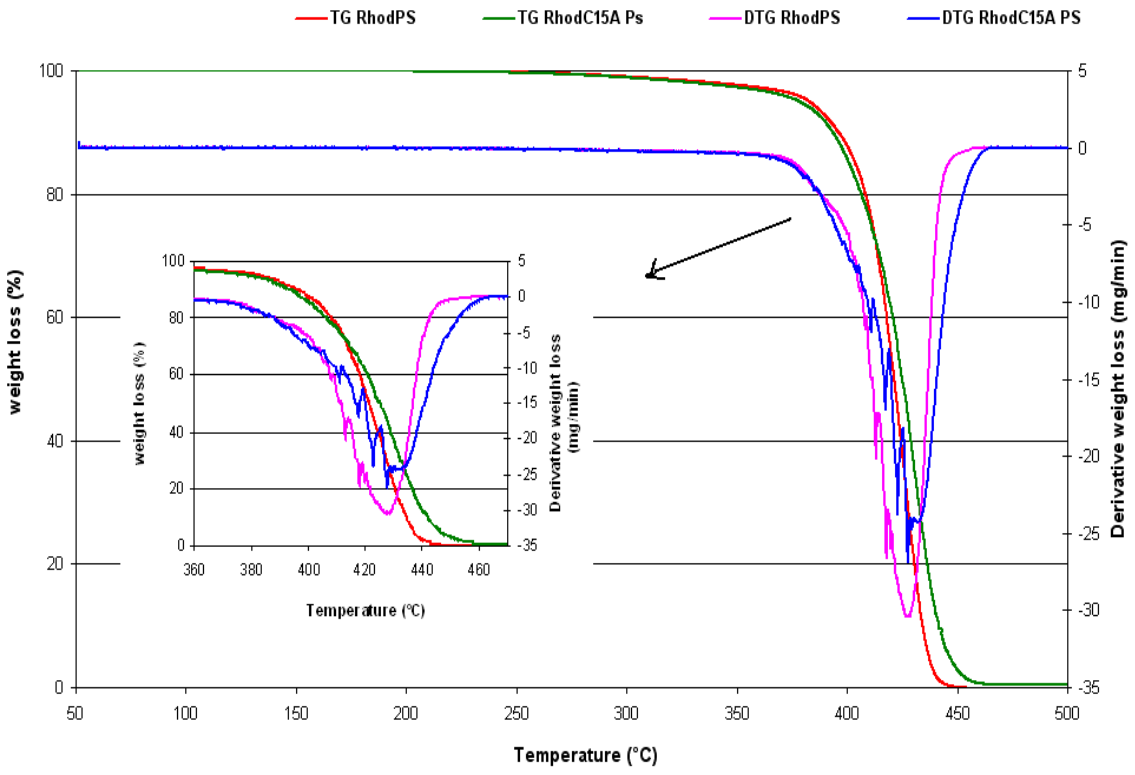

Figure 4-22: TG-DTG curve of modified clay based Rhodamine dye pigment polymer nanocomposites (Rhod B-C15A-PS)

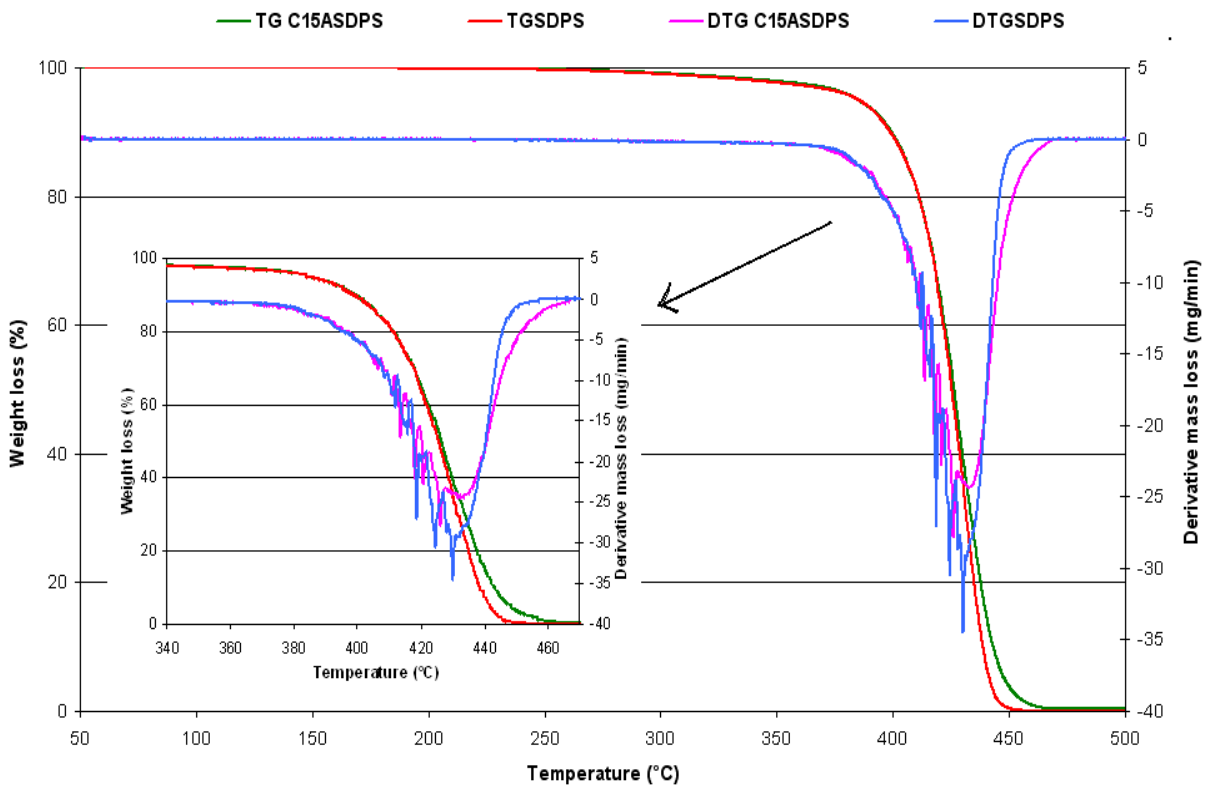

Figure 4-23: TG-DTG curve of modified clay based Solvent dye pigment polymer nanocomposites (PS -C15A- SD)

4.6 Ultra Violet (UV) Stability Study of clay dye pigment polymer nanocomposite

The UV stability of clay dye pigment polymer nanocomposite samples was studied using the test method that covers an accelerated procedure intended to determine the resistance to color change of plastics in typical environments. The test method followed is similar to ASTM D 4674-89. Color change was evaluated by monitoring the visual change throughout the course of the exposure time. Samples were irradiated in the air.

Figure 4-24 shows visual color change of Rhodamine B dye dispersed in Polystyrene (Rhodamine B-PS marked as **1**) after 8 hours of irradiation in comparison with Rhodamine B clay dye pigment with NaMMT (Rhodamine B NaMMT- PS, marked as **2**)and Rhodamine B clay- dye pigment with Cloisite 15 A (Rhodamine B Cloisite15 A- PS, marked as **3**). Exposed area marked as UV. It can be seen that the exposed area of neat Rhodamine B-PS sample lost its transparency and shows discoloration. On the other hand there is no visible change between exposed area and unexposed area for Rhodamine B NaMMT- PS sample. Rhodamine B Cloisite15 A- PS sample shows noticeable color change for the same exposure time. Color change at exposed area for this sample was pale whitened rather than darkening like neat Rhodamine B-PS sample; indicating the presence of long chained alkyl ammonium ion which has poor stability against high energy.

As shown in Figure 4-25 Solvent dye did not show any significant increase in UV stability for both Solvent dye- clay pigment with Cloisite 15A (SD Cloi15A- PS, marked as **2**)and Solvent dye- clay pigment with NaMMT (SD NaMMT- PS, marked as **3**). Unlike Rhodamine B dye, neat Solvent dye-polystyrene sample (SD - PS, marked as **1**) itself shows stability up to 140 hours of UV-irradiation. Similarly modified Solvent dye also did not show (as shown in Figure 4-26) any significant color change for NaMMT based dye pigment polymer (PS) sample compared to neat modified Solvent dye polymer (PS) sample for up to 156 hours of UV irradiation.

The reason for the reduced color degradation in presence of clay was not clearly identified. One possible explanation for increased UV stability arises from barrier action of exfoliated clay layers. Clay layers act as an energy barrier and shelter the organic dye and polymer molecules from high energy load; thus increases the UV stability. However if that is the case then Solvent dye- NaMMT clay pigment incorporated polystyrene sample should also show increased stability compared to neat Solvent dye polystyrene sample for the same exposure time. Therefore as mentioned in section 2.9 it is believed that stabilization occurs due to some specific intermolecular interactions of cationic dye at the clay surface. As Margulies et al [13] described, the energy absorbed by polymer molecule from the UV-radiation may be transferred to organic dye (due to intermolecular interactions between organic dye and polymer) and this energy is immediately transmitted on to the surface of the clay layer via π interaction of cationic dye, which prevents the high energy load to the organic dye molecules and the polymer.

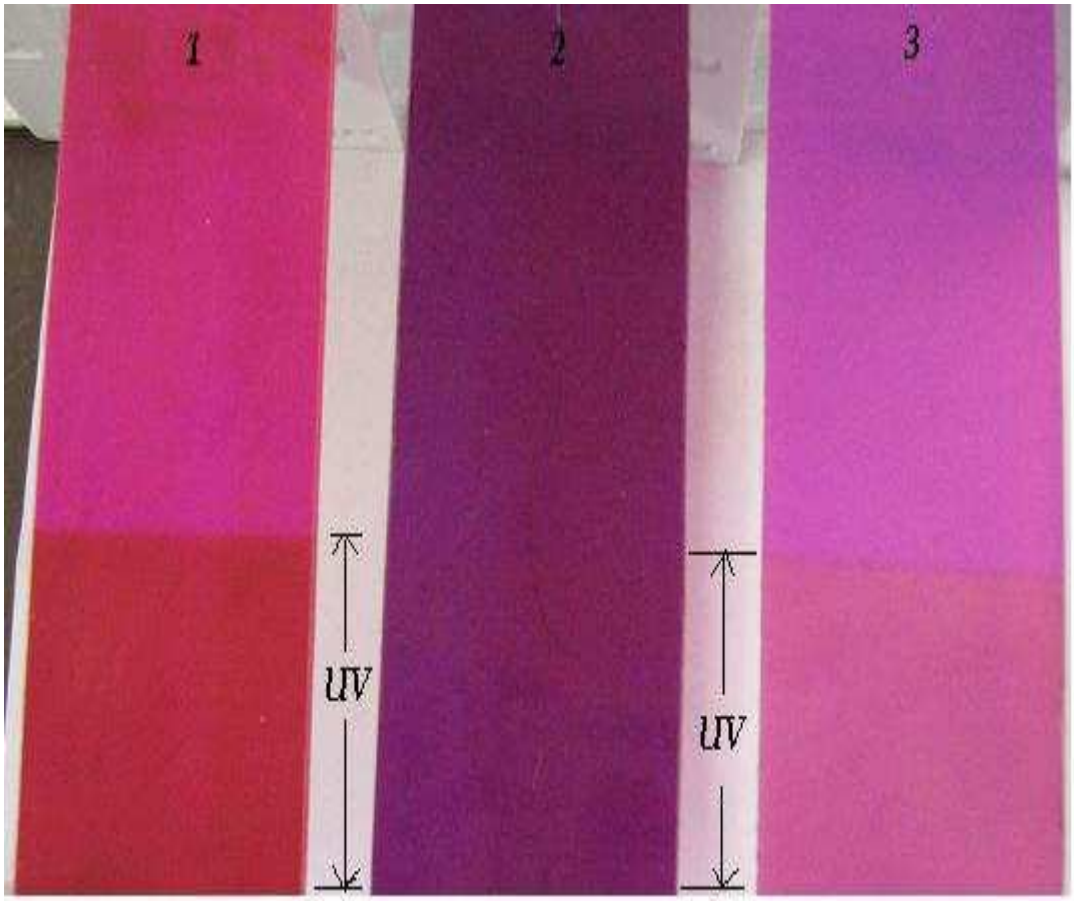

Figure 4-24: Rhodamine B Dye-Polystyrene Composite (1), Rhodamine B Dye-NaMMT Polystyrene Composite (2) Rhodamine B Dye-Cloisite 15A Polystyrene Composite (3) After 8 hrs. of UV-irradiation. (Exposed area to UV irradiation marked as 'UV')

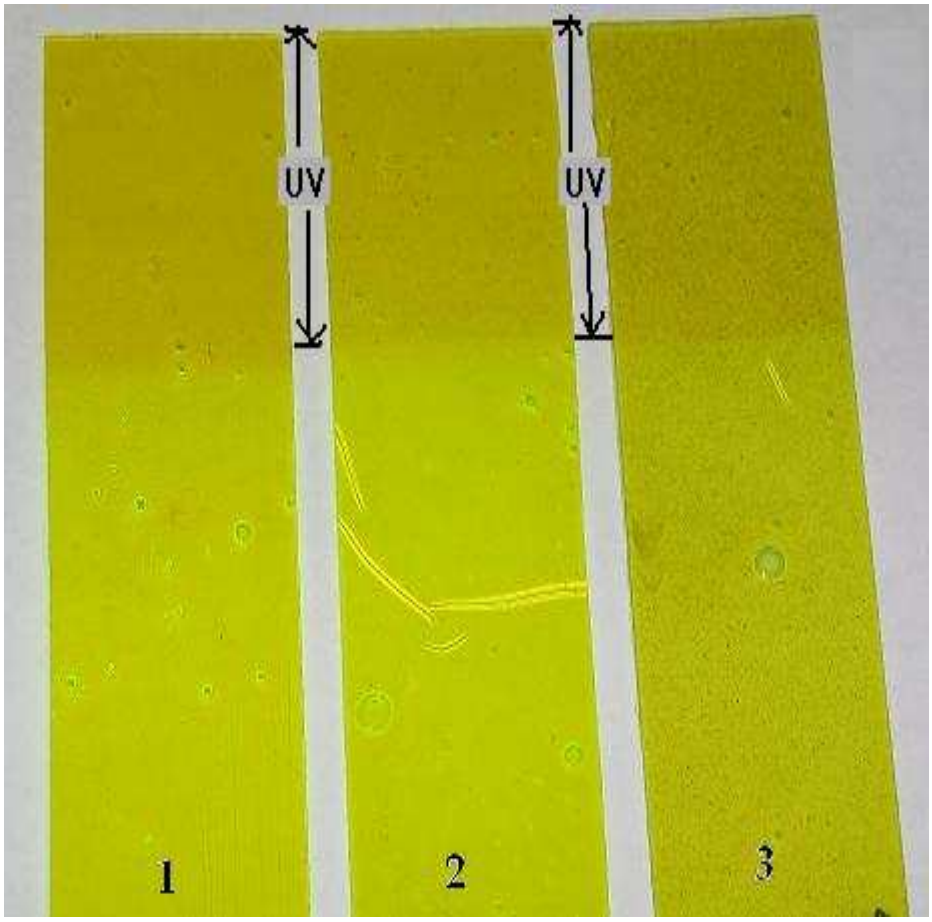

Figure 4-25: Solvent Dye-Polystyrene Composite (1), Solvent Dye- Cloisite 15A Polystyrene Composite (2) Solvent Dye- NaMMT Polystyrene Composite (3) After 140 hrs. of UV-irradiation (Exposed area to UV irradiation marked as 'UV')

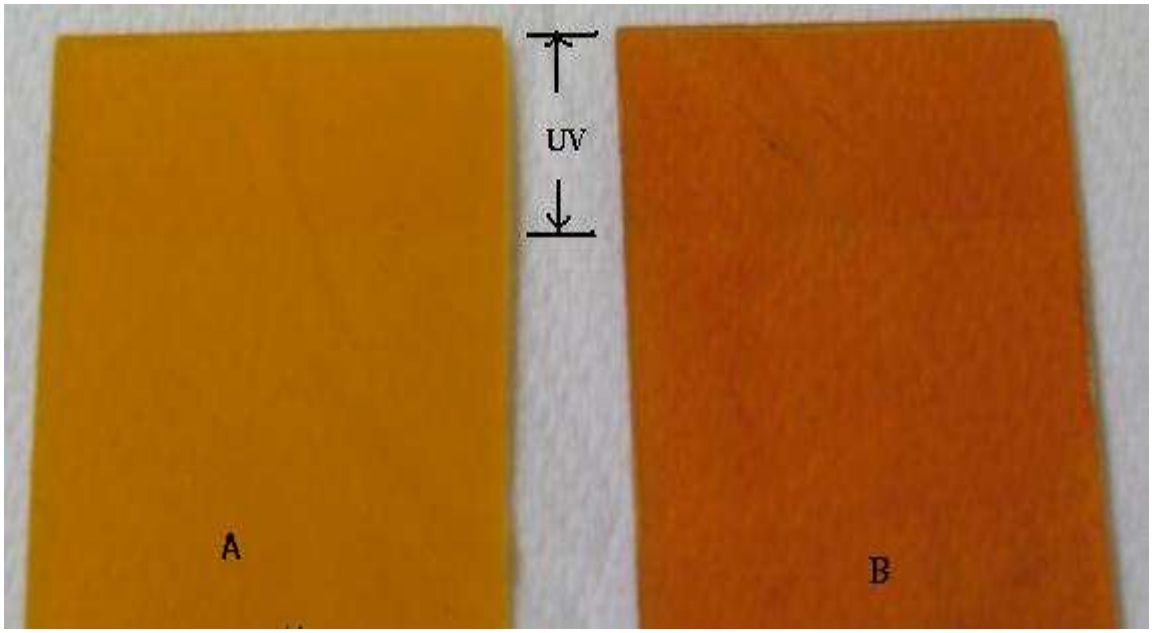

Figure 4-26: Modified Solvent Dye-Polystyrene Composite (A), modified Solvent Dye- NaMMT Polystyrene Composite (B) After 156 hrs. of UV-irradiation. (Exposed area to UV irradiation marked as 'UV')

CHAPTER 5: Conclusion

The following conclusions can be drawn from the experimental results aspects of this thesis.

Wide-angle x-ray scattering (WAXS) analysis of the unmodified clay based dye- pigment samples showed larger d-space increase (Δd= 6.58 Å) for Rhodamine B dye, where as in the case of Solvent dye (SD) –clay complex it showed small increase in d-spacing. This revealed that intercalation of the cationic dye (Rhodamine B) into the interlayer space of unmodified montmorillonite clay was successfully performed by the ion exchange method in aqueous medium. On the contrary solvent dye molecules are more likely to be absorbed onto the clay outer surface oxygen plane (by the formation of monolayer chemisorbed molecules or by hydrogen bonding due to carbonyl group oxygen domination in protonation site rather than the NH_2 group).

SAXS analysis of clay- dye complex, prepared with modified clay in the non aqueous medium showed decrease of d-spacing from the d-spacing of that actual organo clay (Cloisite 15 A: d_{00}= 31.5 Å) for both dyes (Rhodamine B Cloisite 15 A complex: d_{00}= 25.1 Å , Solvent dye- Cloisite 15 A complex: d_{00}= 24.1 Å) suggesting the partial desorption of alkyl ammonium molecule from the organo clay inter layer by organic dye molecule and hence the possible partial replacement of dye molecule to the clay surface

Transmission electron microscopy (TEM) analysis visually confirmed the interlayer space expansion of cationic dye-unmodified clay (Rhodamine B dye-NaMMT) complex

sample and interlayer space decrease for solvent dye-modified clay (SD-Cloisite 15 A) complex. Energy dispersive spectroscopy (EDS) study of solvent dye-modified clay confirmed the penetration of solvent dye into the interlayer of modified clay, located inside the clay layer.

TGA- DTG analysis of unmodified clay based dye-pigment samples revealed that the adsorption of the organic cationic dye (Rhodamine B) mainly takes place inside the clay interlayer space and increases its thermal stability; the main DTG peak of organic matter decomposition temperature range shifted to a higher temperature for Rhodamine B-NaMMT clay complex compared to that of neat Rhodamine B dye (shifted from 380 °C to 405° C). On the contrary the adsorption of solvent dye only takes place on the external surface of the clay and that decreases its thermal stability; the main DTG peak of Solvent dye-NaMMT clay complex shifted to a lower temperature compared to that of neat Solvent dye (Organic matter DTG peak shifted from 425°C to 370° C)

TGA- DTG analysis of modified clay based dye-pigment samples obtained from non aqueous medium indicated the incomplete desorption of clay interlayer alkyl ammonium cation by organic dye molecule for both dyes. DTG curve of solvent dye modified clay complex (Solvent dye-Cloisite 15A) differed from that of neat organo clay (Cloisite 15A), where DTG curve of cationic dye- modified clay sample showed identical DTG peak to that of neat organo clay. This suggests that dye molecular structure and the intercalation medium greatly influenced the intermolecular interactions between the interlayer alkyl ammonium molecule and organic dye molecule.

Intercalation of modified solvent dye into the unmodified clay study with WAXS showed d-space increase from 12.4 Å to 14.01 Å. This suggested the possibility of aromatic entities of dye molecule lying parallel to the silicate layers. DTG peaks of organic matter decomposition shifted to lower temperature to that of neat modified solvent dye; comparing this observation with cationic dye- clay complex (Rhodamine B-NaMMT complex shows DTG peak shift to higher temperature) suggests that the position of the quaternary ammonium ion in the organic dye molecule effects the specific π interaction between oxygen planes of silicate layer and organic dye that facilitates thermal stability.

Thermal and UV stability study of clay-dye pigment incorporated polymer nanocomposites showed significant improvement in thermal and UV stability by cationic dye intercalation into the clay layer. Rhodamine B-NaMMT polymer nanocomposites showed no visible change after 8 hours of UV irradiation; and in the TGA analysis temperatures for 10 % and 50 % weight loss increased by 4 °C and 20 °C respectively, However for the clay content of ~0.9 % (where solvent dye adsorbed on the outer surface of the clay), no significant improvement in the thermal and UV stability was observed. In the case of modified clay dye pigment the presence of remaining long chain aliphatic quaternary ammonium cation (which has poor stability against high energy) shows poor UV stability against UV exposure and it lowers the thermal stability of the polymer clay nanocomposites.

Appendix A

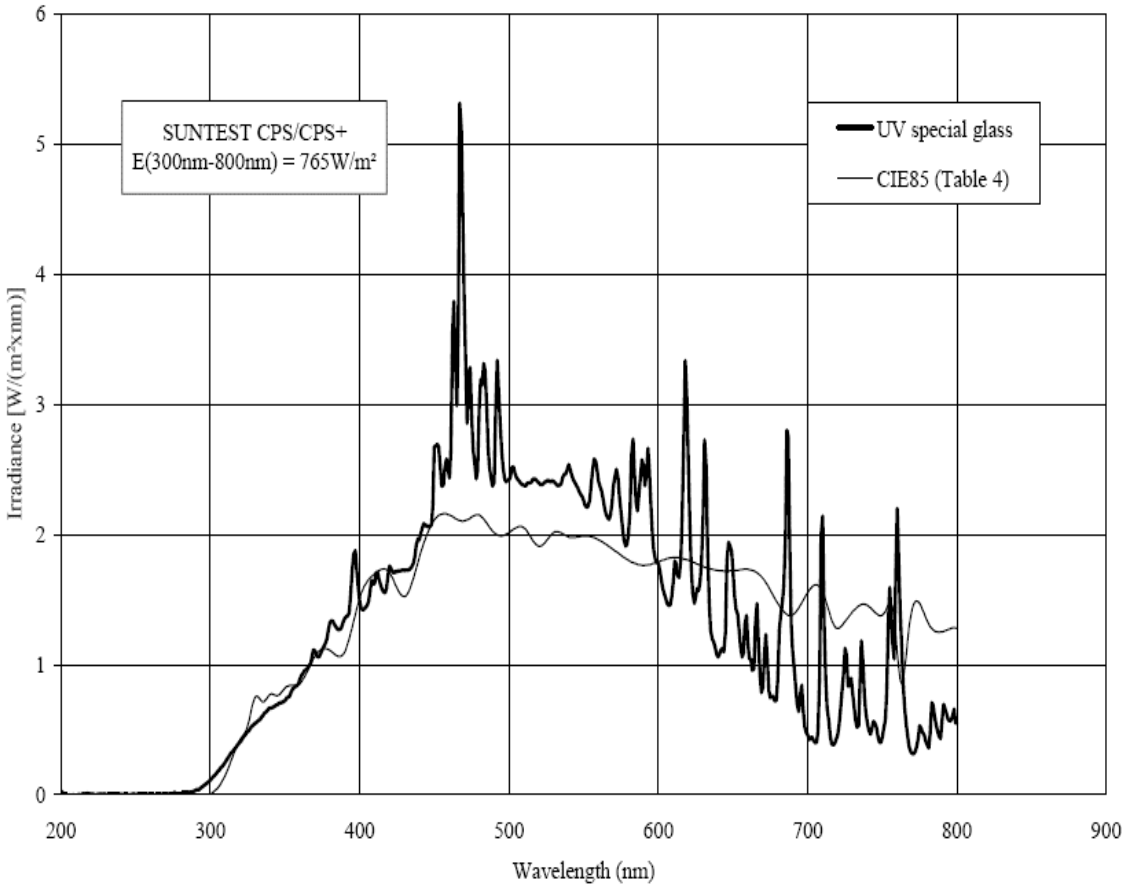

Figure A.1: Spectral distribution of Suntest CPS/CPS+ with additional filters.

Adopted from Suntest CPS/CPS+ Operating Manuel.

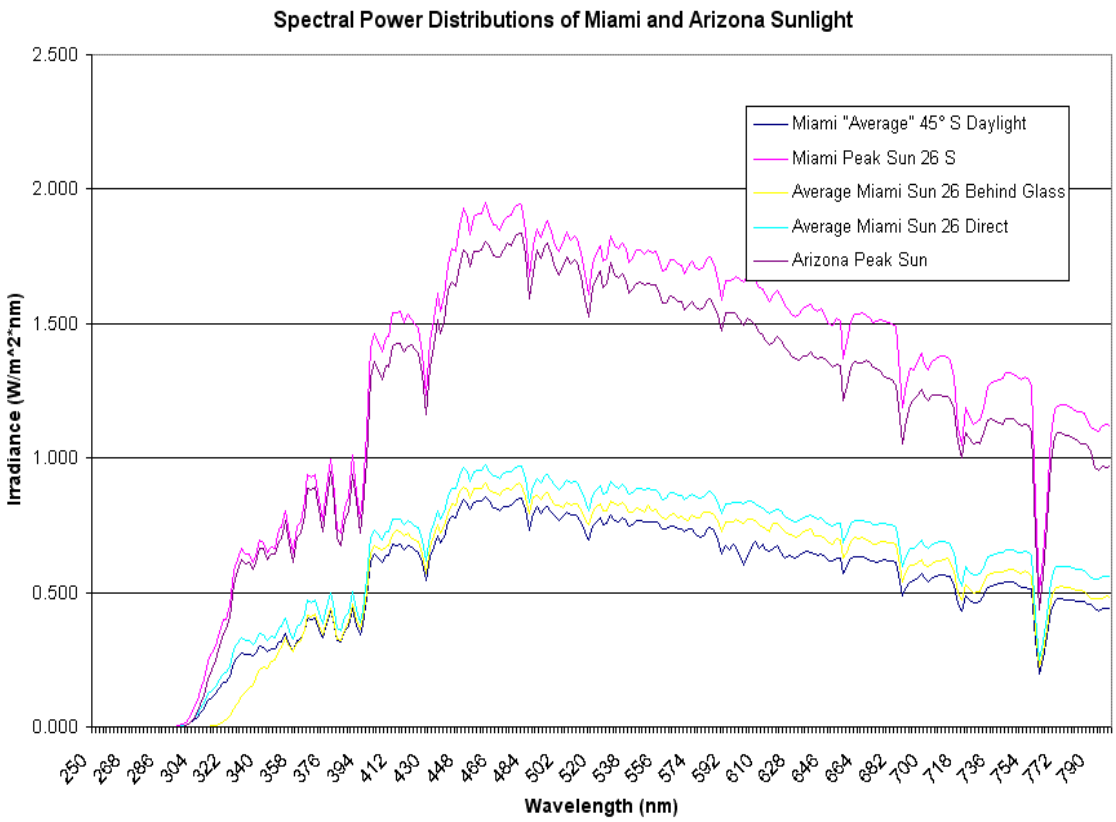

Figure A.2: Spectral distribution of day light and behind the glass from Miami and peak sun of Arizona. Adopted from Suntest CPS/CPS+ Manufacture's website.

Appendix B

SOUTHERN CLAY PRODUCTS / A SUBSIDIARY OF ROCKWOOD SPECIALTIES, INC.

PRODUCT BULLETIN/Cloisite®

Southern Clay Products, Inc.
1212 Church Street
Gonzales, TX 78629
Phone: 800-324-2891
Fax: 830-672-1903
www.scprod.com

Cloisite® 15A

Typical Physical Properties Bulletin

Description:
Cloisite® 15A is a natural montmorillonite modified with a quaternary ammonium salt.

Designed Used:
Cloisite® 15A is an additive for plastics to improve various plastic physical properties, such as reinforcement, HDT, CLTE and barrier.

Typical Properties:

Treatment/Properties:	Organic Modifier (1)	Modifier Concentration	% Moisture	% Weight Loss on Ignition
Cloisite® 15A	2M2HT	125 meq/100g clay	< 2%	43%

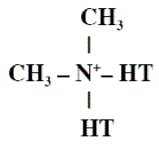

Where HT is Hydrogenated Tallow (~65% C18; ~30% C16; ~5% C14)

Anion: Chloride

(1) 2M2HT: dimethyl, dehydrogenated tallow, quaternary ammonium

Typical Dry Particle Sizes: (microns, by volume)

10% less than:	50% less than:	90% less than:
2µm	6µm	13µm

Color: Off White

Density:

Loose Bulk, lbs/ft^3	Packed Bulk, lbs/ft^3	Density, g/cc
10.79	18.64	1.66

X Ray Results: d_{001} = 31.5Å

For additional information or technical assistance contact Southern Clay Products, Inc. toll free at 800-324-2891.

SOUTHERN CLAY PRODUCTS / A SUBSIDIARY OF ROCKWOOD SPECIALTIES, INC.

PRODUCT BULLETIN/Cloisite®

Southern Clay Products, Inc.
1212 Church Street
Gonzales, TX 78629
Phone: 800-324-2891
Fax: 830-672-1903
www.scprod.com

Cloisite® 20A

Typical Physical Properties Bulletin

Description:
Cloisite® 20A is a natural montmorillonite modified with a quaternary ammonium salt.

Designed Used:
Cloisite® 20A is an additive for plastics to improve various plastic physical properties, such as reinforcement, HDT, CLTE and barrier.

Typical Properties:

Treatment/Properties:	Organic Modifier (1)	Modifier Concentration	% Moisture	% Weight Loss on Ignition
Cloisite® 20A	2M2HT	95 meq/100g clay	< 2%	38%

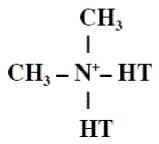

Where HT is Hydrogenated Tallow (~65% C18; ~30% C16; ~5% C14)

Anion: Chloride

(1) 2M2HT: dimethyl, dehydrogenated tallow, quaternary ammonium

Typical Dry Particle Sizes: (microns, by volume)

10% less than:	50% less than:	90% less than:
2μ	6μ	13μ

Color: Off White

Density:

Loose Bulk, lbs/ft^3	Packed Bulk, lbs/ft^3	Density, g/cc
7.35	13.55	1.77

X Ray Results: d_{001} = 24.2Å

For additional information or technical assistance contact Southern Clay Products, Inc. toll free at 800-324-2891.

Appendix-C

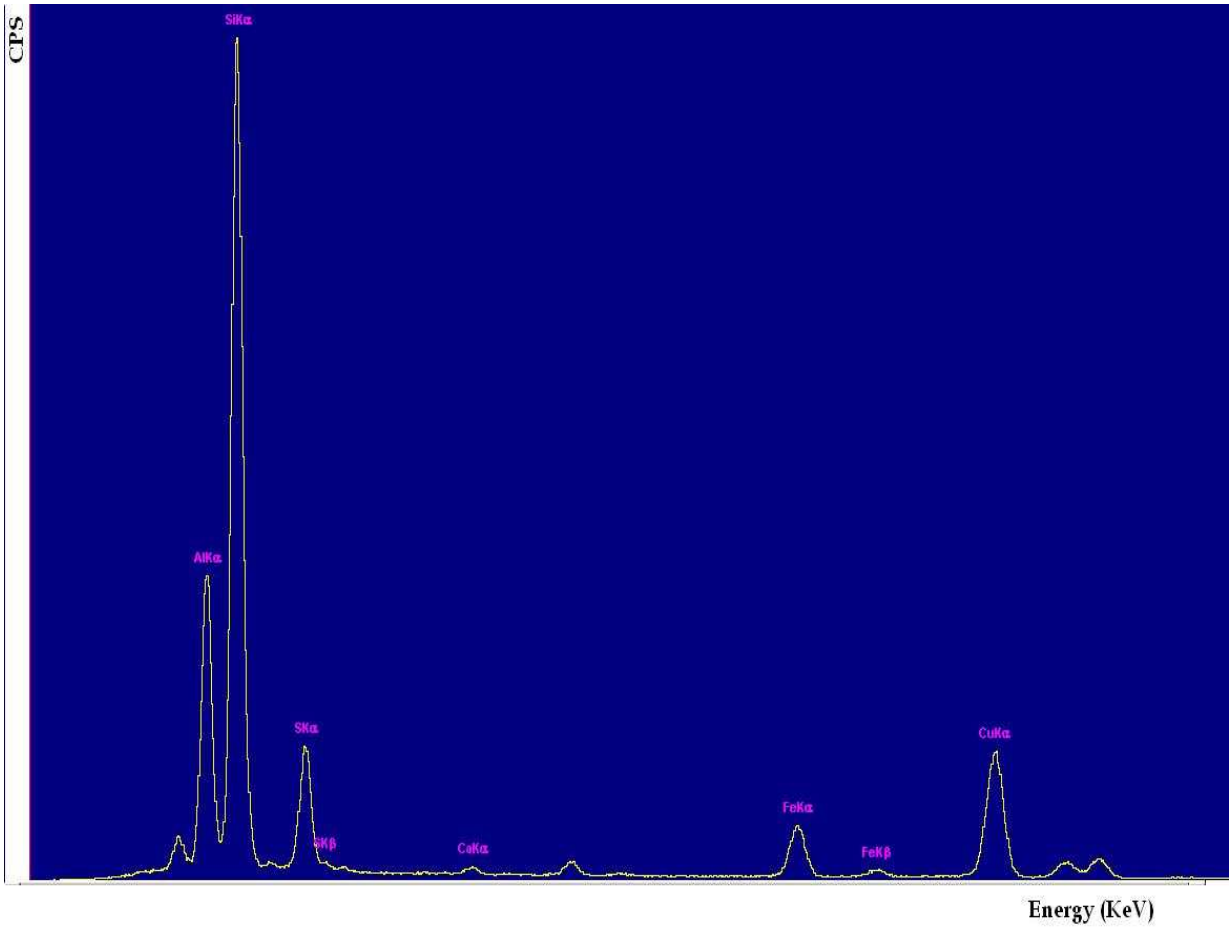

Figure C.1: Energy dispersive spectroscopy of Solvent Yellow 98 - Cloisite 15A Clay complex

References:

1. Zee, F.P.v.d., *Anaerobic azo dye reduction*. 2002, Wageningen University: Wageningen, The Netherlands.

2. Welham, A., *The theory of dyeing (and the secret of life).* J. Soc. Dyers Colour., 2000. **116.**: p. 140-143.

3. Chen K., V., *Mechanistic differences in degradation of Polystyrene and Polystyrene-Clay Nanocomposites of Polystyrene and Polystyrene-Clay Nanocomposite: Thermal and Thermo-Oxidative degradation.* Macromolecular Chemistry and Physics, 2006. **207**: p. 587-595.

4. Chen G., I.N., *Intercalation of rhodamine 6G and oxazine 4 into oriented clay films and their alignment.* Journal of Materials Research Society, 2002. **17**: p. 1035-1040.

5. Hummel, R.E., *Understanding Materials Science*. 1998, New York: Springer-Verlag.

6. Shichi T., T.K., *Clay minerals as photochemical reaction fields.* Journal of Photochemistry and Photobiology, 2000. **1**: p. 113-130.

7. Batenburg L. F., F.H., *PlanoColors® - a combination of organic dyes and layered silicates with nanometer dimensions.* e-Polymers, 2001. **no. T_001**.

8. Zee, F.P.v.d., *Anaerobic azo dye reduction*. 2002, Wageningen University: Wageningen, The Netherlands. p. 2-7.

9. Pospisil M., C.P., Weissmannova H., Klika Z.,Trchova M., Chmielova M., Weiss Z., *Structure analysis of montmorillonite intercalated with rhodamine B: modeling and experiment.* Journal of Molecular Modeling, 2003. **9**: p. 39–46.

10. van Olphen H, F.J., *Data handbook for clay materials and other non-metallic minerals..* 1979, Oxford: Pergamon Press. 19.

11. Utracki, L.A., *Clay Containing Polymeric Nanocomposites*. Vol. 1. 2004, UK: Rapra Technology Ltd. 76-81,98.

12. Ross C. S., H.S.B. in *U.S. Geological Survey professional*. 1945.

13. Margulies L., R.H., Stern. T., Rytwo G., Rubin B.,RUZO L. O.,Shlomo Nir S.,& Cohen E., *Photostabilization of Pesticides by Clays and Chromophores.* Archives of Insect Biochemistry and Physiology, 1993. **22**: p. 467-486.

14. Boyd, S.A., Jaynes, W. F., and Ross, B. S., *Immobilization of organic contaminants by organo-clays. Application to soil restoration and hazardous waste containment: In Organic Substances and sediments in Water (Baker, R. S., ed.).* 1991, Chelsea, MI: Lewis Publishers. 181-200.

15. Yariv, S., *Organo-Clay Complexes and Interactions*. 2002, New York: Marcel Dekker, Inc. 68,69 &84-89, 515-519.

16. Heller-Kallai, L., nad Yariv. S., *Swelling of montmorillonite containing coordination complexes of amines withtransition metal cations.* Journal of Colloid Interface Science, 1981. **79**: p. 479-485.

17. Yariv, S., *Wettability of clay minerals. In Modern Approaches to wetterbility (Schrader, M. E., and Loeb, G., eds.).* 1992, New York: Plenum Press. 279-326.

18. Anderson, M.A., Trouw, F. R., and Tam, C. N., *Properties of water in calcium- and hexadecyltrimethylammonium-exchanged bentonite.* Clay and Clay Minerals, 1999. **47**: p. 28-35.

19. Yariv, S., *Organophilic pores as proposed primery migration media for hydrocarbons in argillaceous rocks.* Clay Science, 1976. **5**: p. 19-29.

20. Barrer, R.M., *Shape-selective sorbents based on clay minerals-a review.* Clay and Clay Minerals, 1989. **37**: p. 385-395.

21. Jordan, J.w., *Organophilic bentonites, Swelling in organic liquids.* Journal of Physics & Colloid Chemistry, 1949. **53**: p. 294-306.

22. Maes A., L.V.L., A. Cremers, and J. Uytterhoevenm, *Electron density distribution as a parameter in understanding organic cation exchange in montmorillonite,.* Journal of colloidal Interface Science, 1980. **77**: p. 14-20.

23. Bergmann, K., and O'Konski, C. T.,, *A Spectroscopic Study of Methylene Blue Monomer, Dimer and Complexes with Montmorillonite.* Journal of Physical Chemistry, 1963. **67**: p. 2169-2177.

24. Neumann M. G., G.F., Schmitt C. C, & Sartori R., *Influence of the Layer Charge and Clay Particle Size on the Interactions between the Cationic Dye Methylene*

Blue and Clays in an Aqueous Suspension. Journal of Colloid and Interface Science, 2002. **255**: p. 254–259.

25. Sethuraman V. V., R., *Colour removal by clays: kinetic study of adsorption of cationic and anionic dyes.* Environmental Science and Technology, 1975. **9**: p. 1139-1140.

26. Ghosal D. N., M.S.K., *Studies on the sorption and desorption of crystal violet on and from bentonite and kaolinite.* Journal of Indian Chemical socity, 1972. **49**: p. 569-572.

27. Rytwo G., N.S., Margulies L., *Competitive adsorption of methylene blue and crystal violet to montmorillonite.* Clay and Clay Minerals, 1993. **28**: p. 139-143.

28. Narine D. R., a.G.R.D., *Interaction of some large organic cations with bentonite in dilute aqueous systems.* Clays and Clay Minerals, 1981. **29**: p. 205-212.

29. Landau A., Z.A., Lapides I., Yariv S., *Montmorillonite Treated with Rhodamine-6G Mechanochemically and Aqueous Suspensions Simultaneous DTA-TG study.* Journal of Thermal Analysis and Calorimetry, 2002. **70**: p. 103–113.

30. Garfinkel-Shweky. D., Y.S., *The effect of exchangeable metallic cation on the colloid properties of laponite treated with acridine orange. A spectrophotometric study.* Colloid Polymer Science, 1995. **273**: p. 453-463.

31. Grauer Z., A.G., Yariv s., *Adsorption characteristics of rhodamine 6G on montmorillonite and laponite, elucidated from electronic absorption and emission spectra.* Canadian Journal of Chemistry, 1984. **62**: p. 1889-1894.

32. Yariv S., N.A., Bar-On P., *Metachromasy in clay minerals. Spectroscopic study of the adsorption of crystal violet by Laponite.* Journal of Chem. Socity Faraday Trans., 1990. **86**: p. 1593-1598.

33. Nevins M. J., W.D.J., *Determination of cation exchange capacity by Methylene blue adsorption.* American Ceramic Socity Bulltion, 1967. **46**: p. 587-592.

34. Hills J. F., P.G.S., *The Clay mineral content of various rock types compared with the methylene blue value.* Journal of Chemistry and Biotechnology, 1984. **35A**: p. 168-180.

35. Fahn R., F.K., *Reaction Products of Organic Dye Molecules with Acid-Treated Montmorillonite.* Clay Minerals, 1983. **18**: p. 447-458.

36. Kengo Ito, M.K., Koushi Fukunishi, & Yoshio Fujiwara, *Thermal Recording Media Using Clay-Fluoran Dye Intercalation as a Stable Colour Former.* Dyes and Pigments,, 1996. **34,**(4): p. pp. 297-306.

37. Fan Q., U.S.C., Wilson A. R., Mani G., Yang Y., *Dyeable Polypropylene via Nanotechnology*, in *National Textile Center Annual Report*. 2003, Dept. of Textile Science, University of Massachusetts Dartmouth: North Dartmouth, MA.

38. Dudkina M. M., T.A.V., Pospiech D., Jehnichen D., Haussler L. and Leuteritz A.,, *Nanocomposites of NLO Chromophore-Modified Layered Silicates and Polypropylene.* Journal of Polymer Science, 2005. **43**: p. 2493-2502.

39. Synder L.R., W.J.W., Journal of Physical Chemistry, 1966. **70**: p. 3941.

40. Kim R. M., P.J.E., Burwell D.A., Groves J.T., Thompsom M.E., Inorg. Chem., 1993. **32**: p. 4509.

41. Yamanaka, F.K., M. Koizumi,, Journal of Physical Chemistry, 1975. **79**: p. 1285.

42. Fredericq E., H.C., *Electric Dichroism and Electric Birefringence,*. 1973, Oxford: Clarendon Press.

43. S.P., S., *Colloid Electrooptics: Theory, Dichroism and Applications*. 1991, New York: Academic Press.

44. Yamagishi A., T.M., Takahashi M., Asada C., and S.H. Matsushita N, J. Chem. Phys., 1994. **98**: p. 7555.

45. Cullity, B.D., *Elements of X-Ray Diffraction*. 2nd ed. 1978, California: Addison-Wesley Publising Company, Inc. 82-87.

46. Shiang J. J., K., A. V., Grubbs R. K. & Alivisatos A. P.J., *Symmetry of Annealed Wurtzite CdSe Nanocrystals: Assignment to the C3v Point Group.* Journal of Physical Chemistry, 1995. **99**: p. 17417-17422.

47. Smith, D.J., *The realization of atomic resolution with the electron microscope.* Reports on Progress in Physics, 1997. **60**: p. 1513-1580.

48. McCulloch, D., *Electron Microscopy*. 2003, Applied Physics, RMIT University: Melbourne. p. 21-24,37.

49. Williams D. B., C.C.B., *Transmission Electron Microscopy: A Test Book for Materials Science*. 1996, New York: Plenum Press. 555-570.

50. Cole, W.F., Rowland, N. M., *An abnormal effect in differential thermal analysis of clay minerals*. Vol. Ch 46. 1961, Am: Mineralogist. 304-312.

51. Stoch, L., *Thermal dehydroxylation of minerals of the Kaolinite group.* Bull. Acad. Polon. Sci., 1964. **12**: p. 173-180.

52. Cebulak, S., and Langier- Kuzniarowa, A., *Some remarks on the methodology of thermal analysis of clay minerals.* Journal of Thermal Analysis, 1998. **53**: p. 375-381.

53. Yariv, S., *Differential thermal analysis (DTA) of organo-clay complexe*. Lecture Notes in Earth Science -Thremal Analysis in the Geosciences. Vol. 38. 1991, Berlin: Springer Verlag. 328-351.

54. Cebulak, S., and Langier-Kuzniarowa, A., *Application of oxyreactive thermal analysis to the examination of organic matter associated with rocks.* Journal of Thermal Analysis, 1997. **50**: p. 175-190.

55. Gilman J. W., J.C.L., Morgan A. B., Harris R.,, *Flammability Properties of Polymer-Layered-Silicate Nanocomposites. Polypropylene and Polystyrene Nanocomposites.* Chemistry of Materials, 2000. **12**: p. 1866-1873.

56. Tanoue S., U.L.A., Garcia-Rejon A., Kamal M. R., Sammut P., Ton-That M. T., Pesneau I., Lyngane- Jorgensen J., *Melt compounding of different grades Polystyrene with organoclay: Rheological properties.* Polymer Engineering Science, 2004. **44**: p. 1061-1076.

57. Zilg C., T.R., Mulhaupt R., Finter J., *Polyurethane nanocomposites containing laminated anisotropic nanoparticles derived from organophilic layered silicates.* Advanced Materials, 1999. **11**: p. 49-52.

58. Fischer H. R., B.L.F., Meinema H. A., Hogerheide M. P., Rentrp C. H. A., *Nanocomposites coatings*. 2001, Nederlandse Centrale Organisatie voor Toegepast- Natuurwetenschappelijk Onderzoek TNO.: Neitherland.

59. Barbee R. B., W.M.A., Matayabas J. C., *A colorant composition, a polymer nanocomposite comprising the colorant compostion and articlesproduced therefrom*. 2000, Eastman Chemical Co.: US.

60. Zhu J, M.A.B., Lamelas F. J., & Wilkie C. A., *Fire properties of polystyrene-clay nanocomposites.* Chem Mater, 2001b. **13**: p. 3774-3780.

61. Bourbigot S., G.J.W., Wilkie C. A, *Kinetic Analysis of the Thermal Degradation of Polystyrene-MontmorilloniteNanocomposite.* Polymer Degradation Stability, 2004. **84**(3): p. 483- 492.

62. A, W.C., *Recent advanced flame retradency.* Polymer Materials, 2000. **11**: p. 55-67.

63. Zhu J., S.P., Mauritz K. A. & Wilkie C. A., *Silicon-methoxide-modified clays and their polystyrene nanocomposites.* Journal of Polymer Science Part A: Polymer Chem., 2002. **40**: p. 1498- 1503.

64. Zhu J, U.F.M., Morgan A. B, , Lamelas F. J., & Wilkie C. A., *Studies on the mechanism by which the formation of nanocomposites enhances thermal stability.* Chem Matter, 2001a. **13**: p. 4649-4654.

65. Jang B. N., W.C.A., *The thermal degradation of Polystyrene nanocomposite.* Journal of Polymer, 2005. **46**: p. 2933-2942.

66. Pickett, J.E., *Permanence of UV Absorbers in Plastics and Coatings*, in *Technical Information Series*. 1997, General Electric Company. p. 1-30.

67. Hirt R. C., S.N.Z., Schmitt R. G. *Ultraviolet degradation of plastics and the use of protective ultraviolet absorbers*. in *SPE Transactions*. 1961.

68. Krenske D, A.S., Van Damme H, Cruz M, Fripiat JJ, *Photochemical and photocatalytic properties of adsorbed organometallic compounds. Luminescence quenching of tris(2,2'- bipyridine) ruthenium (11) and chromium (In) in clay membranes.* Journal of Physical Chemistry, 1980. **84**: p. 2447.

69. DellaGuardia RA, T.J., *Photoprocesses on colloidal clay systems. Tris (2,2'- bipyridine) ruthenium (11) bound to colloidal kaolin and montmorillonite.* Journal of Physical Chemistry, 1983. **87**: p. 990.

70. Schoonheydt F. L., D.P.P., Vliers D., Schrijver F. C.,, *Luminescence of tris (2,2'-bipyridine) ruthenium (11) in aqueous clay mineral suspensions.* Journal of Physical Chemistry, 1984. **88**: p. 5113.

71. Romero, R., Robert, M., Elsass, P. and Garcia, C.,, *Evidence by transmission electron spectroscopy ofweathering microsystems in soil developed from crystalline rocks.* Journal of Clay Minerals, 1992. **27**: p. 21-33.

72. Lagaly, G.E., *In progress in colloid and polymer science*. Vol. 121. 2002, Berlin-Heidelberg: Springer. ch. 6 (111).

73. Tahoun, S.A., and Mortland, M. M., *Complexes of montmorillonite with primary, secondery and tertiary amides. I Protonation of amides on the surface of montmorillonite.* Journal of Colloid soil Science, 1966a. **102**: p. 248-254.

74. Tahoun, S.A., and Mortland, M. M., *Complexes of montmorillonite with primary, secondery and tertiary amides. II Coordination of amides on the surface of montmorillonite.* Journal of soil Science, 1966b. **102**: p. 314-321.

75. Stutzmann, T.a.S., B., *Contribution to the adsorption mechanism of acetamide and polyacrylamide on to caly minerals.* Clays and Clay minerals, 1977. **25**: p. 392-406.

76. Yariv, S., Muller-Vonmoos, M. Kahr, G., & Rub.A., *Thermal analytic study of the adsorption of Crystal violet by montmorillonite.* Thermochim. Acta, 1989a. **148**: p. 457-466.

77. Yariv, S., *Combined DTA-mass spectrometry of organo-clay complexes.* Journal of Thermal Analysis, 1990. **36**: p. 1953-1961.

78. Yariv, S., Muller-Vonmoos, M. Kahr, G., & Rub.A., *Thermal analytic study of the adsorption of Crystal violet by laponite.* Journal of Thermal Analysis, 1989b. **35**: p. 1941-1952.